UNCLASSIFIED

SECURITY CLASSIFICATION OF THIS PAGE (When Data Entered)

REPORT DOCUMENTATION PAGE

READ INSTRUCTIONS BEFORE COMPLETING FORM

1. REPORT NUMBER: NAVENVPREDRSCHFAC Contractor Report CR 83-09	2. GOVT ACCESSION NO.
3. RECIPIENT'S CATALOG NUMBER	
4. TITLE (and Subtitle): Aerosol Characteristics on the Alboran Sea, 9-18 October 1982	5. TYPE OF REPORT & PERIOD COVERED: Final Report 9/17/82 - 9/7/83
6. PERFORMING ORG. REPORT NUMBER: 7076-M-1	
7. AUTHOR(s): E. J. Mack, C. W. Rogers and J. N. Kile	8. CONTRACT OR GRANT NUMBER(s): N00228-82-C-8170
9. PERFORMING ORGANIZATION NAME AND ADDRESS: Arvin/Calspan Advanced Technology Center, Box 400, Buffalo, NY 14225	10. PROGRAM ELEMENT, PROJECT, TASK AREA & WORK UNIT NUMBERS: PE 62759N PN WF59-553 TA 1 NEPRF WU 6.2-9
11. CONTROLLING OFFICE NAME AND ADDRESS: Naval Air Systems Command, Department of the Navy, Washington, DC 20361	12. REPORT DATE: December 1983
	13. NUMBER OF PAGES: 144
14. MONITORING AGENCY NAME & ADDRESS (if different from Controlling Office): Naval Environmental Prediction Research Facility, Monterey, CA 93943	15. SECURITY CLASS. (of this report): UNCLASSIFIED
	15a. DECLASSIFICATION/DOWNGRADING SCHEDULE

16. DISTRIBUTION STATEMENT (of this Report)

Approved for public release; distribution unlimited.

17. DISTRIBUTION STATEMENT (of the abstract entered in Block 20, if different from Report)

18. SUPPLEMENTARY NOTES

19. KEY WORDS (Continue on reverse side if necessary and identify by block number)

Aerosols	Size Spectra	Alboran Gyre
Marine	Chemical Composition	Mediterranean Sea
Coastal	Boundary Layer	Alboran Sea
Optical Depth	Sun Photometry	
Visibility	Scattering coefficient	

20. ABSTRACT (Continue on reverse side if necessary and identify by block number)

An at-sea study of aerosol characteristics was conducted on the Alboran Sea to obtain data for potential correlation with sun photometry, overflight imagery and radiance data and for study of possible atmospheric/aerosol effects produced by sea surface temperature gradients of the Alboran Gyre. Observations of Aitken nuclei concentrations, aerosol size spectra (0.3 to 30 μm diameter), visibility (scattering coefficient), optical depth (sun photometry), air temperature, relative humidity, winds and cloud cover were acquired hourly during daylight hours of the cruise; samples for aerosol chemical analyses were obtained at approxi-

DD FORM 1 JAN 73 1473

UNCLASSIFIED

SECURITY CLASSIFICATION OF THIS PAGE (When Data Entered)

Block 20, Abstract, continued.

mate 3-hr intervals. The data show that aerosol populations, even in mid-Alboran, were typical of those observed previously at other near-coastal locals, although characterized by high proportions of NaCℓ aerosols. The cold water of the Alboran Gyre was apparently responsible for a stable atmospheric boundary layer, along the northern shore of the Alboran, which trapped aerosol plumes from the Gibraltar area at low levels. Finally, optical depth was found to correlate with surface level visibility integrated as a function of the relative humidity profile over the boundary layer, assuming a well-mixed boundary layer with respect to aerosols.

AN (1) AD-A134 872
FG (2) 040200
CI (3) (U)
CA (5) ARVIN/CALSPAN ADVANCED TECHNOLOGY CENTER BUFFALO NY
TI (6) Aerosol Characteristics on the Alboran Sea, 9-18 October 1982.
TC (8) (U)
DN (9) Final contractor rept. 17 Sep 82-7 Sep 83,
AU (10) Mack,E. J.
AU (10) Rogers,C. W.
AU (10) Kile,J. N.
RD (11) Dec 1983
PG (12) 151p
RS (14) CALSPAN-7076-M-1
CT (15) N00228-82-C-8170
PJ (16) F59553
TN (17) WF595531
RN (18) NEPRF-CR-83-09
RC (20) Unclassified report
DE (23) *Aerosols, Mediterranean Sea, East(Direction), Concentration(Composition), Chemical analysis, Particle size, Visibility, Meteorological data, Variations
DC (24) (U)
ID (25) Alboran Sea, FE62759N
IC (26) (U)
AB (27) An at-sea study of aerosol characteristics was conducted on the Alboran Sea to obtain data for potential correlation with sun photometry, overflight imagery and radiance data and for study of possible atmospheric/aerosol effects produced by sea surface temperature gradients of the Alboran Gyre. Observations of Aitken nuclei concentrations, aerosol size spectra (0.3 to 30 micrometers diameter), visibility (scattering coefficient), optical depth (sun photometry), air temperature, relative humidity, winds and cloud cover were acquired hourly during daylight hours of the cruise; samples for aerosol chemical analyses were obtained at approximate 3-hr intervals. The data show that aerosol populations, even in mid-Alboran, were typical of those observed previously at other near-coastal locals, although characterized by high proportions of NaCl aerosols. The cold water of the Alboran Gyre was apparently responsible for a stable atmospheric boundary layer, along the northern shore of the Alboran, which trapped aerosol plumes from the Gibraltar area at low levels. Finally, optical depth was found to correlate with surface level visibility integrated as a function of the relative humidity profile over the boundary layer, assuming a well-mixed boundary layer with respect to aerosols.
AC (28) (U)
DL (33) 01

SE (34) F
CC (35) 414301

NAVENVPREDRSCHFAC
CONTRACTOR REPORT
CR 83-09

NAVENVPREDRSCHFAC CR 83-09

AEROSOL CHARACTERISTICS ON THE ALBORAN SEA, 9-18 OCTOBER 1982

Prepared By:

E. J. Mack, C. W. Rogers and J. N. Kile
Arvin/Calspan Advanced Technology Center
Buffalo, NY 14225

Contract No. N00228-82-C-8170

DECEMBER 1983

Prepared For:
NAVAL ENVIRONMENTAL PREDICTION RESEARCH FACILITY
MONTEREY, CALIFORNIA 93943

TABLE OF CONTENTS

Section	Title	Page
1	INTRODUCTION AND SUMMARY	1
2	RESULTS	4
	2.1 Summary Discussion of the Alboran Data Set	4
	2.1.1 Experiment Protocol and Instrumentation	4
	2.1.2 Background and Overview of Maritime Aerosol Populations	7
	2.1.3 Summary of the Alboran Data Set	11
	2.2 A Relationship Between Optical Depth and Surface-Level Visibility	21
3	INTERPRETATION OF INDIVIDUAL DAILY DATA SETS	27
	3.1 9 October 1982	31
	3.2 10 October 1982	37
	3.3 11 October 1982	43
	3.4 12 October 1982	48
	3.5 13 October 1982	54
	3.6 14 October 1982	59
	3.7 15 October 1982	64
	3.8 16 October 1982	69
	3.9 17 October 1982	75
	3.10 18 October 1982	81
	REFERENCES	86
	APPENDIX A CALSPAN'S DATA LOG	88
	APPENDIX B REDUCED DATA	103
	B-1 Optical Depth Computations	104
	B-2 Aerosol Size Spectra; and Number, Cross-section and Volume	107
	B-3 Extinction Estimates based on Aerosol Size Spectra	124
	B-4 Aerosol Chemistry	131
	B-5 Summary Discussion of the Alboran Gyre	137

LIST OF FIGURES

Figure	Title	Page
1	Approximate Cruise Tracks of the USNS BARTLETT during Daylight Hours (0600-1900 GMT) Showing where Aerosol Measurements were Obtained on the Indicated Days of October 1982	6
2	Meteorological Parameters as Functions of Time, Measured from Aboard the USNS BARTLETT on the Alboran Sea, 9-18 October 1982 .	13
3	Optical Depth, Scattering Coefficient and Aerosol Cross-section as Functions of Time, Measured from Aboard the USNS BARTLETT on the Alboran Sea, 9-18 October 1982	14
4	Aerosol Number Concentrations at Four Size (diameter) Intervals as Functions of Time, Measured from Aboard the USNS BARTLETT on the Alboran Sea, 9-18 October 1982.	15
5	Percentage of Aerosols >0.2μm dia by Compositional Classification as a Function of Time, Measured from Aboard the USNS BARTLETT on the Alboran Sea, 9-18 October 1982	16
6	Aerosol Optical Depth for Two Sites as Functions of a) Scattering Coefficient and b) Visibility Measured at the Surface.	22
7	Integrated Boundary Layer Extinction Coefficient, Derived from Surface-Level Aerosol Extinction (at .474μmλ) and Vertical Profile of Relative Humidity within the Boundary Layer, vs. Surface Measured Total Atmospheric Aerosol Optical Depth at 0.502 μmλ.	26
8a	Approximate Cruise Track of the USNS BARTLETT, 0030 9 October to 1730 GMT 11 October 1982	28
8b	Approximate Cruise Track of the USNS BARTLETT, 1730 11 October to 1700 GMT 15 October 1982	29
8c&d	Approximate Cruise Track of the USNS BARTLETT, 1700 15 October to 1800 GMT 18 October 1982	30
9	Meteorological Parameters, 9 October 1982	32
10	Optical Depth, β_{scat} and Aerosol Cross-section, 9 October 1982 . . .	33
11	Aerosol Concentrations at Three Size Intervals, 9 October 1982 . . .	34
12	Chemical Classification of Aerosols >0.2μm dia, 9 October 1982 . . .	35
13	Meteorological Parameters, 10 October 1982	38
14	Optical Depth, β_{scat} and Aerosol Cross-section, 10 October 1982 . .	39
15	Aerosol Concentrations at Three Size Intervals, 10 October 1982 . .	40
16	Chemical Classification of Aerosols >0.2 μm dia, 10 October 1982 . .	41
17	Meteorological Parameters, 11 October 1982	44

LIST OF FIGURES (Cont'd)

Figure	Title	Page
18	Optical Depth, β_{scat} and Aerosol Cross-section, 11 October 1982 . .	45
19	Aerosol Concentrations at Three Size Intervals, 11 October 1982 . .	46
20	Chemical Classification of Aerosols >0.2 μm dia, 11 October 1982. .	47
21	Meteorological Parameters, 12 October 1982.	49
22	Optical Depth, β_{scat} and Aerosol Cross-section, 12 October 1982 . .	50
23	Aerosol Concentrations at Three Size Intervals, 12 October 1982 . .	51
24	Chemical Classification of Aerosols >0.2 μm dia, 12 October 1982. .	52
25	Meteorological Parameters, 13 October 1982.	55
26	Optical Depth, β_{scat} and Aerosol Cross-section, 13 October 1982 . .	56
27	Aerosol Concentrations at Three Size Intervals, 13 October 1982 . .	57
28	Chemical Classification of Aerosols >0.2 μm dia, 13 October 1982. .	58
29	Meteorological Parameters, 14 October 1982.	60
30	Optical Depth, β_{scat} and Aerosol Cross-section, 14 October 1982 . .	61
31	Aerosol Concentrations at Three Size Intervals, 14 October 1982 . .	62
32	Chemical Classification of Aerosols >0.2 μm dia, 14 October 1982. .	63
33	Meteorological Parameters, 15 October 1982.	65
34	Optical Depth, β_{scat} and Aerosol Cross-section, 15 October 1982 . .	66
35	Aerosol Concentrations at Three Size Intervals, 15 October 1982 . .	67
36	Chemical Classification of Aerosols >0.2 μm dia, 15 October 1982. .	68
37	Meteorological Parameters, 16 October 1982.	70
38	Optical Depth, β_{scat} and Aerosol Cross-section, 16 October 1982 . .	71
39	Aerosol Concentrations at Three Size Intervals, 16 October 1982 . .	72
40	Chemical Classification of Aerosols >0.2 μm dia, 16 October 1982. .	73
41	Meteorological Parameters, 17 October 1982.	76
42	Optical Depth, β_{scat} and Aerosol Cross-section, 17 October 1982 . .	77
43	Aerosol Concentrations at Three Size Intervals, 17 October 1982 . .	78
44	Chemical Classification of Aerosols >0.2 μm dia, 17 October 1982. .	79
45	Meteorological Parameters, 18 October 1982.	82
46	Optical Depth, β_{scat} and Aerosol Cross-section, 18 October 1982 . .	83
47	Aerosol Concentrations at Three Size Intervals, 18 October 1982 . .	84
48	Chemical Classification of Aerosols >0.2 μm dia, 18 October 1982. .	85

LIST OF TABLES

Table	Title	Page
1	Calspan Observations, Instrumentation and Measurement Schedule (USNS BARTLETT, 9-18 October 1982, Alboran Sea).	5
2	Typical Aerosol Concentrations Observed in the Marine Boundary Layer.	8
3	Average Percentage of Particles in the Size Range 0.2-10.0 μm Diameter as Functions of Composition and Sampling Location . . .	9
4	Synopsis of Meteorological Circumstances and Summary of the Data Set at BARTLETT's Location	12
5	Average Optical Depth, Extinction and Boundary Layer Data for Each of Four Days on the Alboran Sea (October 1982) and Valkaria, Florida (July 1982).	24

Section 1

INTRODUCTION AND SUMMARY

Under Contract No. N00228-82-C-8170 with the Naval Environmental Prediction Research Facility (NEPRF), Calspan provided aerosol characterization support to the Naval Oceanographic Research and Development Activity's (NORDA) Project ¿Donde Va?, a study of the oceanographic features of the Alboran Gyre. The observation effort, Task 1, was carried out from aboard the USNS BARTLETT during a 10-day cruise in October 1982 on the Alboran Sea, the western-most portion of the Mediterranean immediately inside the Straits of Gibraltar. While the aerosol characterization measurements were obtained in cooperation with and in support of Project ¿Donde Va?, the aerosol data were collected primarily for use in NEPRF's investigation of atmospheric optical properties and 'gray' shades. Since obscuration in the atmosphere is largely dependent on that portion of the aerosol population at sizes >0.1 μm diameter and because deliquescent aerosols fluctuate in size with fluctuating relative humidity, the observation effort centered on both the physical and chemical properties of aerosols of size >0.1 μm and on supporting meteorological variables.

As Task 2 of this contract, the data were reduced and analyzed to provide information for interpretive analyses of boundary-layer aerosol characteristics along specific ship-tracks. The reduced data were intended for potential correlation with overflight imagery and radiance data, with optical depth estimates from sun photometry data, and with possible atmospheric effects related to sea surface temperature gradients in the northern half of the Alboran Gyre. However, for Calspan's analyses, radiance data were not yet reduced and only limited imagery were available. Hence, Calspan's efforts focused on providing reliable aerosol, optical depth and meteorological documentation for future use in interpretation of overflight imagery and radiance data; our analyses were limited to correlations between aerosol

population characteristics, optical depth estimates, and attendant meteorologic/oceanographic/geographic scenarios.

The findings of this study are briefly summarized as follows:

- Optical depth as computed from sun photometer observations appears to be well correlated with surface measurements of visibility (scattering coefficient) integrated as a function of the relative humidity profile over the boundary layer, assuming a well-mixed boundary layer with respect to aerosols.

- Colder water in the northern portion of the Alboran Gyre is apparently directly responsible for lowering air temperature, increasing relative humidity and producing a shallow, stable boundary layer over the northern portion of the Alboran Sea. There is some evidence to suggest that the inversion capping this shallow boundary layer, on occasion, traps aerosol plumes in the surface layer, causing these plumes to extend in an easterly direction from the Gibraltar area, parallel to and directly over east-west oriented isotherms of the Alboran Front.

- Aerosol populations over the Alboran, although characterized by high proportions of NaCℓ, are typical of aerosols observed at other near-coastal locales: i.e., concentrations of small particulates peak at mid-day due to photochemical processes and anthropogenic activities while concentrations at large sizes exhibit minima at mid-day due to daytime relative humidity minima. In the near shore areas (within 35 km), total particle concentrations average ∿50% greater than those observed in the mid-Alboran; while particle concentrations at sizes >0.3 μm diameter, on the average, were comparable for both near-shore and mid-Alboran locations.

This report documents these findings and summarizes results of the analyses efforts. Section 2 presents a summary of cruise and experiment protocol, an overview of the data set, and results. Discussion of the observed relationship between optical depth and surface-level extinction may be found in Section 2.2. A synopsis of cruise activities, detailed presentation of the data and interpretive analyses of the data sets in the context of the attendant meteorologic/oceanographic/geographic scenario are presented in Section 3, organized chronologically for each day of the observation period. The hourly data recorded by Calspan are provided in 'log' format, along with discussion of individual variables and description of instrumentation, in Appendix A. Supporting analyses and reduced data are provided in Appendix B. A brief discussion of the Alboran Gyre is reproduced in Appendix B-5.

Section 2

RESULTS

The objective of Calspan's participation in the Alboran Sea Experiment, i.e., Project ¿Donde Va?, was to provide aerosol characterization for potential correlation with satellite-derived 'gray-shade' imagery (References 1, 2) and radiance data and with possible atmospheric effects resulting from sea surface temperature gradients associated with the Alboran Gyre. In this context, we have attempted to provide an overall assessment of the aerosol population encountered during the 10-day observation period. In addition, we were able to correlate optical depth with integrated boundary-layer extinction coefficient estimated from surface-level measurements. This section provides discussion of these results, a brief description of instrumentation and experiment protocol, summaries of the data, an overview of marine aerosol characteristics, and results of interpretive analyses. Additional information on NORDA's Project ¿Donde Va? and more detail on the oceanographic features of the Alboran Gyre may be found in References 3-6 and in Appendix B-5.

2.1 SUMMARY DISCUSSION OF THE ALBORAN DATA SET

2.1.1 Experiment Protocol and Instrumentation

Calspan measurements were obtained from aboard the USNS BARTLETT during the period 9 through 18 October 1982, principally during daylight hours from 0600 to 1900 GMT. An hourly observation schedule was maintained, with special observations occasionally made at half-hour intervals or later into the evening hours. Approximately 150 observation sets (particle concentrations at sizes >0.003 (Aitken), 0.32 and 3.2 μm, scattering coefficient, air temperature, RH, visibility, winds, and cloud cover) were obtained during the daylight hours of the cruise. In addition, more than 50 aerosol samples were acquired (at 3-hr intervals during daylight) for subsequent chemical composition analyses, and more than 50 impactor samples were collected (simultaneously with the chemical samples) for later analysis to provide large-particle (3 to >50μm) size-spectra data. Sun photometry data were also

Table 1

CALSPAN OBSERVATIONS, INSTRUMENTATION AND MEASUREMENT SCHEDULE

(USNS BARTLETT, 9-18 October 1982, Alboran Sea)

PARAMETER	INSTRUMENT	MEASUREMENT INTERVAL
Total aerosol concentration (sizes >.003 μm dia)	Gardner Small Particle Detector	hourly
Aerosol size spectra (0.3-5.0 μm dia)	Royco Model 225 Particle Counter	10 min.
Aqueous aerosol size spectra (3.0->50.0 μm dia)	Calspan Sea Spray Sampler (gelatin repl.)	3 hr.
Individual particle class by chemistry (>0.1 μm)	Casella-Type Cascade Impactor	3 hr.
Scattering Coefficient ($0.1\text{-}100 \times 10^{-4} m^{-1}$) Visibility (2-80 km)	MRI Integrating Nephelometer, Mod. 2050	continuous
Sun Photometry (0.4-1.1, 0.502 μm λ 5° aperture)	UDT Mod. 40x Opto-meter (Calspan modified)	hourly
Wet/Dry bulb temperatures, RH	Sling Psychrometer	hourly
Winds, Weather, Cloud Cover	Manual Meteorologic Observations	hourly

obtained (hourly, when possible) on six days and for several hours on 2 other days. Instrumentation, observed variables and measurement intervals are listed in Table 1.

Since NORDA's primary objective was study of the Alboran Gyre, the cruise plan was designed to produce cross-sectional observations (primarily north-south) of the oceanographic features of the Gyre. Interest also centered on possible atmospheric or aerosol effects resulting from the sea surface temperature gradient which develops in the northern half of the Gyre. The BARTLETT's track, based on NORDA's experiment requirements, resulted in daylight (0600-1900 GMT) positions and tracks as shown on the chart in Figure 1.

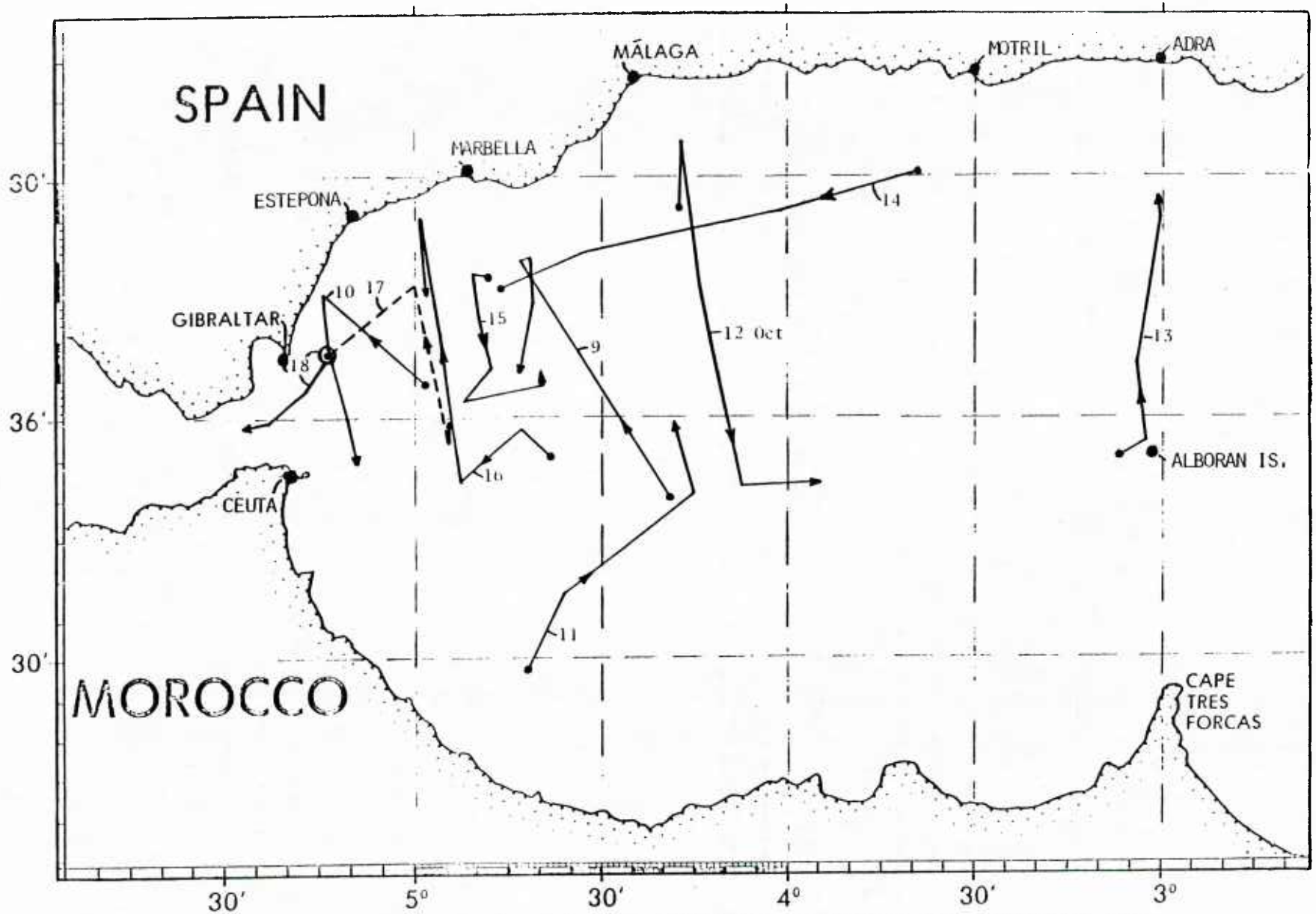

Figure 1. Approximate Cruise Tracks of the USNS BARTLETT during Daylight Hours (0600-1900 GMT) Showing where Aerosol Measurements were obtained on the Indicated Days of October 1982.

Since aerosol characterization was intended principally for correlative analyses with overflight data, Calspan's data acquisition was concentrated during the daylight hours represented by the tracks in Figure 1. It is obvious from the chart that the bulk of the aerosol data set was obtained in the northern half of the Alboran Sea. (Some additional aerosol data were acquired in the area offshore of Marbella by NEPRF personnel aboard a Spanish vessel, the Naucrates.)

2.1.2 Background and Overview of Maritime Aerosol Populations

In recent years, Calspan has made observations of aerosol characteristics at a number of maritime locales in North America and Europe as well as in the mid-Atlantic (References 7-15). Briefly summarizing, the data show that the marine aerosol population varies considerably in number concentrations and chemical composition, both spatially and temporally and does not necessarily comprise solely sea salt aerosols; continental/anthropogenically-derived materials--i.e., sulfates, organics, fly ash, silicates and other minerals--can be found over several thousand kilometers offshore. These data are summarized in Tables 2 and 3.

In remote or mid-ocean areas, total particle concentrations are typically <500 cm^{-3}, while number concentrations at sizes >0.1 µm and >1.0 µm diameter are typically 100 and 1 cm^{-3}, respectively. Particle concentrations, particularly at larger sizes, fluctuate by an approximate order of magnitude over periods of days; fluctuations of these predominantly sea spray particles appear primarily dependent on sea state and relative humidity. Direct measurements of sea spray (away from surf zones) suggest that number concentrations are constant in the vertical in the lowest few 10's of meters and that sea spray droplets are not necessarily locally generated; maximum sizes at wind speeds of <15m/sec are typically ~40 µm diameter. These observations demonstrate that, while continental-source aerosols can at times account for up to 50% of the aerosol at sizes >0.2 µm, mid-ocean aerosols are principally sea salt with equilibrium concentrations controlled by a balance between production and evaporation.

Table 2

Typical Aerosol Concentrations Observed in the Marine Boundary Layer

Location	Date of Study	Visibility (km)	RH (%)	Total Particle Conc. (cm^{-3})	Particle Concentration at Diameters >0.1 μm (cm^{-3})	>0.3 μm (cm^{-3})	>1.0 μm (cm^{-3})	CCN @ 0.2% SS (cm^{-3})	CCN @ 1.0% SS (cm^{-3})
Offshore Coast of Portugal (within 1200 km)	May 77	20-50	75-90	900-5000	400-2000	7-70	0.9-3.0	300-500	600-1000
Offshore Coastal Europe (30-50°N.Lat) (within 1000 km)	Apr 83	-	70-85	1000-20000	50-2000	0.1-80	0.1-0.5	-	-
Mediterranean (150-250 km offshore)	Jun 77	25-60	65-80	800-3500	250-1500	7-30	0.7-3.0	150-900	400-2000
Alboran Sea (Western Mediter.)	Oct 82	25-80	60-85	1500-10000		2-20	0.5-2.0	-	-
Offshore Coast of Nova Scotia (within 150 km)	Aug 75	-	-	400-2000	-	-	-	130	450
Offshore New England Coast of U.S. (200-400 km)	Aug 75	-	-	2000-6000	-	-	-	580	1350
Offshore New England Coast of U.S. (within 300 km)	May 77	20-80	65-75	4000-15000	1000-5000	2-40	0.3-6.0	350	990
Offshore Southeast Coast of U.S. (within 1000 km)	Mar 83	-	55-70	1500-15000	500-2000	0.2-40	0.1-1.0	-	-
Gulf of Mexico (20 km offshore)									
Marine flow (Panama City, FL)	Feb 77	43	65-95	3400	-	2.0	0.1-1.3	-	-
Marine flow	Nov 78	23	75-95	1700	300-1200	-	1.0-10.0	730	1450
Continental flow	Feb 77	32	40-75	5500	-	4.0	0.1-1.2	-	-
Continental flow	Nov 78	20	35-85	3800	1500-3500	-	0.1-1.0	1010	2130
Offshore Coast of S.California									
(within 150 km)	Oct 76	10-40	70-95	400-4000	-	-	-	50-1000	400-2200
(within 150 km)	May 78	10-30	75-95	300-10000	100-2000	-	6.0	100-700	300-3500
(beyond 150 km)	Sep 76	30-80	70-95	<200-600	-	-	-	20-200	100-400
Offshore N. California (100-150 km)	Aug 74	-	-	-	-	-	-	60	200
Mid-Atlantic (40-45°N Lat.)	May 77	80	50-75	<200-500	30-150	2-10	0.8-4.0	60-140	90-200
Mid-Atlantic (20°N Lat.)	Mar 83	-	65-85	300-1000	50-500	1-15	0.2-5.0	-	-
Cape Cod (12km inland, Otis AFB)	Jul 80	4-60	50-95	4000-35000	500-4000	-	0.5-100	60-600	400-2000
Cape Cod (12km inland, Otis AFB)	Jun 82	-	-	2000-30000	-	-	-	250-1100	300-3000
Coastal Cape Cod (Woods Hole)	Jun 82	-	-	1000-11000	-	-	-	100-900	350-2000
Coastal Maine (~2km inland at Corea)	Jul 81	3-80	40-95	1000-10000	-	2.0	0.2-1.0	-	-
Coastal Florida (~5km inland, Valkaria)	Jul 82	5-80	60-90	3000-15000	-	0.5-100	<1.0	-	-

* Single numbers represent averages; multiple figures are typical range values and do not include extremes.

Table 3

Average Percentage of Particles in the Size Range 0.2-10.0 μm Diameter as Functions of Composition and Sampling Location

Location	Date	Sea Salt (%)	Other Salts Without NaCl or Si (%)	Organics (%)	Silicates (%)	Number of Particles Counted
Offshore Coast of Portugal (within 1200 km)	May 77	42	13	33	12	200
Mid-Mediterranean	Jun 77	30	44	17	9	400
Alboran Sea (Western Mediterr.)	Oct 82	70	17	<1	13	3600
New England Coast (within 300 km offshore)	May 77	92	3	2	2	150
Gulf of Mexico						
Marine air (20 km offshore)	Nov 78	81	2	14	3	240
Continental air (20 km offshore)	Nov 78	28	34	27	11	280
Coast of South California (within 150 km offshore)	May 78	16	24	39	21	1350
Mid-Atlantic (40-45°N.Lat)	May 77	78	8	12	2	300
Cape Cod (12 km inland at Otis AFB)	Jul 80	17	16	21	46	360
Cape Cod (12 km inland at Otis AFB)	Jun 82	61	22	1	17	350
Coastal Cape Cod (Woods Hole)	Jun 82	60	31	<1	8	300
Meppen, West Germany (∿80km inland)	Nov 80	16	47	1	36	675
Coastal Maine (∿2km inland at Corea)	Jul 81	74	8	4	14	500
Coastal Florida (∿5km inland at Valkaria)	Jul 82	23	18	<1	58	1150

In immediate coastal areas total particle concentrations (Aitken nuclei) are of the order of 10^4 cm^{-3}, while number concentrations at sizes >0.1 μm and >1.0 μm diameter are typically $\sim 10^3$ and 1 cm^{-3}, respectively. Dramatic fluctuations in the aerosol population (including up to several orders of magntiude in number concentration) occur diurnally as a result of at least four diurnal cycles: photochemical gas-to-particle conversion processes, industrial and other anthropogenic activity, and land/sea breeze and relative humidity cycles. At mid-day concentrations of small particles <0.1 μm diameter peak due to photochemical processes and anthropogenic activity, while concentrations of larger particles reach minima as a result of daytime heating and relative humidity minima. With the onset of the afternoon sea breeze and influx of fresh 'marine' air, small-particle concentrations rapidly decrease and concentrations of larger particles (>0.1 μm diameter) begin to increase. Large-particle concentrations reach maxima during noctural hours, coincident with maxima in relative humidity. Independent of changes in the large particle spectrum due to deliquescence effects, wind shifts produce local changes in aerosol chemistry related to sources and source regions, air mass characteristics, and anthropogenic activities. As a result of the combined effects of these processes in coastal regions, particle concentrations at opposite ends of the size spectrum can fluctuate simultaneously in opposite directions, while aerosol composition can fluctuate independently of number concentration.

Our prior measurements demonstrated that continental/anthropogenic effects can extend to distances $>10^3$ kilometers to sea. It is not unexpected, therefore, that aerosol data obtained on the 150 km wide (north to south) Alboran Sea reflect the proximity of two continents. With continental influences superimposed on Atlantic airmasses which typified the observation period, the 'average' aerosol population on the Alboran is generalized as follows: moderate concentrations (1500-10000 cm^{-3}) of small particulates (<0.1 μm dia) fluctuating by a factor of ∿50 with a tendency to peak at mid-day; and moderate concentrations (2-20 cm^{-3}) of larger particles (>0.3 μm) with a tendency to minima at mid-day; aerosol composition was dominated by sea salt (averaged 70% of the aerosols >0.2μm dia during the 10 day cruise) with an occasional fluctuation to higher proportions of silicates or sulfates.

The averaged Alboran data are compared with data obtained at other maritime locales in Tables 2 and 3. Inspection of the Tables reveals that total aerosol concentrations on the Alboran were not as high as have been observed on shore nor as low as observed at remote mid-ocean locations. Further, while the NaCℓ (sea salt) fraction appears unusually high, silicate and other salts were found in higher proportions than observed in more remote marine locales. Thus, it is readily apparent that the general character of the Alboran aerosol population is comparable to that observed at other offshore coastal locations.

2.1.3 Summary of the Alboran Data Set

The period 9-18 October 1982 on the Alboran was a meteorologically active period, with a succession of upper-level troughs and surface fronts producing considerable cloud cover, alternating periods of strong and light winds, whitecapping and calm seas. Daylight winds were generally from within the direction 230°-300°, bringing Atlantic air of various continental exposure to the Alboran. Cloud-free skys (<0.2 cloud cover) were observed during daylight on only 3.5 days. Meteorological information and the data sets for each day are summarized in Table 4.*

The various data** collected by Calspan are plotted for the entire 10-day cruise in Figures 2-5 to illustrate daily and day-to-day fluctuations.*** Figure 2 presents time histories of air temperature, relative humidity, wind speed and direction, and visibility. Figure 3 presents optical depth, scattering coefficient and aerosol cross-section data. Figure 4 provides time histories of aerosol concentration at four size ranges:

---

* Boundary layer depth estimates were derived from mini-sonde data obtained from aboard the BARTLETT by R. Sylvia, CSI-LSU.

** Numerical values for the data set are provided in Appendix A.

*** Throughout this report all references to time are GMT; on data plots, dates are labelled at the 0000 hour.

TABLE 4. SYNOPSIS OF METEOROLOGICAL CIRCUMSTANCES AND SUMMARY OF THE DATA SET AT BARTLETT'S LOCATION

DAY	CHARACTER OF DAY AT BARTLETT'S LOCATION	Hourly Observations Interval (GMT)	Average total Particle conc. (#/cc)	Avg. conc. Aerosols >0.3μm dia. (#/cc)	Average SEA SALT Fraction >0.2μm (%)	Bndy. Layer Depth at Mid-Day (m)	Optical Depth at Mid-Day
9 Oct	Near overcast dense cloud cover most of day, associated with a pre-frontal trough, with WNW-WSW winds of 3-10 m/s; RH remained in 75-81% range, while northward movement of the trough and a ridge building from the Atlantic improved visibilities from 20 to 60 km.	0700-1900	4000	6.5	75	2750	-
10 Oct	Totally sunny day with exception of some fair wx cu over land; westerly winds of ∿5 m/s increased to >10 m/s in PM, producing lots of whitecaps; visibility fluctuated in 40-65 km range, while RH of ∿90% in AM dropped to <70% in late PM.	0600-2200	7600	6.0	57	1500	0.10
11 Oct	Totally sunny day, with exception of thin Ci veil during 1630-1800; winds were near calm and no whitecaps were observed; visibility was in 50-65 km range & RH was ∿70% most of day; visibility dropped to ∿22 km in lt haze as RH increased to >80% after 1700 GMT.	0600-1900	2300	5.0	72	1130	0.12
12 Oct	Increasing thin Ci cloud cover during AM (7/10 by 1100) and ∿8/10 overcast in PM; winds were lt to calm and no whitecaps were seen; visibility was ∿42 km, and RH ranged from 72 to 85%. In advance of an approaching front, winds picked-up from W late in day.	0600-1820	3500	7.0	22	100	0.21 (Thru Ci)
13 Oct	Skies cleared from 9/10 Ci cloud cover to <1/10 by 1330; westerly winds picked-up to >13 m/s by 0830, peaking at >18 m/s in late afternoon and producing considerable whitecapping all day. Through the day, RH dropped from 80 to 70%, and visibility improved from 35 to >50 km.	0600-1845	5400	10.5	68	150	0.12
14 Oct	After mid-morning frontal passage, visibility increased from 50 to ∿80 km as RH dropped from 85 to ∿60%, winds dropped from 14 to 5 m/s and shifted from ∿275° to 240°, and overcast skies briefly cleared to ∿8/10 in mid-afternoon. Moderate whitecapping of morning gave way to only occasional whitecaps by 1700.	0600-1900	7700	7.0	92	1035	-
15 Oct	An upper-level trough caused an increase in cloud cover from 2/10 at 0600 to 9/10 in Ci by 1200 and for the remainder of the day; winds were lt at <4 m/s from WSW-WNW. Visibilities were typically 50-60 km thru the day, but RH dropped from >80% in AM to <70% in late afternoon.	0600-1800	4600	6.5	90	1330	0.22 (Thru Ci)
16 Oct	Skies mostly clear thru day with ∿1/10 Ci; winds were <3 m/s until late afternoon when speeds picked-up. Visibility remained in 29-38 km range, and RH fluctuated 77-82% throughout the day.	0600-1800	4300	10.0	48	2010	0.20
17 Oct	Skies remained nearly overcast with middle & high cloud and imbedded showers & thunderstorms; lt precip observed at ∿1500. Winds turned into SW at ∿5 m/s after 1000. RH dropped from ∿87% in AM to ∿83% in PM; visibility lowered to ∿35 km for the afternoon.	0600-1800	3700	8.0	98	1710	-
18 Oct	Near overcast skies with middle cloud, nimbostratus and showers (0845-1100) gave way to gusty NW wind, cooler & much drier air and clearing skies (2/10 by 1500) after a strong, mid-morning frontal passage; moderate whitecaps began forming after 1330. Late afternoon, visibility improved to ∿80 km as RH dropped to <60%.	0600-2100	7800	5.5	99	1920	-

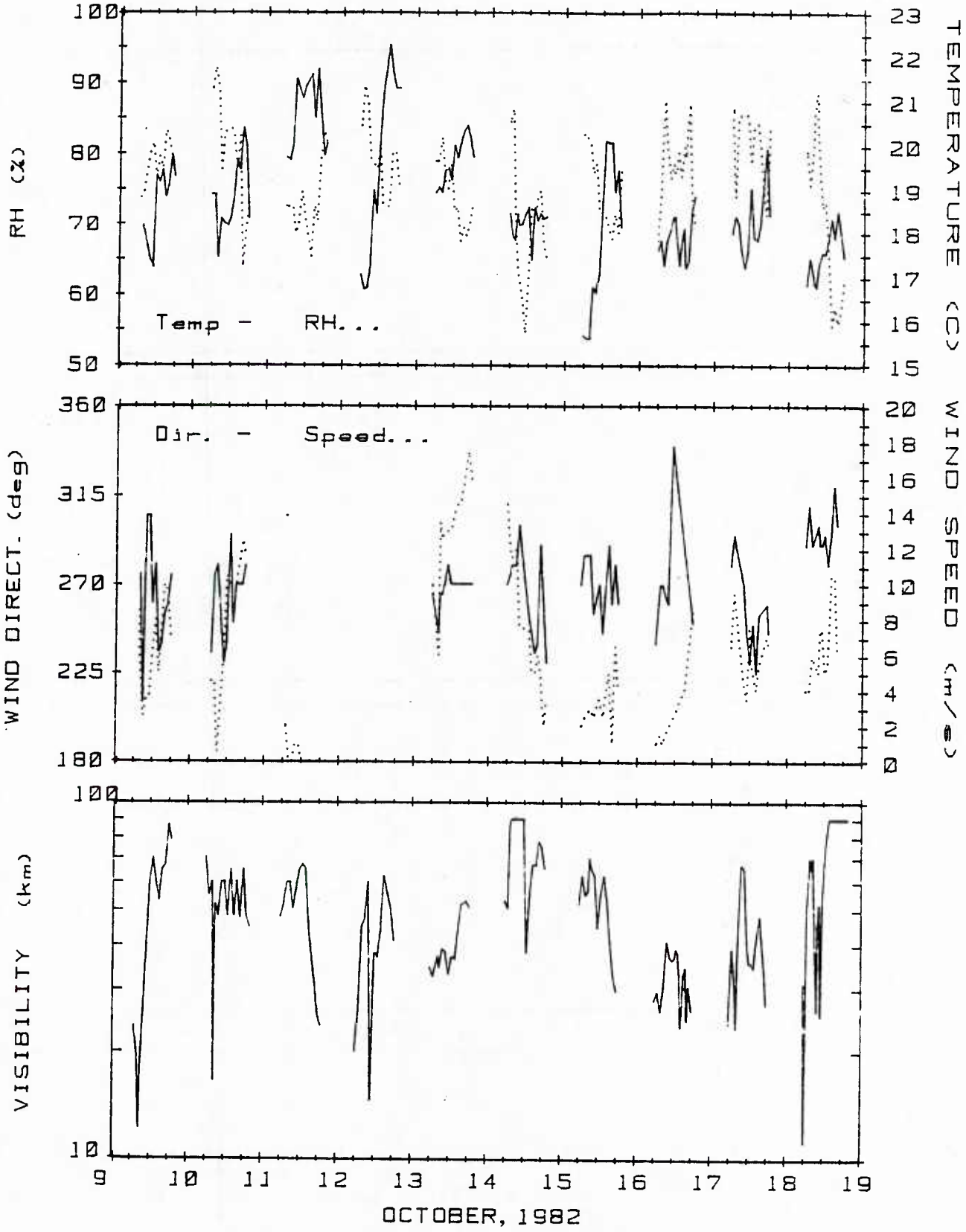

Figure 2. Meteorological Parameters as Functions of Time, Measured from Aboard the USNS BARTLETT on the Alboran Sea, 9-18 October 1982.

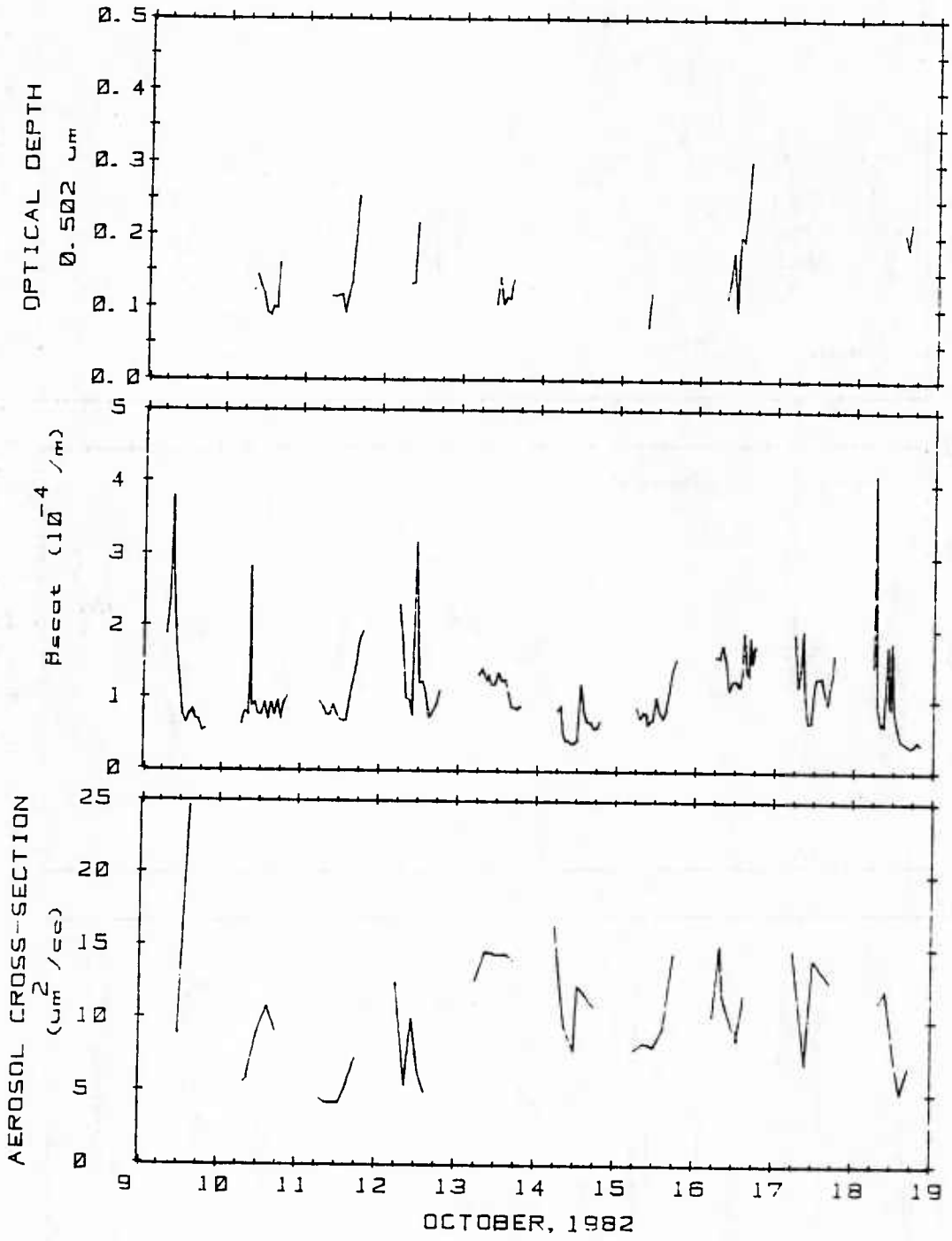

Figure 3. Optical Depth, Scattering Coefficient and Aerosol Cross-Section as Functions of Time, Measured from Aboard the USNS BARTLETT on the Alboran Sea, 9-18 October 1982.

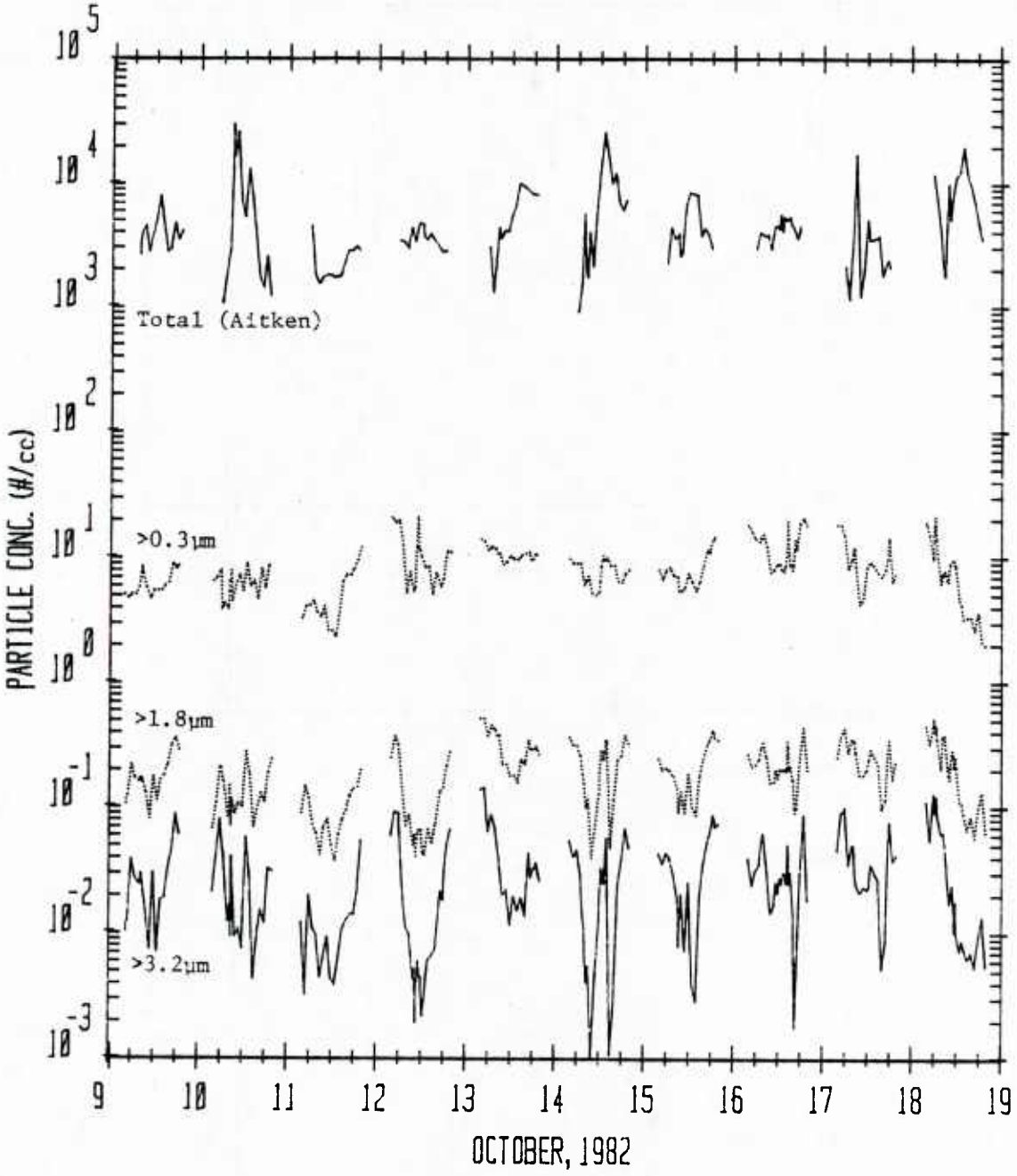

Figure 4. Aerosol Number Concentrations at Four Size (diameter) Intervals as Functions of Time, Measured from Aboard the USNS BARTLETT on the Alboran Sea, 9-18 October 1982.

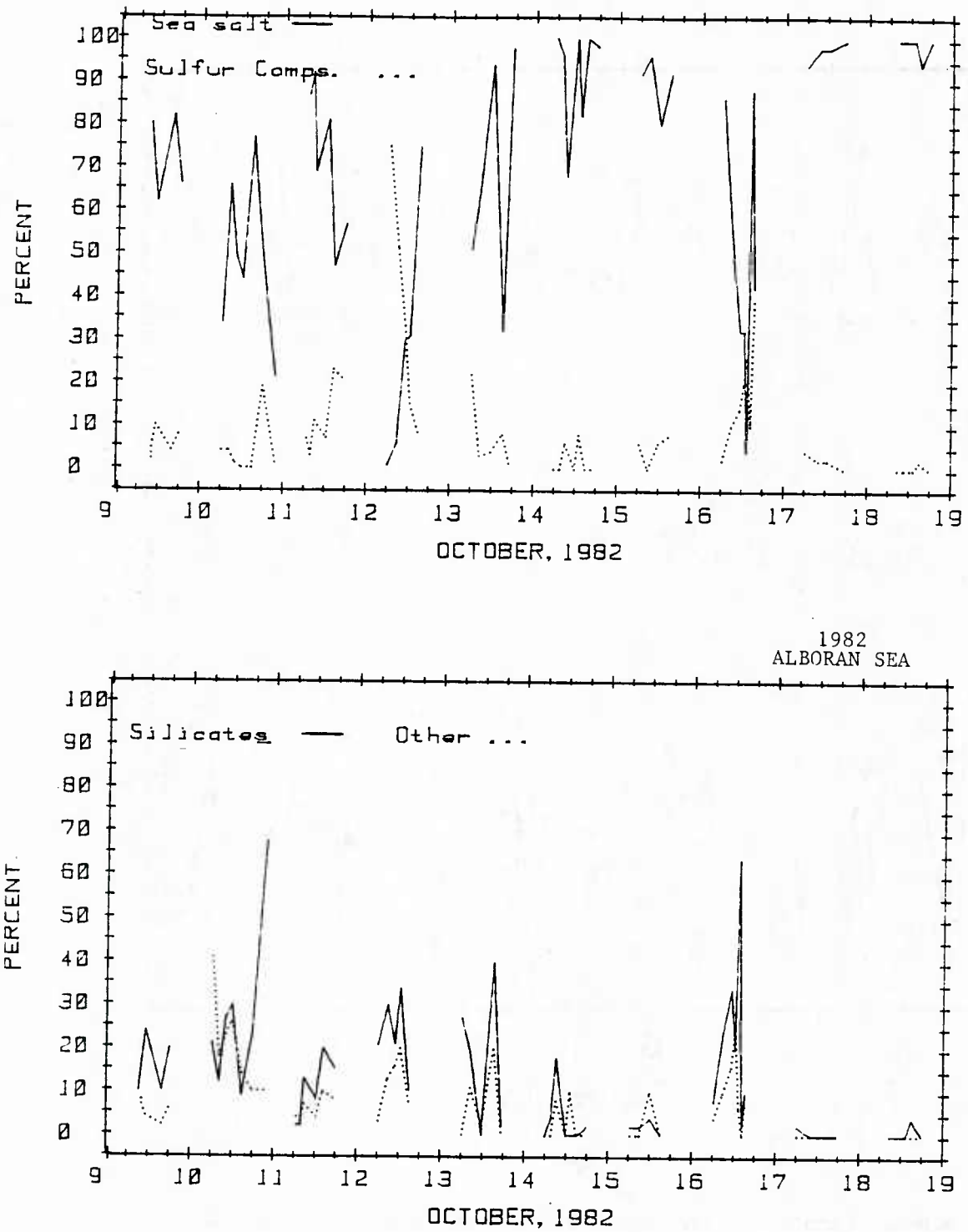

Figure 5. Percentage of Aerosols >0.2μm dia by Compositional Classification as a Function of Time, Measured from Aboard the USNS BARTLETT on the Alboran Sea, 9-18 October 1982.

>0.003 μm (Total or Aitken nuclei), >0.32 μm, >1.8 μm and >3.2 μm diameter. The proportions of the aerosol population at sizes >0.2 μm which comprised NaCℓ (sea salt), sulfur compounds, silicates, or other minerals, salts and organics are presented in Figure 5. The instrumentation, analyses techniques and other aspects relating to gathering and reducing these data are discussed in Appendices A & B.

The data presented in Table 4 and Figures 2-5 and overall conclusions drawn from analyses presented in Appendix B may be summarized in the context of ship's position (Figure 1), meteorological events and diurnal cycles as follows:

- Concentrations of small particles (Aitken nuclei) in general, exhibited daytime maxima and diurnal fluctuations of approximately one to two orders of magnitude, both characteristics probably associated with photochemical processes and anthropogenic activity.

- Total particle concentration averaged 6000 cm^{-3} within 35 km of the shoreline and 4000 cm^{-3} in areas outside of the 35 km distance, probably reflecting the respective distances from their continental sources.

- The highest total particle concentrations were observed on 10, 14 and 18 October when the ship was closest (for the longest periods) to the northern shore (and industrial sources in the vicinity of Gibraltar) and over the cold water of the Gyre.

- Lowest total particle concentrations (and lowest concentrations of aerosols at sizes >0.3 μm diameter) were measured on 11 October under nearly calm wind conditions when the ship was over the warm core of the Gyre.

- Concentrations of large particles were slightly greater farther from the coastline, averaging 8.0 cm^{-3} and 7.2 cm^{-3} at sizes >0.3 μm for mid-Alboran and coastal locales, respectively.

- In general, daytime warming gave rise to daytime minima in relative humidity, and consequent drying of aerosols produced daytime minima in concentrations at large particle sizes and daytime maxima in visibility.

- Maximum concentrations of the larger particles were observed on 13 October (when maximum wind speeds for the period were measured) and on 16 October; high concentrations observed on 16 and 17 October (and early on the 18th) were probably a result of local contamination of the area by aerosol sources in the vicinity of Gibraltar.

- Minimum average daytime visibilities occurred on 16 October and 13 October as a direct result of the high concentrations of aerosols near 0.3 μm diameter.

- A large proportion of the aerosol populations at sizes >0.2 μm diameter comprised sea salt (or NaCℓ), particularly during the period 14-18 October when the ship was in the immediate vicinity and downwind of the Gibraltar area. High winds and whitecapping such as occurred during mid-afternoon on 10 October, late afternoon on 12 October, on 13 October, on the morning of 14 October and on the afternoon of 18 October probably resulted in the higher sea salt proportions observed at those times. However, on several occasions, aerosol 'plumes' were observed to comprise NaCℓ particles, and it is suspected that local sources of NaCℓ particles--either industrial or surf-generated in the Strait--were responsible for general 'contamination' of the northwest corner of the Alboran between Gibraltar and Malaga.

- Low-level inversions at mid-day capped surface boundary layers at heights of <150m on 12, 13, 14, 16 and 17 October, and these shallow surface layers were generally associated with the colder water on the north side of the Alboran Front. It is speculated that the presence of a stable boundary layer in the northern portion of the Alboran probably helped to trap aerosol plumes emanating from the Gibraltar area. Predominantly westerly winds then advected such aerosol material parallel to- and directly over the isotherms of the Alboran Front, giving rise to the observed 'contamination' in the NW Alboran and the coincidence of aerosol 'plumes' over the Alboran Front.

- Optical depth data obtained for correlation with surface-level parameters, are considered valid for that purpose only for 10, 11, 13 and 16 October, due to intervening cloud cover on other days. Data shown for 12 and 15 October were obtained through nearly overcast thin cirrus. The mean mid-day optical depth data for 10, 11, 13 and 16 October were found to be correlated with surface-level scattering coefficient (extinction or visibility) integrated as a function of relative humidity through the boundary layer, assuming well-mixed conditions with respect to aerosols (see Section 2.2). It is concluded that the well-mixed assumption is valid and that most of the atmospheric aerosol optical depth (in the absence of cloud) occurs in the planetary boundary layer.

- The scope of the observation effort purposely precluded definitive measurement of the aerosol size spectrum at sizes <0.3μm diameter (except for Aitken nuclei) because in more remote marine locales the small particle population contributes only a small fraction of the total scattering cross-section (Ref. 11). However, the Aitken particle concentrations observed in the highly polluted air on the Alboran and extrapolation of Royco size spectra (Appendix B-2) to sizes <0.3μm suggested that aerosol concentrations at optically effective sizes <0.3μm were much greater than anticipated--perhaps, at sizes of ∿0.1μm diameter, as much as two orders of magnitude greater than concentrations at 0.3 μm diameter. Mie calculations (Appendix B-3) of extinction

for the portion of the size spectrum >0.3μm, show that these larger particles can account for only 25-75% of the measured extinction. If particle concentrations at 0.1 μm were ∿100X greater than those >0.3 μm diameter, the extinction attributable to these particles would be sufficient to account for the differences in measured and calculated extinction. Thus, it is concluded that high concentrations of particles <0.3μm diameter, which were purposely not measured, accounted for a significant fraction (∿25-75%) of the measured extinction on the Alboran Sea.

2.2 A Relationship Between Optical Depth and Surface-level Visibility

During the Alboran Sea Experiment, sun photometry* data were collected at hourly intervals, regardless of cloud cover except during periods of thick overcast. The data are listed in the "log" reproduced in Appendix A. Aerosol optical depth was then computed from these data for a 5 nm wide band centered at 0.502μm wavelength (see Appendix B-1) for correlation with surface-level visibility (or scattering coefficient). Scattering coefficient (β_{scat})** was measured directly (centered at 0.475μm wavelength) and visibility (V) calculated according to

$$V = \frac{4.605}{\beta_{scat}} .$$

Previously, a β_{scat} and sun photometry data set was acquired at Valkaria, Florida, an Atlantic coastal site (Ref. 16). When plotted against aerosol optical depth, β_{scat} was generally found to increase as optical depth increased in the Florida data. When data from the Alboran Sea were added to the plot, the same general trend was suggested but two distinct relationships were indicated. These data are plotted in Figure 6. In the Figure, individual hourly data points are indicated by the small symbols, while the averages of each of four day's data for each site are represented by the large circles. (The mid-day data were averaged in order to filter-out scatter due to local aerosol sources, passing clouds or measurement error and to provide a single value for correlation with meteorological-scale variables.) Note in Figure 6 (a and b) that the two data sets appear offset: i.e., for a given surface-level visibility or scattering coefficient, greater optical depth (by a factor of 2 to 3) was observed in the Florida situation.

---

* Details of instrumentation may be found in Appendix A.

** An MRI Integrating Nephelometer was used to measure scattering coefficient (β_{scat}). In the absence of absorption at visible wavelengths, we equate β_{scat} to extinction coefficient and use the terms interchangeably.

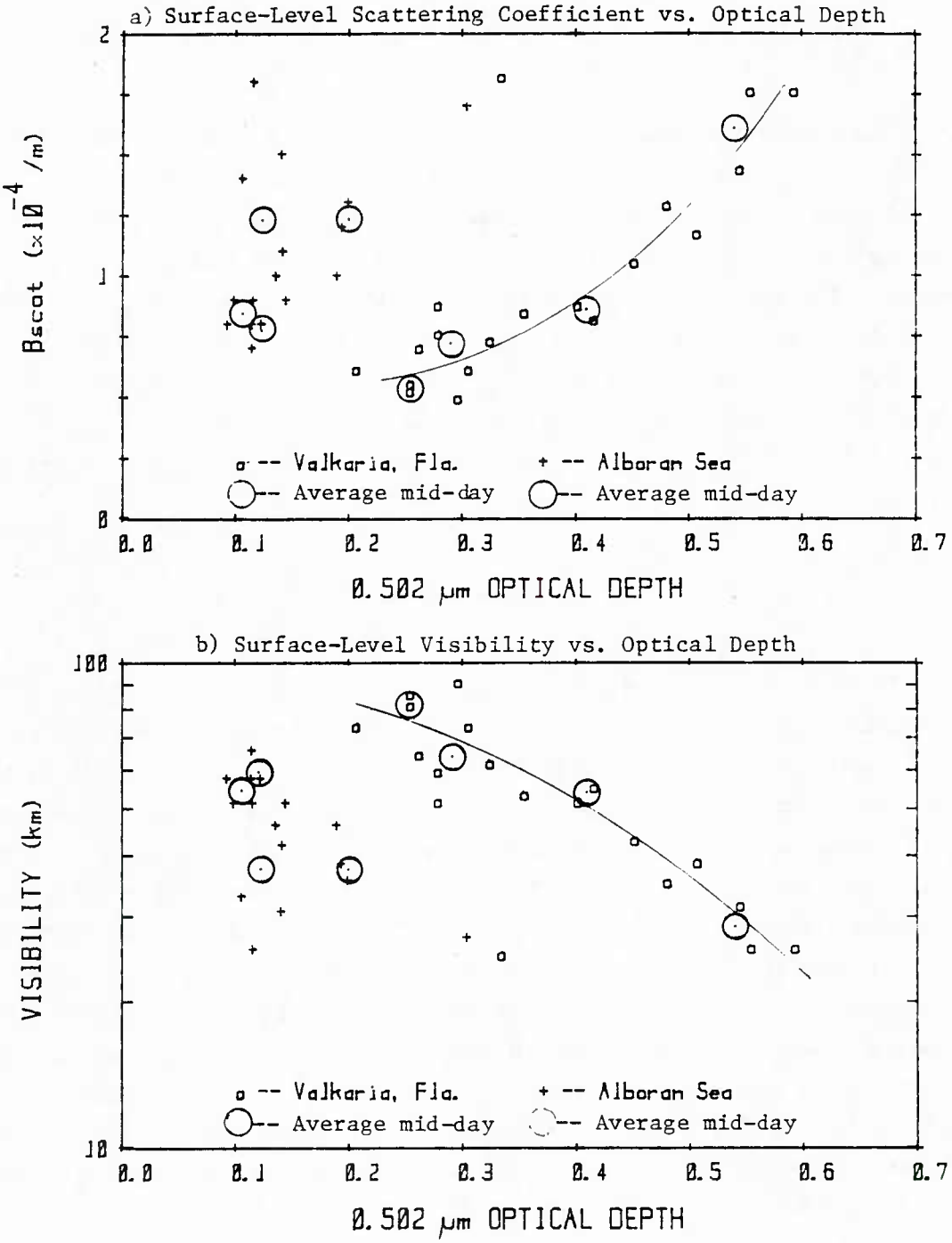

Figure 6. Aerosol Optical Depth for Two Sites as Functions of a) Scattering Coefficient and b) Visibility Measured at the Surface

The above result should not be surprising since the Florida data were obtained at a subtropical location in mid-summer while the Alboran data were acquired at a more northerly latitude in the Fall. The meteorological circumstances and, in particular, boundary layer characteristics would be expected to differ between the two regimes. Further, surface-level measurements would be more or less representative of the atmosphere through which optical depth measurements were obtained depending on the depth of the planetary boundary layer.

In an attempt to merge the two data sets, the mean mid-day data were normalized to account for day to day differences in boundary layer depth and humidity structure. The mean data (optical depth, surface relative humidity, scattering/extinction coefficient and boundary layer depth) for the indicated hours and dates at the Alboran and Florida sites are tabulated in Table 5. Assuming a well-mixed boundary layer with respect to aerosol, aerosol β (not including molecular scattering) within the boundary layer was computed by relating vertical variation in β to vertical variation in relative humidity, according to the relation suggested by Hanel (Reference 17):

$$\frac{\beta_{sfc}}{\beta_z} = \left(\frac{(1 - f_z)}{(1-f_{sfc})}\right)^{2\varepsilon^*}$$

in which f is relative humidity and β is aerosol extinction coefficient; and ε^* is a function of the aerosol type, which takes on the value of 0.26 for the maritime aerosol assumed here. The surface value of β was obtained by subtracting the atmospheric molecular scattering ($0.23 \times 10^{-4} m^{-1}$) from the surface measured β_{scat} value. For the Alboran data, the relative humidity profile was obtained from the LSU radiosonde data; for the Valkaria, Florida data set, the Waycross, GA radiosonde profiles were used. The top of the boundary layer was determined independently from the radiosonde data using meteorological

TABLE 5

Average Optical Depth, Extinction and Boundary Layer Data for Each of Four Days on the Alboran Sea (October 1982) and Valkaria, Florida (July 1982)

ALBORAN DATA

Date	Time of Day (GMT)	Measured Average Optical Depth	Surface-Level Average (measured) Relative Humidity (%)	Surface-Level Average (measured) Scattering Coefficient ($\times 10^{-4} m^{-1}$)	(β_{mean}) Estimated Mean Boundary Layer Aerosol Scattering Coefficient ($\times 10^{-4} m^{-1}$)	Measured Boundary Layer Depth (m)	Calculated Integrated Boundary Layer Extinction (O.D.)
10 Oct.	10-15	0.10	82	0.85	0.43	1500	0.07
11 Oct.	10-14	0.12	70	0.78	0.58	1130	0.07
13 Oct.	11-15	0.12	71	1.23	0.96	150	0.01
16 Oct.	10-14	0.20	79	1.23	0.94	2010	0.19

FLORIDA DATA

	(EDT)						
26 Jul.	12-14	0.54	67	1.61	1.20	5180	0.62
27 Jul	9-11	0.41	73	0.97	1.01	4000	0.40
28 Jul.	10-12	0.25	64	0.56	0.68	4440	0.30
29 Jul.	10-11	0.29	72	0.73	0.87	3130	0.27

judgment and a combination of height of the features: inversion, isothermal layer, boundary between layers of different wind directions and rapid decreases in relative humidity. The estimated mean boundary-layer scattering coefficients (β_{mean}) were determined as functions of the RH profile from Hanel's relationship and tabulated in Table 5. These mean boundary layer extinction data were then multiplied by boundary layer depth to provide a dimensionless integrated extinction parameter for the boundary layer, a quasi-optical-depth, tabulated in the right-hand column in Table 5.

The integrated extinction parameters determined for each of 4 days for the two data sets are plotted in Figure 7. The two data sets now lie on the same line with the Alboran data at small values and the Florida data at large values. Since the range of surface β_{scat} is essentially the same in both data sets, the distribution of the normalized data primarily represents the difference in boundary layer depths.

The relationship shown in Figure 7 may be applicable to the estimation of surface β_{scat} or visibility from satellite radiance measurements. Given a relationship between measured radiance and aerosol optical depth, then with an estimate of the boundary layer depth, the mean boundary layer aerosol scattering coefficient (β_{mean}) could be obtained. Assuming that the surface aerosol $\beta_{scat} = \beta_{mean}$, the surface visibility could then be computed from

$$V = \frac{4.605}{(\beta_{mean} + 0.23)}$$

where the atmospheric molecular scattering has been added and the constant for the MRI nephelometer, 4.605, is used to convert β_{scat} to visual range. Of course, relative humidity profile information would help provide better definition of surface-level visibility through use of the Hanel equation.

The foregoing analysis is based on a very limited data set. Additional observations at other locations and for other meteorological scenarios are required to substantiate the relationship.

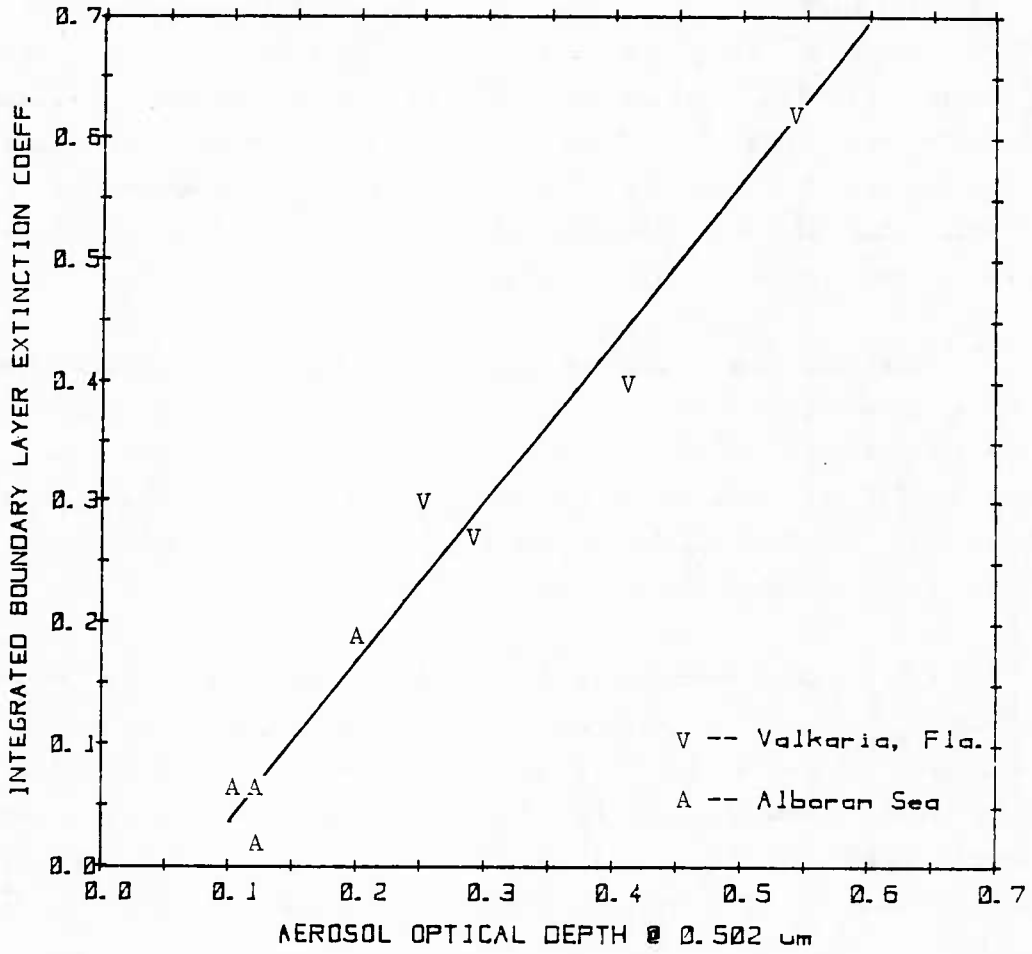

Figure 7. Integrated Boundary Layer Extinction Coefficient, Derived from Surface-Level Aerosol Extinction (at .474μmλ) and Vertical Profile of Relative Humidity Within the Boundary Layer, vs. Surface Measured Total Atmospheric Aerosol Optical Depth at 0.502μmλ.

Section 3

INTERPRETATION OF INDIVIDUAL DAILY DATA SETS

Instrumentation set-up was begun on the morning of 8 October 1982, and initial measurements were obtained by 2000 GMT while in port at Malaga, Spain. The BARTLETT was underway by 2215, passing through the harbor entrance by 2240 GMT on 8 October. Continuous measurements of visibility and particle concentrations at sizes >0.3 μm were obtained thereafter until the ship departed the Port of Tangiers at 0005, 19 October. Manual observations were obtained hourly each day, during the period ∿0600 to ∿1900 GMT and occasionally later into the evening hours. The approximate track of the BARTLETT during the 10-day cruise is plotted in Figure 8a-d.

The following provides a detailed summary of daily cruise activities, the meteorologic/geographic scenario, events, observations and measurements aboard the BARTLETT, principally for daylight hours. For each day, plots of meteorological variables, optical depth, scattering coefficient, aerosol concentrations and aerosol composition are provided for reference and interpretation in the context of the environmental scenario. Discussion of weather patterns was derived from synoptic analyses supplied by R. Fett (NEPRF) and by personnel of the Buffalo Office of the National Weather Service. Boundary layer information was derived from minisonde soundings obtained by R. Sylvia (Coastal Studies Institute, LSU) from aboard the BARTLETT and from the Gibraltar soundings. This information was condensed to provide the summaries presented in Figure 1 and Table 4. In the following narrative, reference to Figures 1 and 8, Table 4, and to the Logs and reduced data in Appendices A & B is suggested for additional detail. The reader is cautioned that much of the discussion presented herein is without benefit of quantitative sea surface temperature data or overflight imagery.

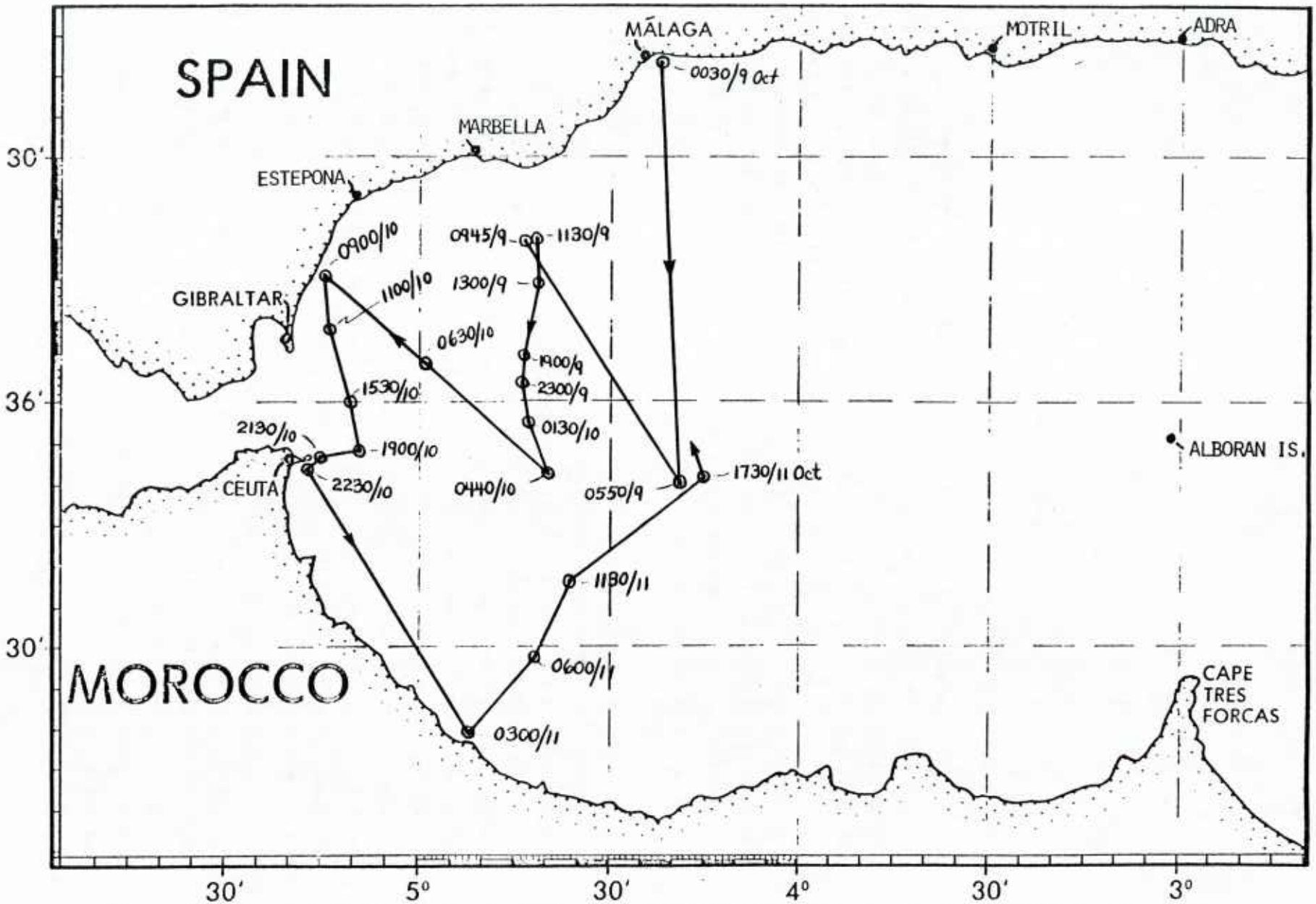

Figure 8a. Approximate Cruise Track of the USNS BARTLETT, 0030 9 October to 1730 GMT 11 October 1982.

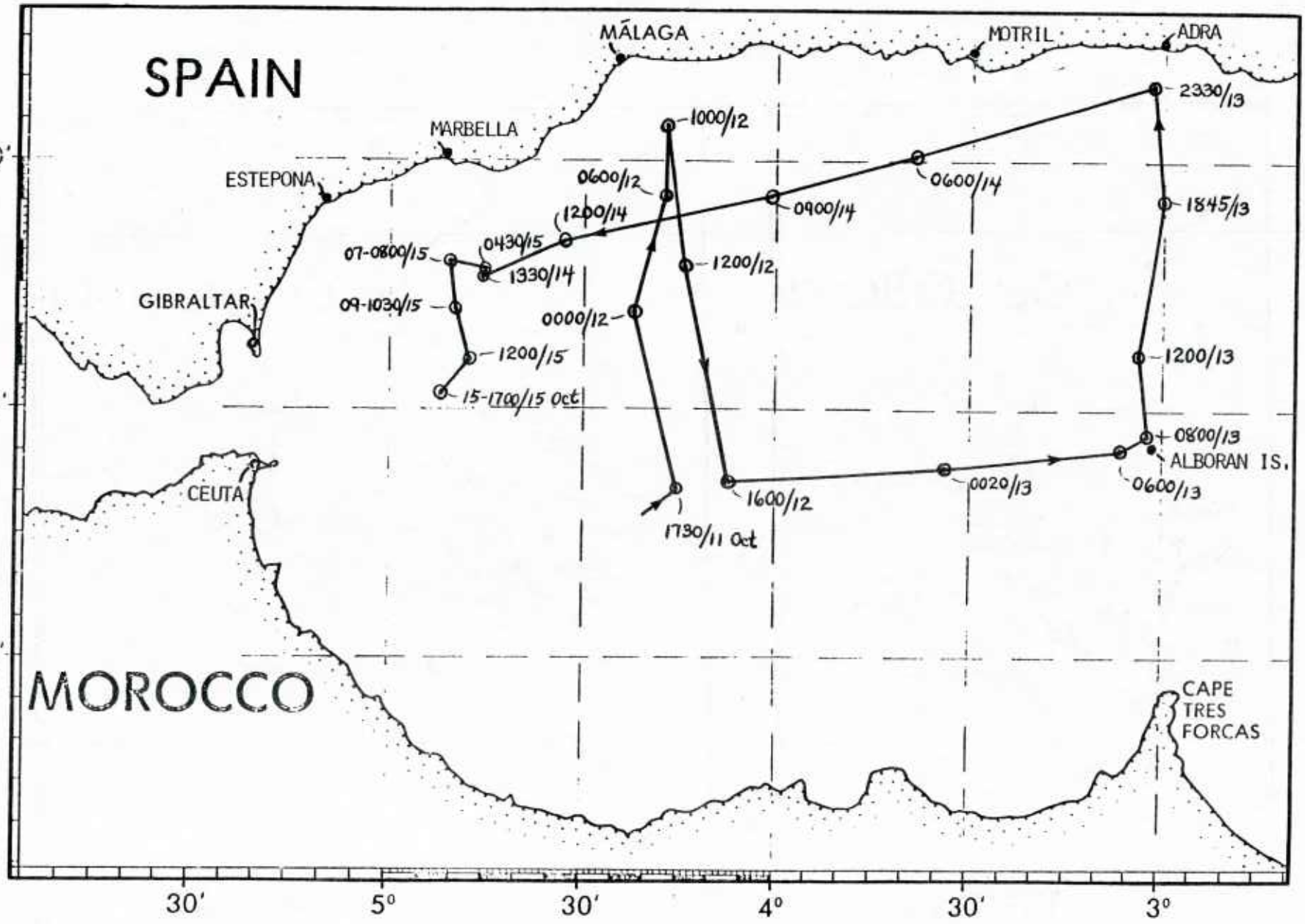

Figure 8b. Approximate Cruise Track of the USNS BARTLETT, 1730 11 October to 1700 GMT 15 October 1982.

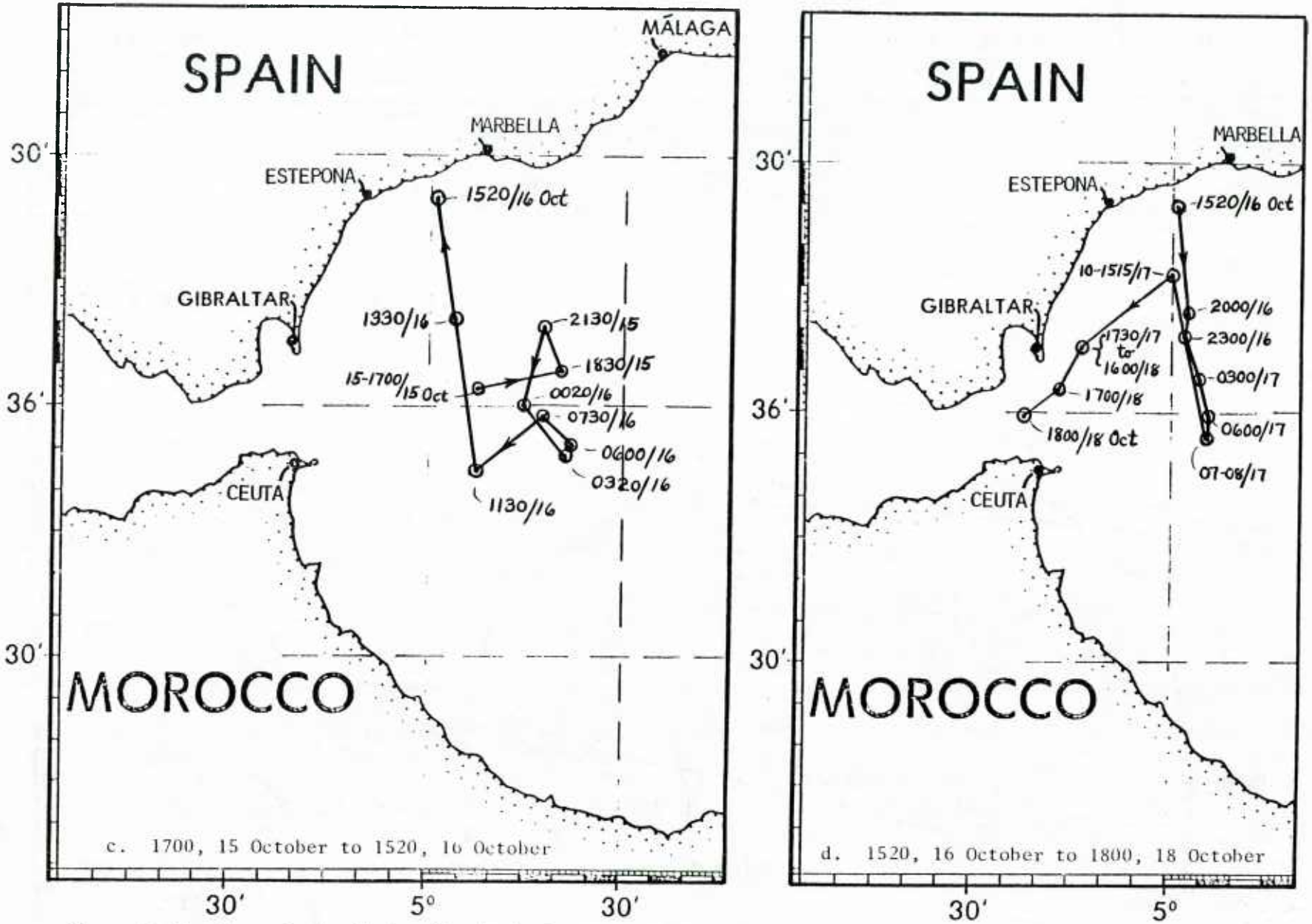

Figure 8c&d. Approximate Cruise Track of the USNS BARTLETT, 1700 15 October to 1800 GMT 18 October 1982.

3.1 9 October 1982

Summary After departing Malaga late on 8 October, the BARTLETT reached the southern end of the Malaga line (approximately mid-way across the Alboran) by dawn. During daylight hours, the ship cruised northwesterly from the southern end of the Malaga line to a point along the Marbella line ∿17 km offshore and then southward to 45 km offshore. (See Figure 8a). Skys were near overcast most of the day with visibilities improving from 20 to 60 km after ∿1100 GMT. Winds were from WNW-WSW, averaging ∿ 8 m/s in the afternoon, and RH remained in the 75-81% range for the entire day. A plume which reduced visibility to ∿12 km was encountered at ∿ 0845 GMT. Sun photometry data were not obtained this day due to dense cloud cover. Data for 9 October are plotted in Figures 9-12.

Lower air temperature at the northern end of the track may be a result of cold water on northern side of the Alboran Gyre. The aerosol plume was also found over the cold water.

Meteorology A NE-SW oriented trough over the Alboran at dawn weakened and moved to the north shore by mid-day as ridging from the Atlantic built-in over the southern portion of the Alboran. By 1800 GMT, the trough deepened over the northern shore in advance of a weak cold front and an upper-level trough. While the upper-level trough produced nearly overcast skys of thick alto stratus, the ridging at mid-day caused winds to decrease to 3-4 m/sec; air temperature increased by ∿2C and visibility improved to >60 km; wind speeds increased to 10 m/s in late afternoon as the trough deepened. (See Figures 9 and 10.)

The lower air temperature on the northern portion of the track (0900-1100) may be a result of cold water in the northern half of the Gyre. However it cannot be determined whether the increase in visibility and temperature by mid-day and afterwards is due to sea surface temperature effects, mid-day warming or changes in the meteorological pattern.

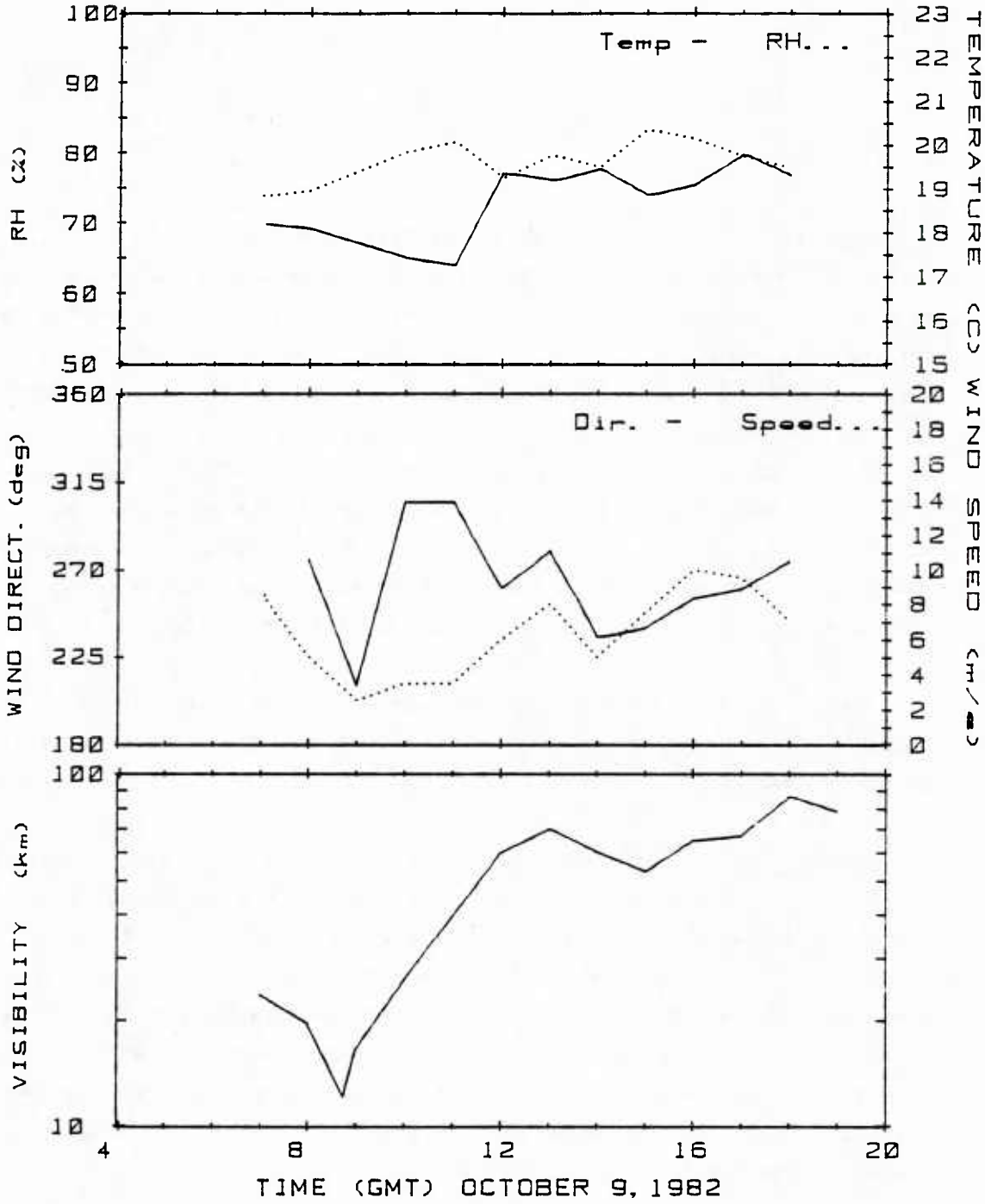

Figure 9: Meteorological Parameters, 9 October 1982

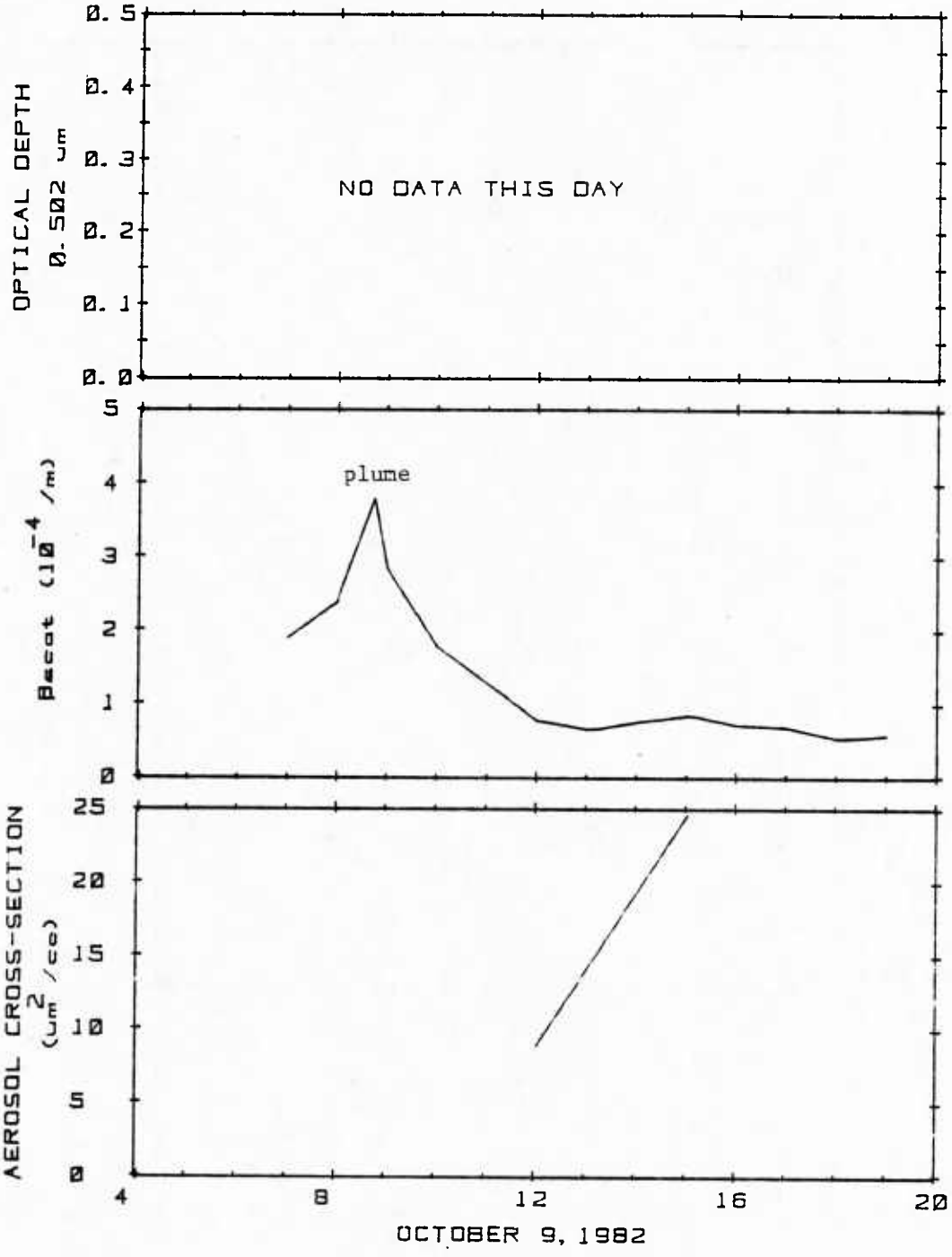

Figure 10 Optical Depth, β_{scat} and Aerosol Cross-section, 9 October 1982

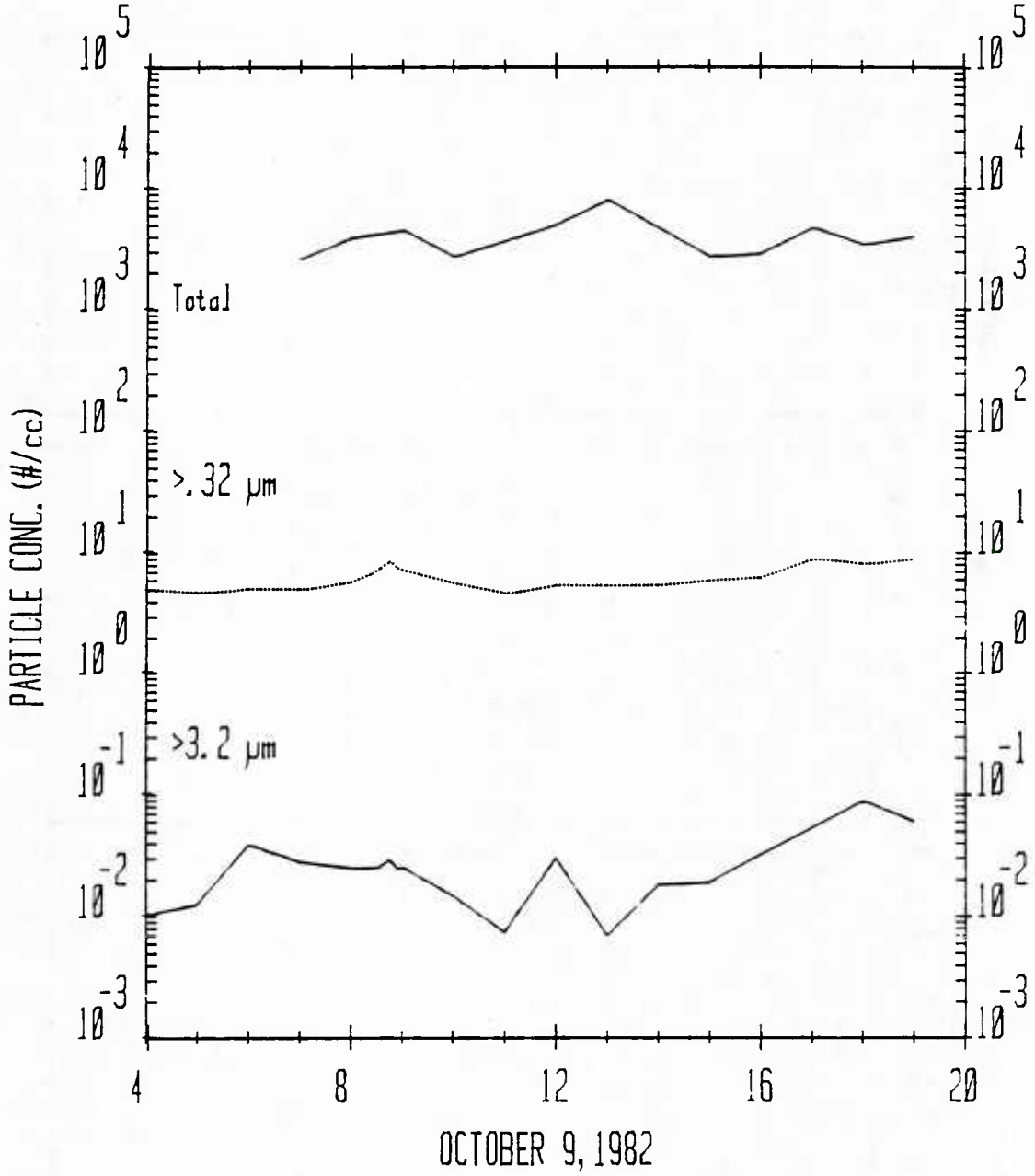

Figure 11: Aerosol Concentrations at Three Size Intervals, 9 October 1982

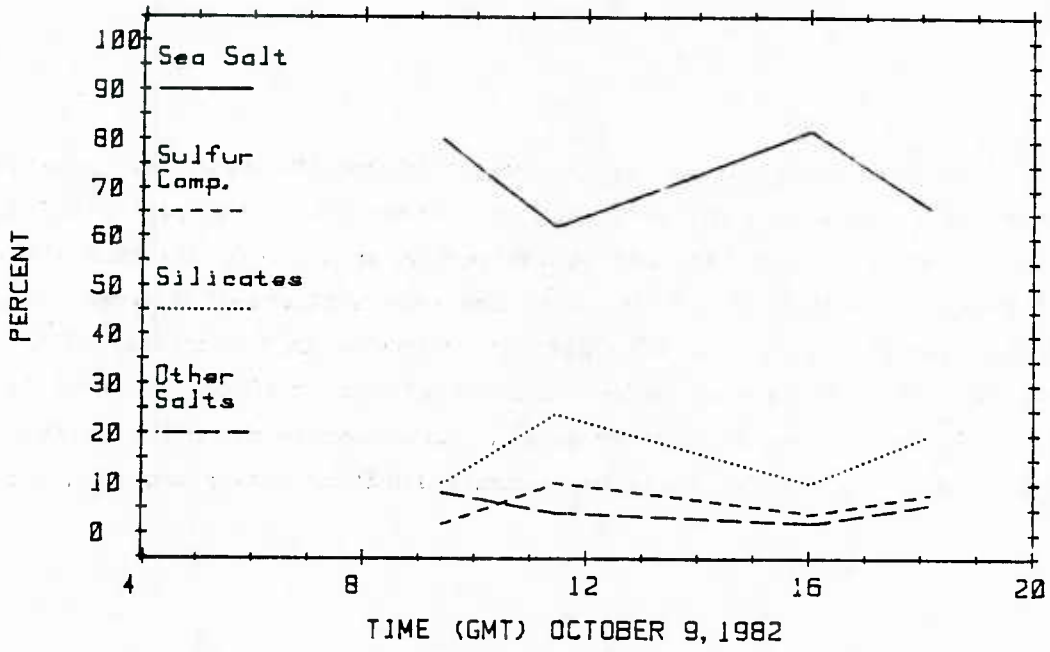

Figure 12: Chemical Classification of Aerosols >0.2μm dia, 9 October 1982

The plume encountered at ∿0845, evidenced by the visibility and scattering coefficient data, occurred without change in humidity. The plume appeared to lie along the boundary of the Alboran Front on the cold water side. Wind direction at the time of the plume encounter suggests that the plume came from the Gibraltar area.

Aerosols Figures 11 and 12 present the aerosol concentration and composition data for 9 October. Figure 11 shows aerosol concentration for three size intervals: Total (Aitken), >0.32 μm and >3.2 μm diameter. Note that total particle concentrations reached maxima at mid-day and nearer the shore at 0900-1300 GMT; while concentrations at size >0.3 μm generally increased throughout the day with a peak in the plume at 0845 GMT and a slight minimum at mid-day. The largest particles (>3.2 μm) also exhibited minima at mid-day.

Aerosol classification by chemistry (Figure 12) shows fairly uniform composition throughout the day, with an average 75% of the particles >0.2 μm diameter being NaCℓ and apparently reflecting an Atlantic air mass source for these aerosols; 15% of the particles were silicates. However, the aerosol sample acquired at ∿0920, perhaps obtained in the fringes of the plume, shows a high proportion of NaCl--a characteristic of plumes observed later in the study (see 10 and 16 October data); the extent to which the entire area of this day's track might be 'contaminated' by this plume is unknown.

3.2 10 October 1982

Summary During the morning hours, the BARTLETT cruised NW from near the southern end of the Marbella line to the north end of the Gibraltar section and then southward after 0900 along the Gibraltar line (offshore of Gibraltar by ∿1200 GMT) to its southern end by 1900 (see Figure 8a). A full day of sun photometry data was obtained as ridging produced clear skys, with the exception of some fair weather cu over land, through the entire day after 0700. Winds were approximately westerly at ∿5 m/s in the morning but increased to >10 m/s in the afternoon producing numerous whitecaps. Visibility fluctuated between 40 and 65 km throughout the day, while RH gradually dropped from ∿90% in the morning to <70% in the late afternoon. A plume was encountered 15 km NE of Gibraltar at 0830 GMT in which visibility was reduced to 17 km. Hourly sun photometry data were obtained from dawn to dusk this day. Data for this day are plotted in Figures 13-16.

The data for this day, while not conclusive, suggest that a clear zone (downwind of Ceuta) in a broad field of gray shade may be the result of a warm dry 'tongue' from the African continent -- perhaps a wind shadow or localized area of subsidence. Optical depth data did not correlate with fluctuations in surface-level parameters on this day.

Meteorology A minor frontal passage prior to 0600 GMT and ridging aloft were responsible for clearing skys in the early morning. A secondary trough tightened the gradient and caused the wind increase observed at mid-day (see Figure 13); but skys remained totally clear. Boundary layer depth was ∿1500m. Cruising southward after 0900, air temperatures gradually increased and then jumped to a maximum at ∿1600 GMT just south of the mid-line through the straits; relative humidity remained nearly constant and then dropped rapidly (due to a decrease in dewpoint and an increase in temperature) in the warm, dry zone encountered at 1600; relative humidity remained low at least through 2200 GMT as we approached close to Ceuta. (NOAA-7 imagery shows a 'gray-shade' field through the straits and into the Alboran with a clear zone downwind (east) of Ceuta at 1342 GMT.) Visibility at the BARTLETT's locations remained relatively constant throughout the day (except for the

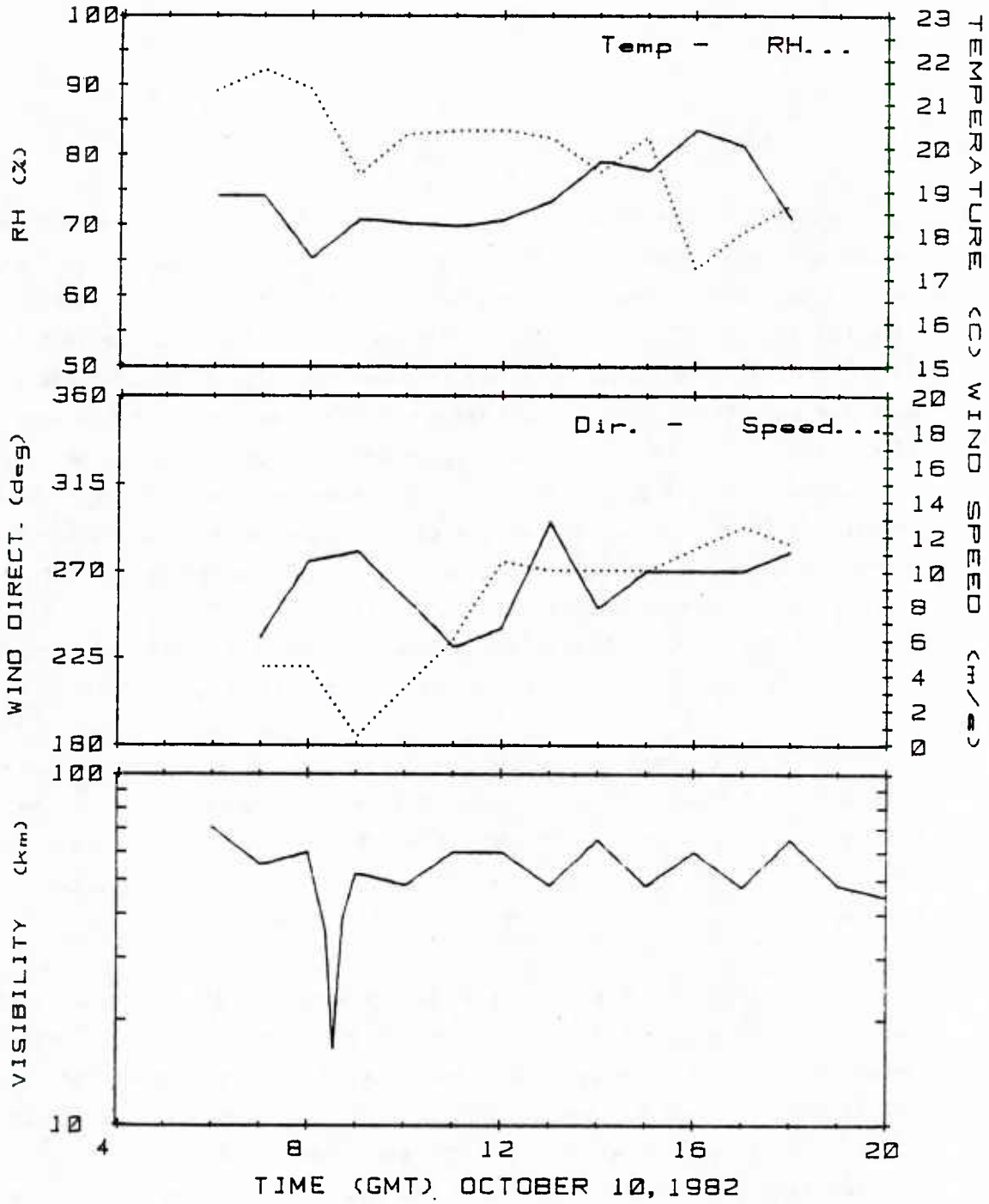

Figure 13: Meteorological Parameters, 10 October 1982

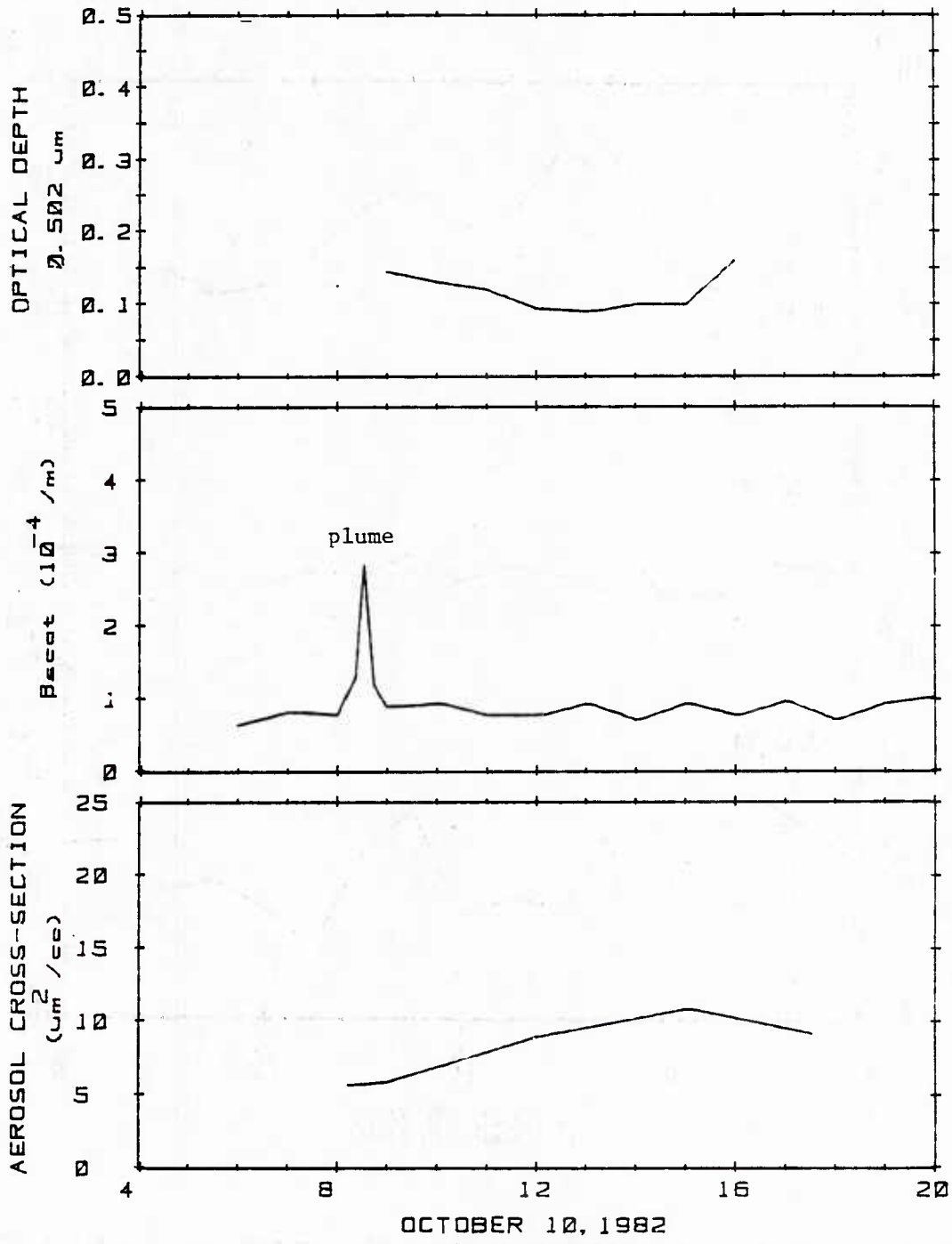

Figure 14: Optical Depth, β_{scat} and Aerosol Cross-section, 10 October 1982

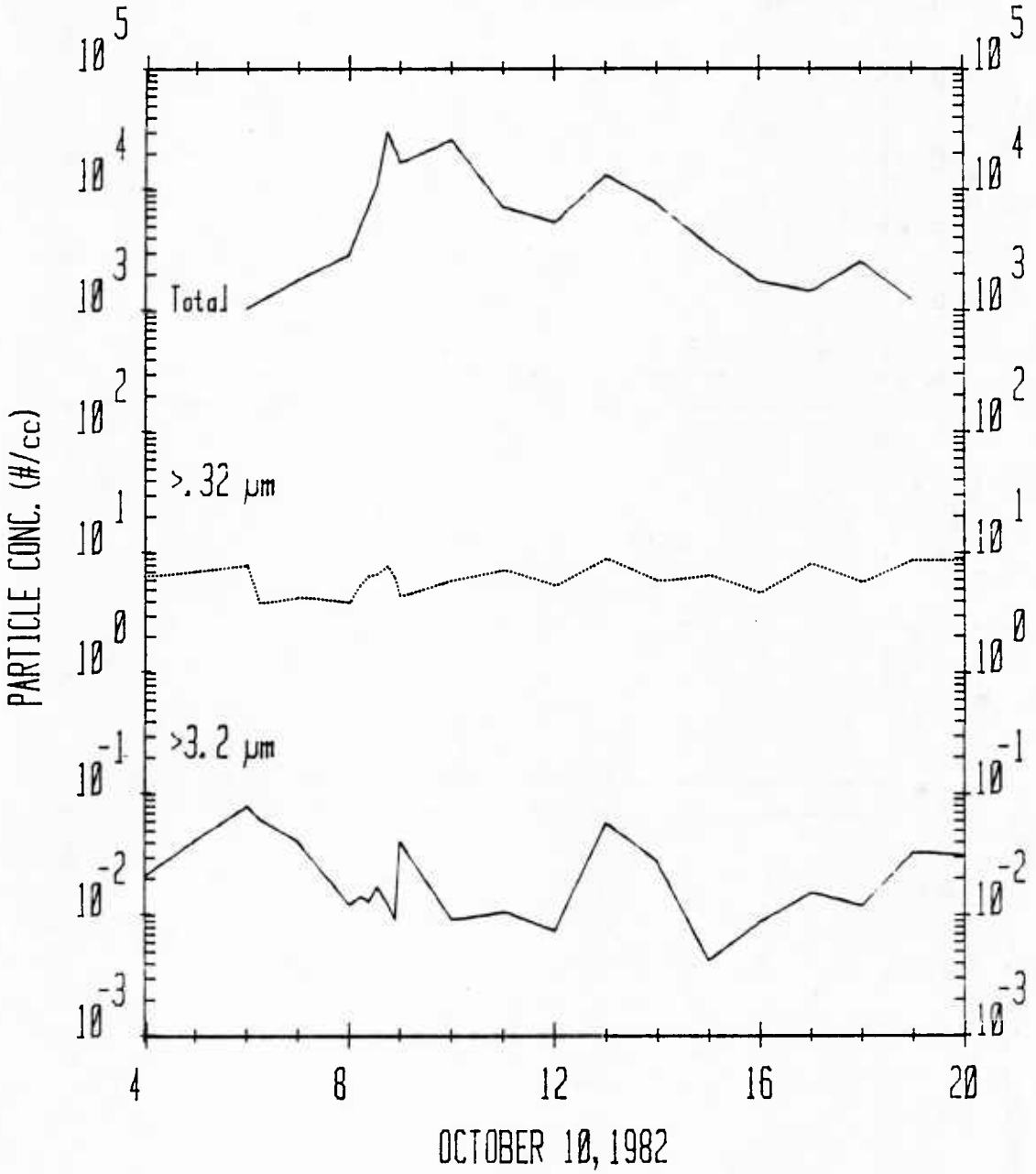

Figure 15: Aerosol Concentrations at Three Size Intervals, 10 October 1982

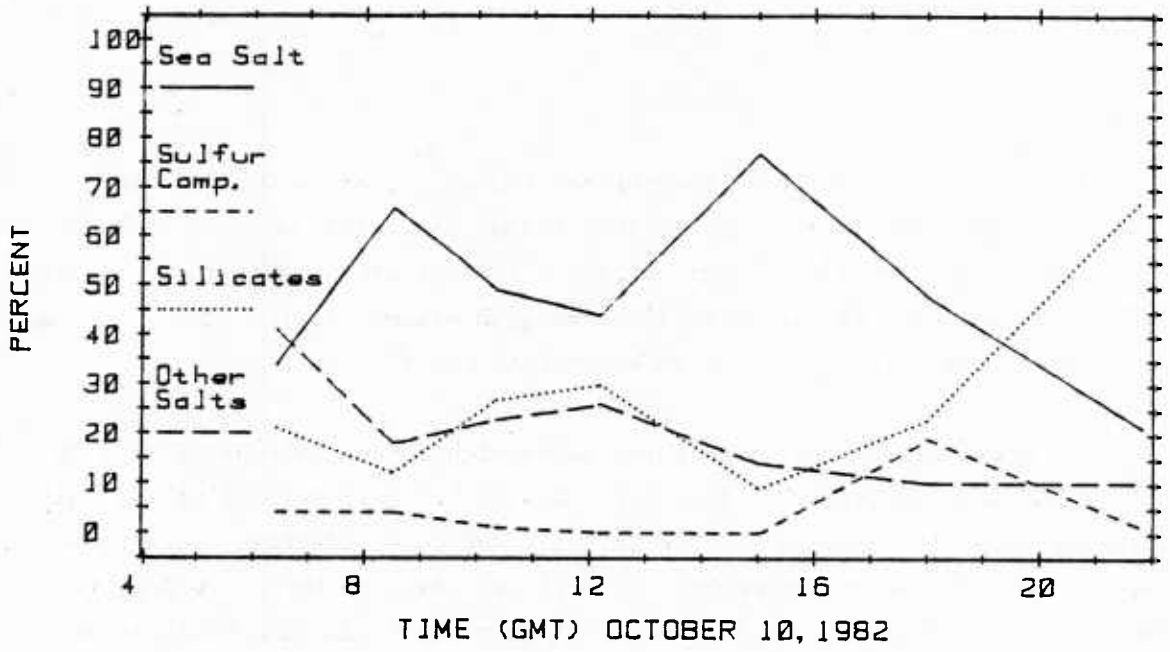

Figure 16: Chemical Classification of Aerosols >0.2 μm dia, 10 October 1982

plume encounter at 0835) showing little response to changes in RH or whitecap-produced sea spray. Whitecapping began at ∿1100 as wind speeds increased, peaked during the period 1300-1500, and ceased by 1700 GMT. Visual observations at 1200 and 1500 GMT make note of considerable "surf-zone" haze along both shores of the Straits visible from the BARTLETT's position. Aerosol cross-section data (Figure 13) shows maxima coinciding with whitecapping during afternoon hours, but optical depth estimates show unexplainable minima during the afternoon.

Aerosols Figure 15 shows the aerosol concentration data and Figure 16 shows aerosol composition analyses for 10 October. Note that total particle concentrations (the highest observed during the cruise) peaked in the morning (associated with the plume) and early afternoon hours when the ship was downwind of the Gibraltar area; after 1300, total particle concentration decreased

until 1900 GMT when we began to approach Ceuta. At sizes >0.3 μm particle concentrations increased slightly from mid-morning minimums to a maximum just off Ceuta at ∿2130. Large particle concentrations show much greater fluctuations, peaking during early morning RH maxima, in the plume, in the afternoon whitecapping, and as we approached Ceuta.

The chemistry data (Figure 16) shows high concentrations of NaCℓ in the plume at 0830 (see also data for 9 and 16 October) and during the whitecapping event of the afternoon; relatively low concentrations of sulfates were observed. As we approached the Moroccan coast in early evening, the sea salt proportion of the aerosol population was replaced by silicates.

3.3 11 October 1982

Summary The BARTLETT was in the southern half of the Alboran for most of the day as it cruised northeasterly from near the coast of Morocco to the south end of the Malaga line, all within the warm sector of the Gyre (see Figure 8a). Strong ridging maintained totally clear skys this day, except for a thin Ci veil which passed over during the period 1630-1800 GMT. Winds were virtually calm all day; not a single whitecap was observed. Visibilities remained in the 50-65 km range with RH of ∿70% most of day until a light haze was encountered late in the day; visibility dropped to 22 km in the haze as RH increased to >80% during the period 1600-1900 GMT. Dawn to dusk sun photometry data was obtained this day. Data for this day are provided in Figures 17-20.

The haze of later afternoon was produced by aerosol growth with increased relative humidity and apparently was responsible for the increase in optical depth which was observed in the afternoon.

Meteorology Low pressure over the Alboran before dawn was replaced by mid-morning by high pressure building-in from the south. The small ridge crested by mid-afternoon and was gone by 0000 on 12 October. Figure 17 shows the light to calm winds, warm temperatures, low relative humidities and high visibilities resulting from this fair weather pattern. A very shallow surface boundary layer developed this day: 480 m at 1100 GMT and 170 m at 1630. The reduction in visibility in haze during the late afternoon appears to be correlated with the increase in RH after 1400 brought on by increased moisture and decreased air temperatures. Figure 18 shows optical depth, scattering coefficient and aerosol cross-section increasing simultaneously with the occurrence of haze. A thin cirrus cloud precluded sun photometry after 1600.

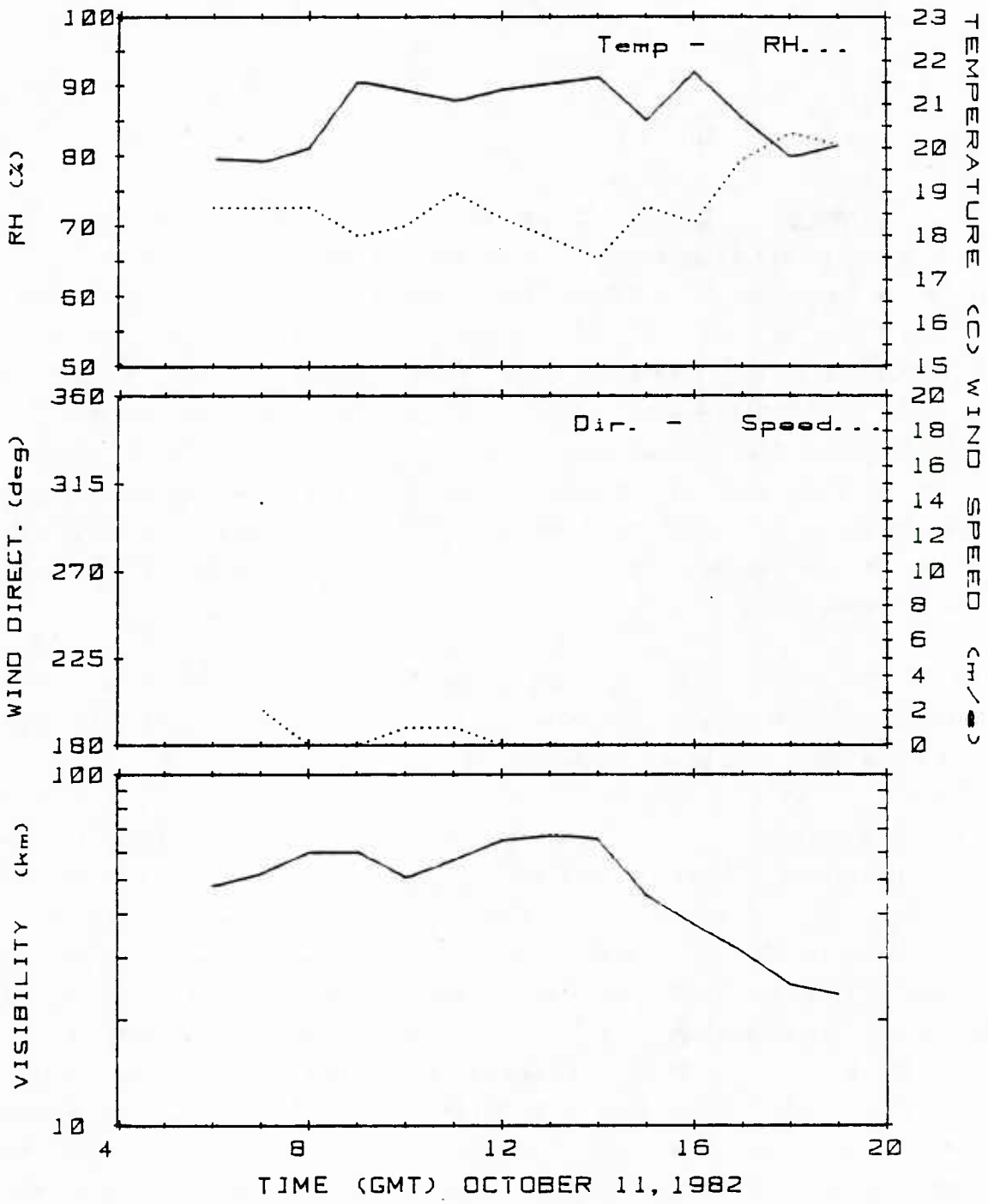

Figure 17: Meteorological Parameters, 11 October 1982

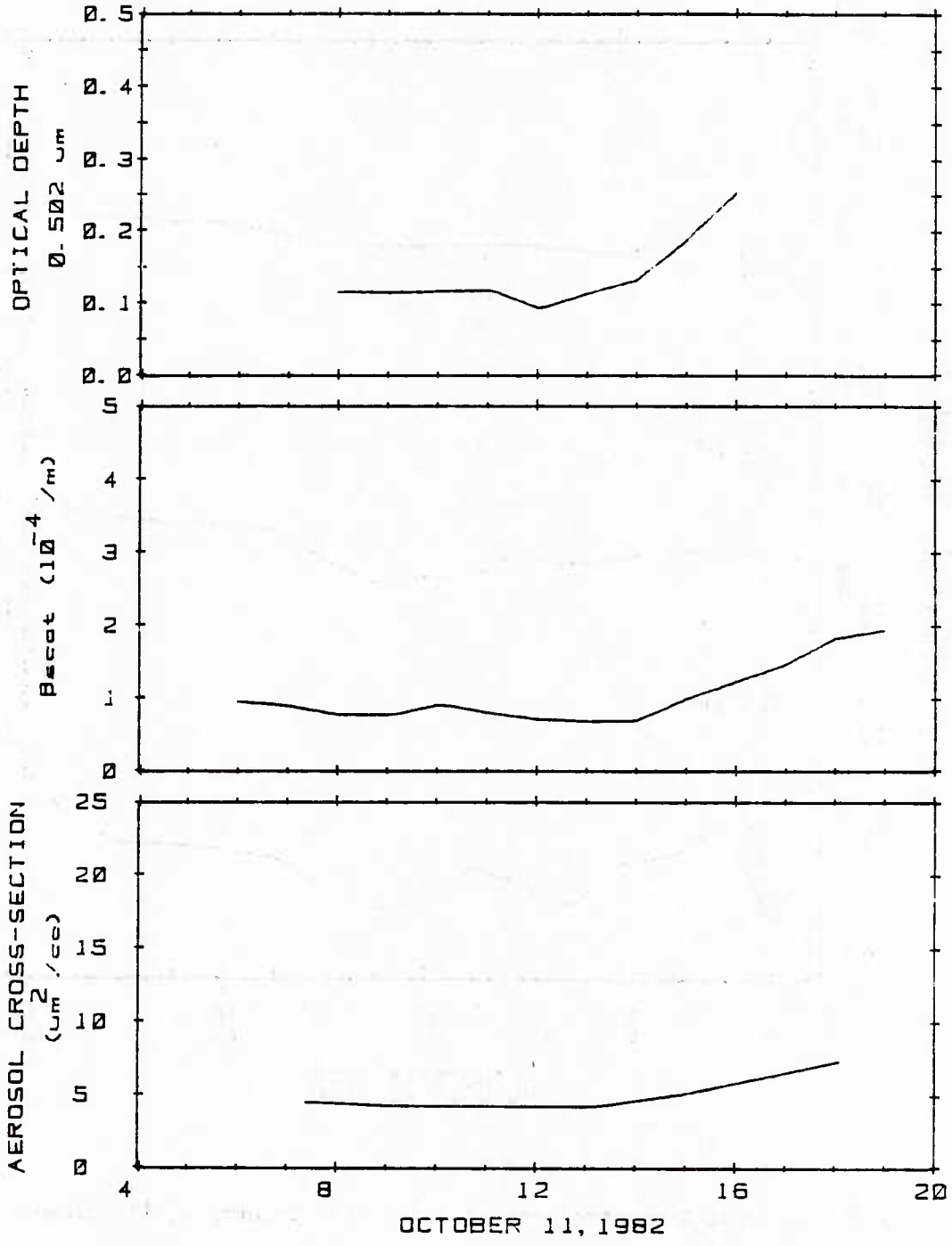

Figure 18: Optical Depth, β_{scat} and Aerosol Cross-section, 11 October 1982

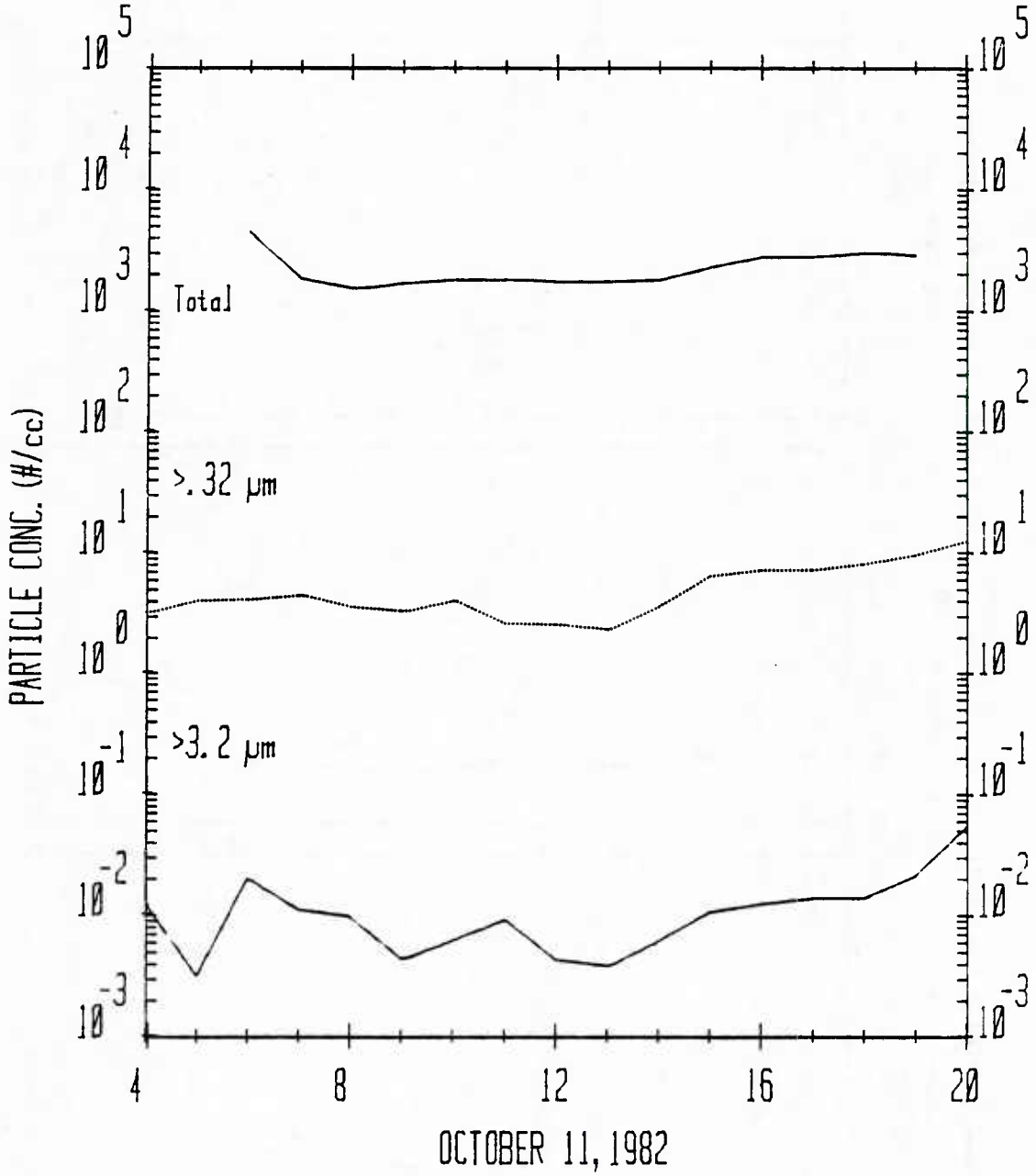

Figure 19: Aerosol Concentrations at Three Size Intervals, 11 October 1982

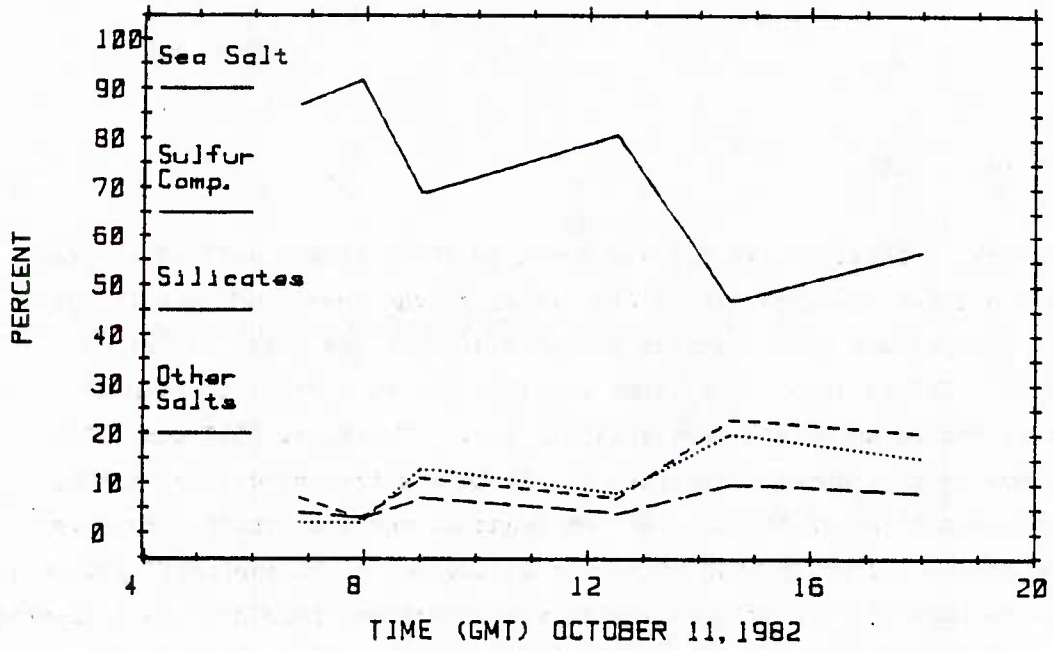

Figure 20: Chemical Classification of Aerosols >0.2 μm dia, 11 October 1982

Aerosols Aerosol concentrations measured during the first half of this day were among the lowest observed on the 10-day cruise. Particle concentrations at all size intervals (see Figure 19) were relatively constant during the morning but increased monotonically after 1300 reflecting the developing haze. The greatest relative increase in particle concentration occurred at larger sizes. The sea salt component of the aerosol population dropped from about 90% in the morning to ∿50% (except for a peak a mid-day) in the late afternoon haze (see Figure 20). Increases in all other composition categories accounted for the reduction in the sea salt component. Naucrates chemistry data show similar trends.

3.4 12 October 1982

Summary Most of the day was spent in the northern half of Alboran along Malaga line, traversing from its center to the coast and back (Figure 8b). The morning was characterized by increasing Ci overcast, 0.3 cloud cover at 0600 GMT to >0.8 cloud cover by 1230. Winds were lt to calm in the morning and no whitecaps were seen all day. (Twice, at 0330 and 1100 GMT, a plume which reduced visibility to <15 km was traversed.) By ∿1600, we reached centerline of the Alboran and began an easterly track. By this time, the pressure gradient had tightened in advance of an approaching front, and winds picked-up; so that a following wind precluded regular data collection. Eleven hours of sun photometry were acquired through a Ci overcast. Data obtained from aboard the BARTLETT are plotted in Figures 21-24.

This day's data suggest that cold water on the north side of the Alboran Gyre helped establish a low-level inversion and was responsible for cool air temperatures, increased RH, growth of aerosols, reduced visibility in that area. An aerosol plume was found lying approximately along the Alboran Front over the cold water.

Meteorology Very light winds during the morning gave way to stronger winds in the afternoon as a trough developed and deepened along the northern shore of the Alboran. Inspection of overflight imagery reveals that the ship crossed the sea surface temperature gradient twice this day: at ∿0300-0400 and at ∿1100. The records reproduced in Figure 21 show that the coldest air was observed in northern half of this track before 1100. Relative humidity was highest and visbility also lowest in the area of colder temperatures. Minisonde data show a low-level inversion base at 45 m over the cold water at 0800 (beneath a higher level inversion at 315 m developed by the receding

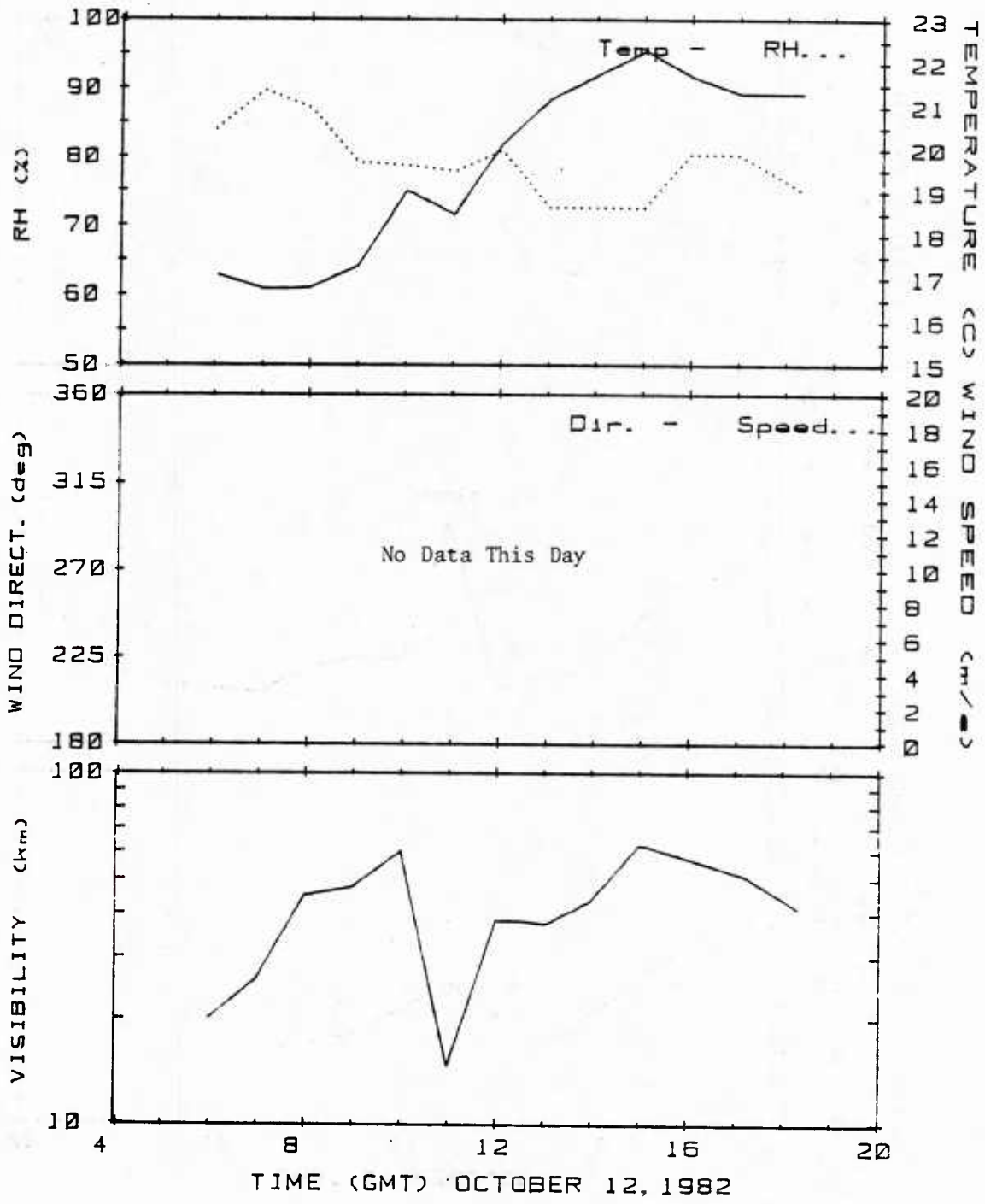

Figure 21: Meteorological Parameters, 12 October 1982

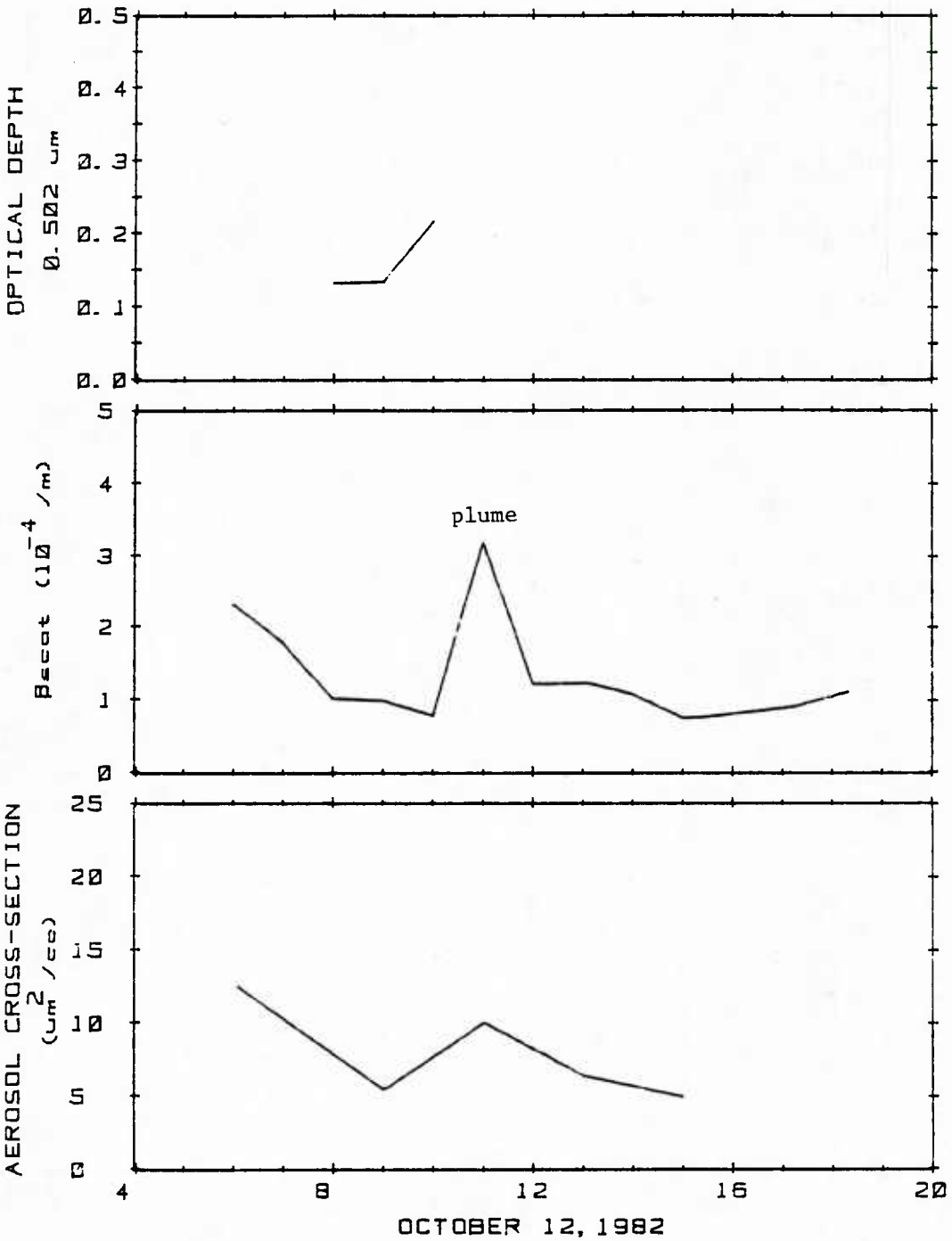

Figure 22: Optical Depth, β_{scat} and Aerosol Cross-section, 12 October 1982

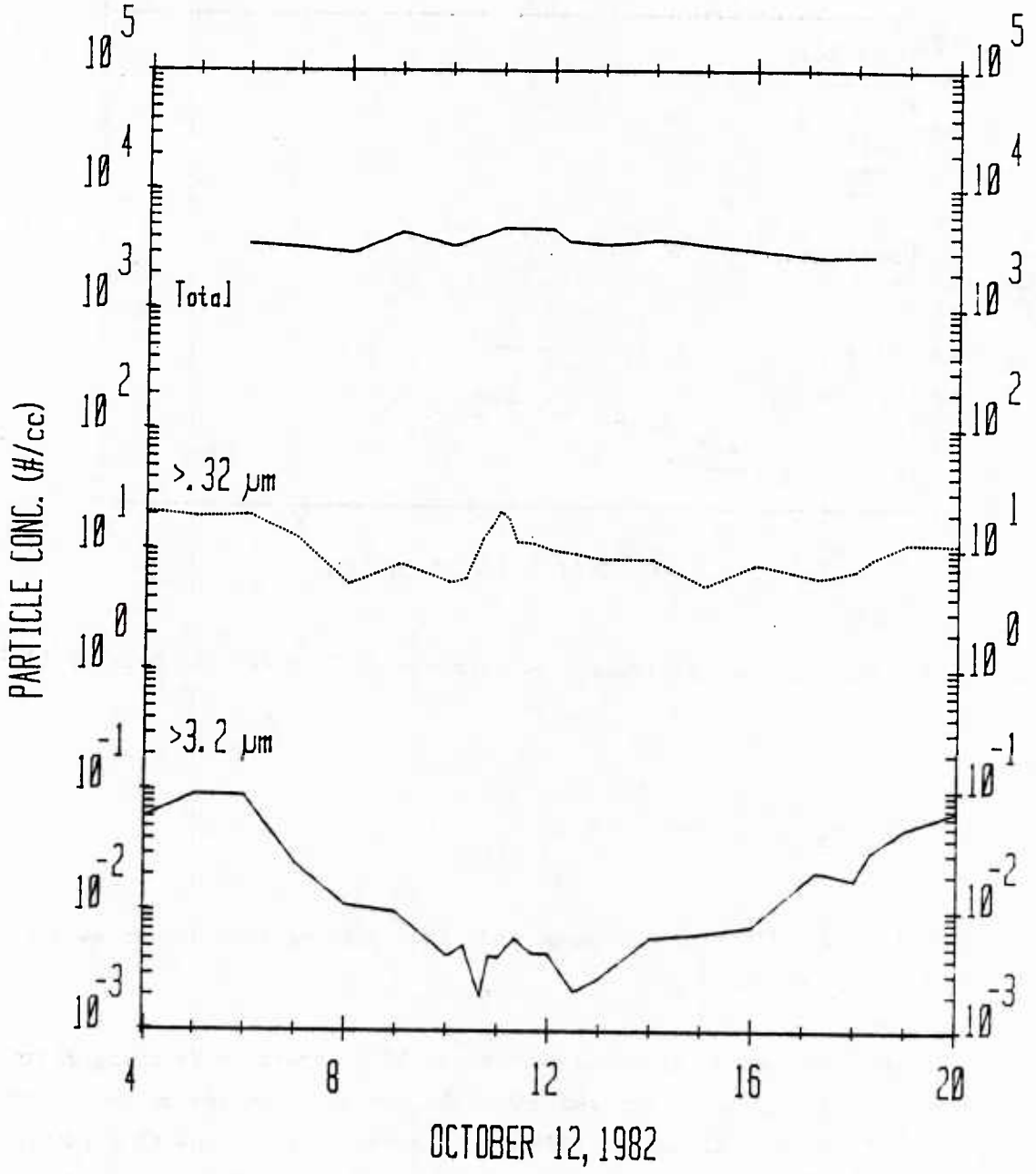

Figure 23: Aerosol Concentrations at Three Size Intervals, 12 October 1982

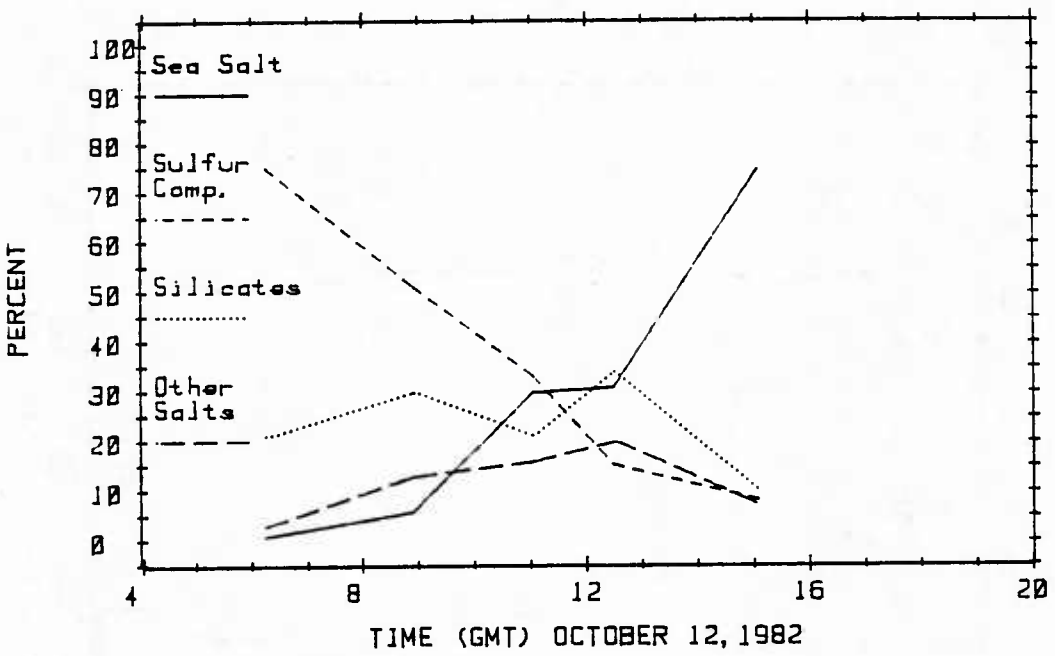

Figure 24: Chemical Classification of Aerosols >0.2 μm dia, 12 October 1982

synoptic ridge.) (Inversion base at 1630 GMT, perhaps over warmer water, was at a height of ∿100m.)

Plumes observed at 1100 and perhaps at 0330 appear to be lying along the Alboran Front, perhaps trapped under the low level inversion generated over the cold water. The aerosol data in Figures 23 & 24 show that particle concentrations increased in the plume, but no change in RH was observed and no specific chemical constituent can be attributed to the plume.

Aerosols Aerosol data presented in Figure 23 show that total concentrations remained relatively constant throughout the day. However, concentrations of the largest particles (>3.2μ dia) exhibit distinct maxima during the high RH morning hours, in the 1100 GMT plume, and early in the evening when whitecapping began.

The chemistry data in Figure 24 shows that sulfate compounds comprised a very high proportion of the aerosols during early morning hours -- perhaps material of continental/anthropogenic origin trapped beneath the low-level inversion. As the day progressed and winds and wave action increased, the proportion of sea salt aerosols increased from near zero to ∿75% in concert with the increase in whitecapping. Chemistry data from the Naucrates show sulfate and sea salt proportions of ∿30 and ∿25%, respectively, at 1130 GMT; by 1500, sea salt had increased to ∿85% and sulfates had dropped to ∿5% of the aerosols >0.2 μm diameter.

3.5 13 October 1982

Summary The entire day was spent traversing the Adra line from the center of the Alboran to the coast (see Figure 8b). Westerly winds picked up to >13 m/s by 0830 producing high seas and considerable whitecapping throughout the day; peak winds in excess of 18 m/s were observed in late afternoon. During daylight hours, RH dropped from 80 to 70%, visibility improved from 35 to >50 km, and skys cleared from 0.8-0.9 Ci cloud cover to <<0.1 (by 1400). Good sun photometry data were obtained during the hours 1100-1500. The data for this day are plotted in Figures 25-28.

The data for this day, show that a low level inversion was established over the cold water along the north shore. A gray shade area along the north shore does not appear to be correlated with surface-level aerosol characteristics, although it may have been detected by sun photometry.

Meteorology A developing surface trough, oriented along the north shore of the Alboran continued to deepen through 1800 producing strong NW (offshore) winds immediately along the coast, but W to WSW winds with good fetch farther to sea (see Figure 25). Air temperatures gradually increased through 1600 GMT producing a decrease in RH and improvement in visibility. Warm air aloft apparently gave rise to the observed warming, a low-level inversion and shallow boundary-layer over the cold water: 150 m and 70 m inversion bases were observed respectively, at 1100 and 1630 GMT at the BARTLETT's locations; an upper level inversion was also present at ∿3400 m at least at 1630 GMT. NOAA-7 imagery suggest that the ship passed through or beneath a gray-shade boundary and into the gray shade area along the coast at ∿1500 GMT; however surface visibility was improving at that time and visibility remained at high values thru ∿2000 GMT. Optical depth increased between 1400 and 1500 GMT; unfortunately, ship motion due to high seas precluded optical depth data after 1500. As the ship approached nearer to shore during evening hours, visibility dropped from ∿51 km at 2000 GMT to 43 km at 2330 GMT (see Appendix A).

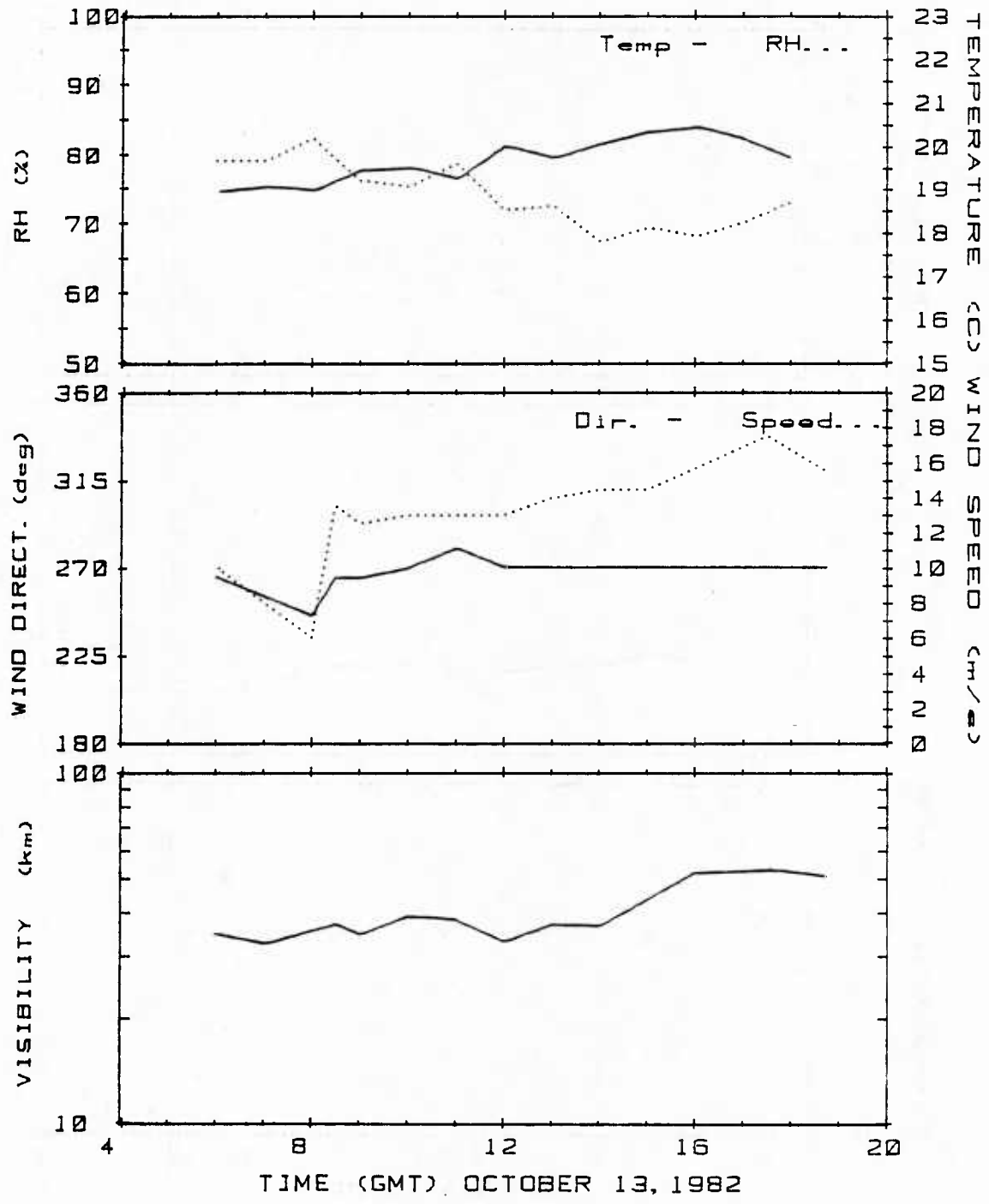

Figure 25: Meteorological Parameters, 13 October 1982

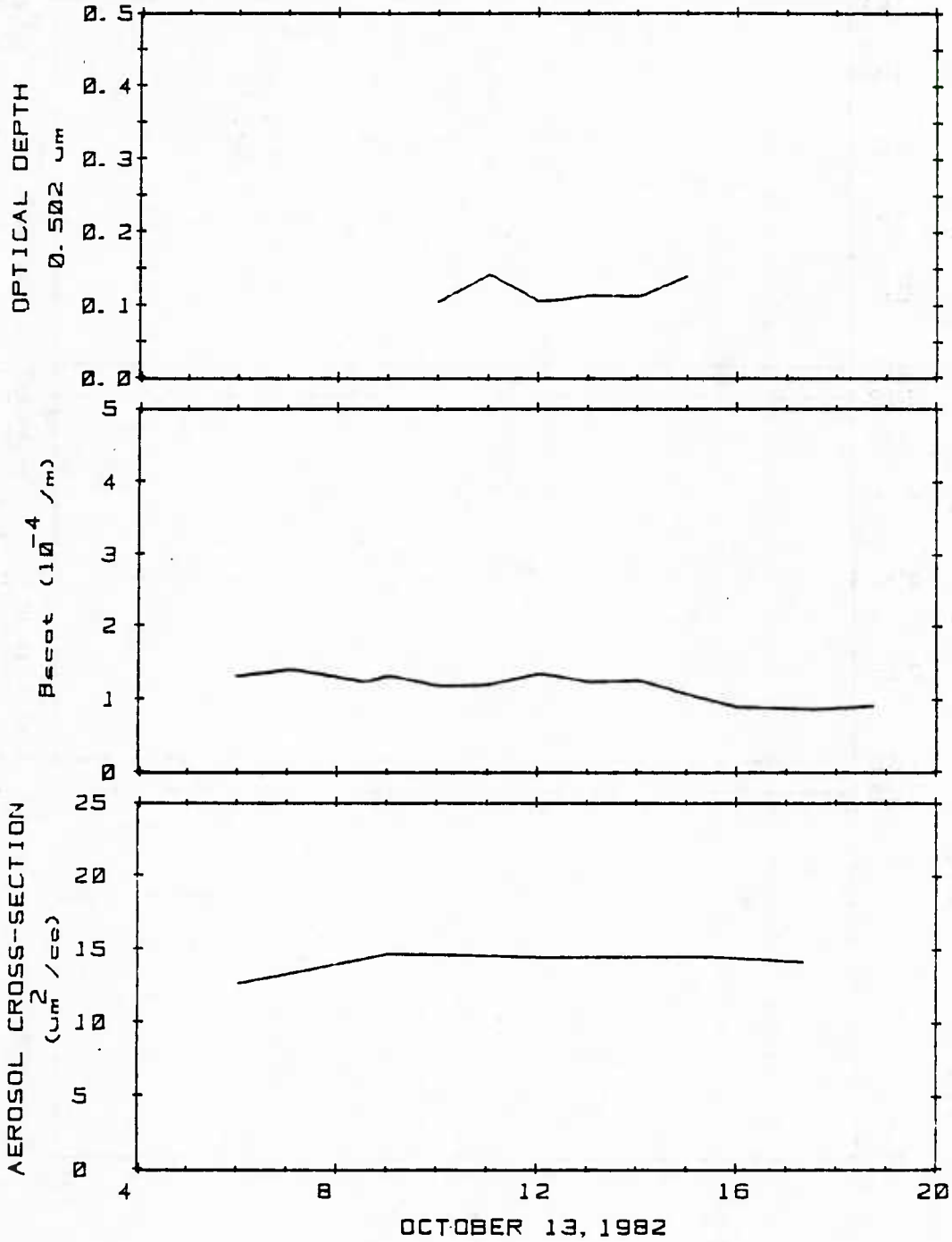

Figure 26: Optical Depth, β_{scat} and Aerosol Cross-section, 13 October 1982

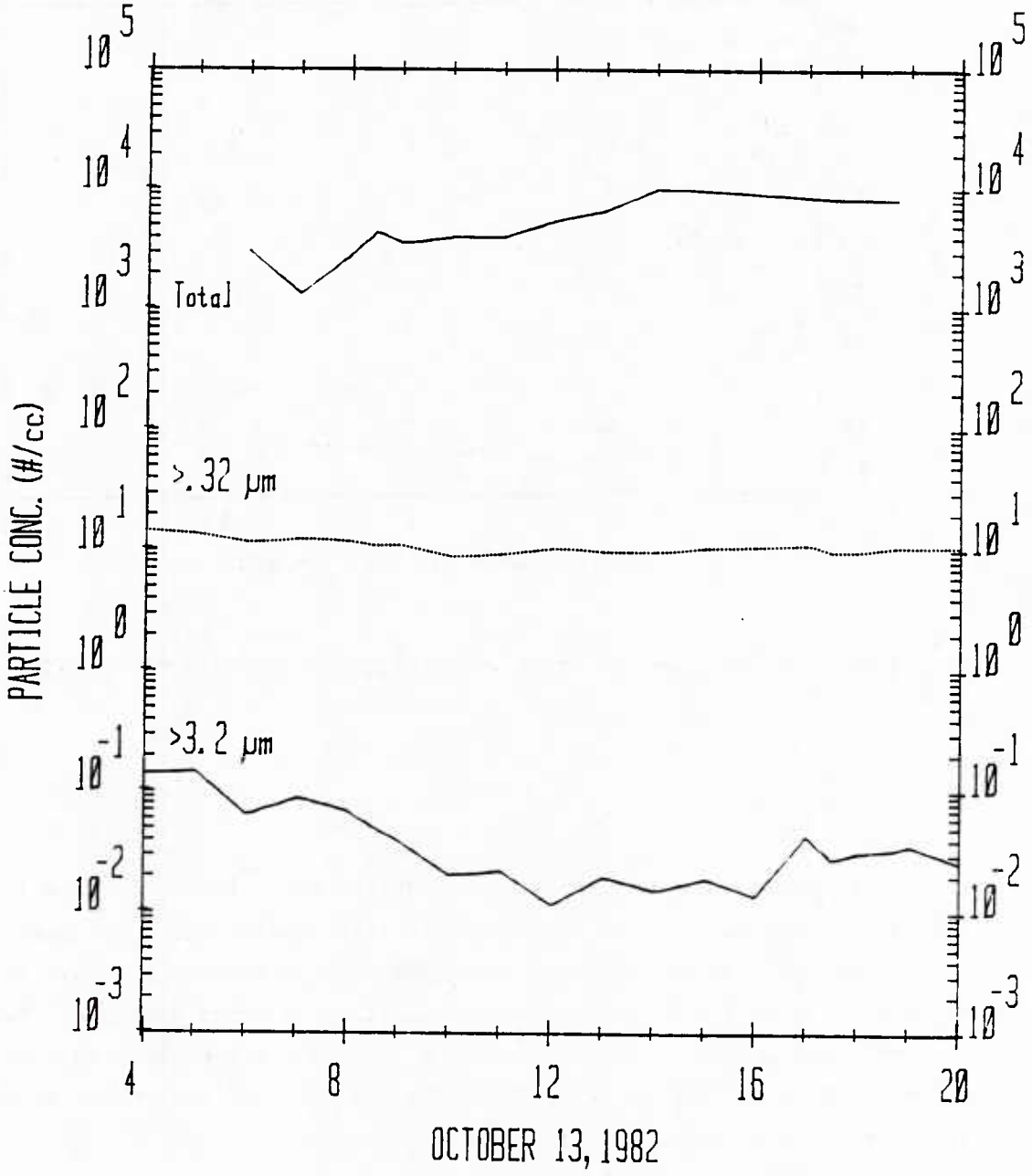

Figure 27: Aerosol Concentrations at Three Size Intervals, 13 October 1982

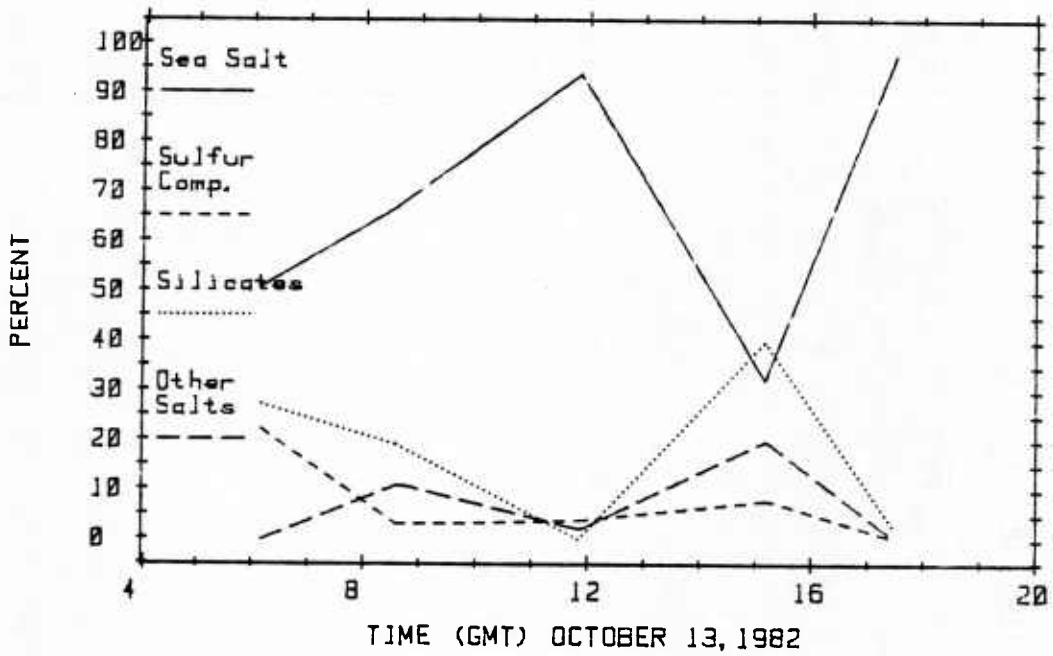

Figure 28: Chemical Classification of Aerosols >0.2 μm dia, 13 October 1982

Aerosols Figures 27 and 28 provide the aerosol data for the daylight portion of this day. Note that total particle concentration increased with time as the ship moved closer to the coast. Aerosol concentrations at sizes >0.3 μm were nearly constant with a slight minimum during mid-day. At sizes >3.2 μm, particle concentration shows a distinct minimum during mid-day. Between 2000 and 2300 GMT while the ship was presumably in the gray shade area, particle concentrations at sizes >0.3 μm and >3.2 μm increased by ∿30% and ∿300%, respectively, in concert with the observed decrease in visibility.

The chemical analyses show an increasing proportion of sea salt aerosol through the day to near 100% at 1730 GMT, except for an anomalous low sea salt value at 1500. Perhaps a wave on the shallow inversion pushed it closer to the surface for a brief period; the sample could then have been obtained from air above the boundary layer.

3.6 14 October 1982

Summary The ship tracked on a WSW line from offshore at Adra (at 0000 GMT) to a point SSW of Marbella (∿30 km offshore) by 1330, where it remained on approximate station until the morning of 15 October (see Figure 8b). Weather gradually improved during the day after a mid-morning frontal passage: winds dropped from 275° @ 14 m/s to 240° @ 3 m/s by late afternoon, and visibility increased from 50 to >80 km as RH dropped from 85 to <60% before mid-day. Moderate whitecapping of the morning hours gave way to only an occasional whitecap by 1700. Overcast skys briefly cleared to 0.8 in the early afternoon, and 3 hr of sun photometry data were attempted. The ship passed thru a distinct plume at ∿1300 GMT in which particle counts peaked and visibility dropped to ∿35 km. The data for this day are presented in Figures 29-32.

Meteorology The trough over the north shore was maintained, but it gradually weakened during the day. Minimum atmospheric pressure at the BARTLETT occurred at ∿0100 but a large jump in pressure occurred as the front passed over the ship's location at ∿0700 GMT. With the frontal passage, winds shifted to WNW-NW and speeds began to drop; dewpoint temperature and RH dropped and visibility improved (see Figure 29). Air temperature remained relatively constant through the day, but RH increased to >70% by afternoon. The plume encounted at ∿1300 was not associated with an increase in RH and occurred about the time winds shifted to place Gibraltar upwind of the BARTLETT.

Aerosols As the ship cruise along the northern shore, high winds and whitecapping produced copious quantities of large sea salt aerosols. After the frontal passage, offshore flow brought an increase in concentrations of very small particles (the second-highest observed on the cruise) to our location. The aerosol immediately behind the front also comprised higher proportions of silicates, sulfates and other minerals at the larger sizes (Figure 32). The plume observed at 1300 was accompanied by increases in particle concentrations at all sizes and by increases in the proportions of sulfates and other minerals; silicates were not detected in the plume.

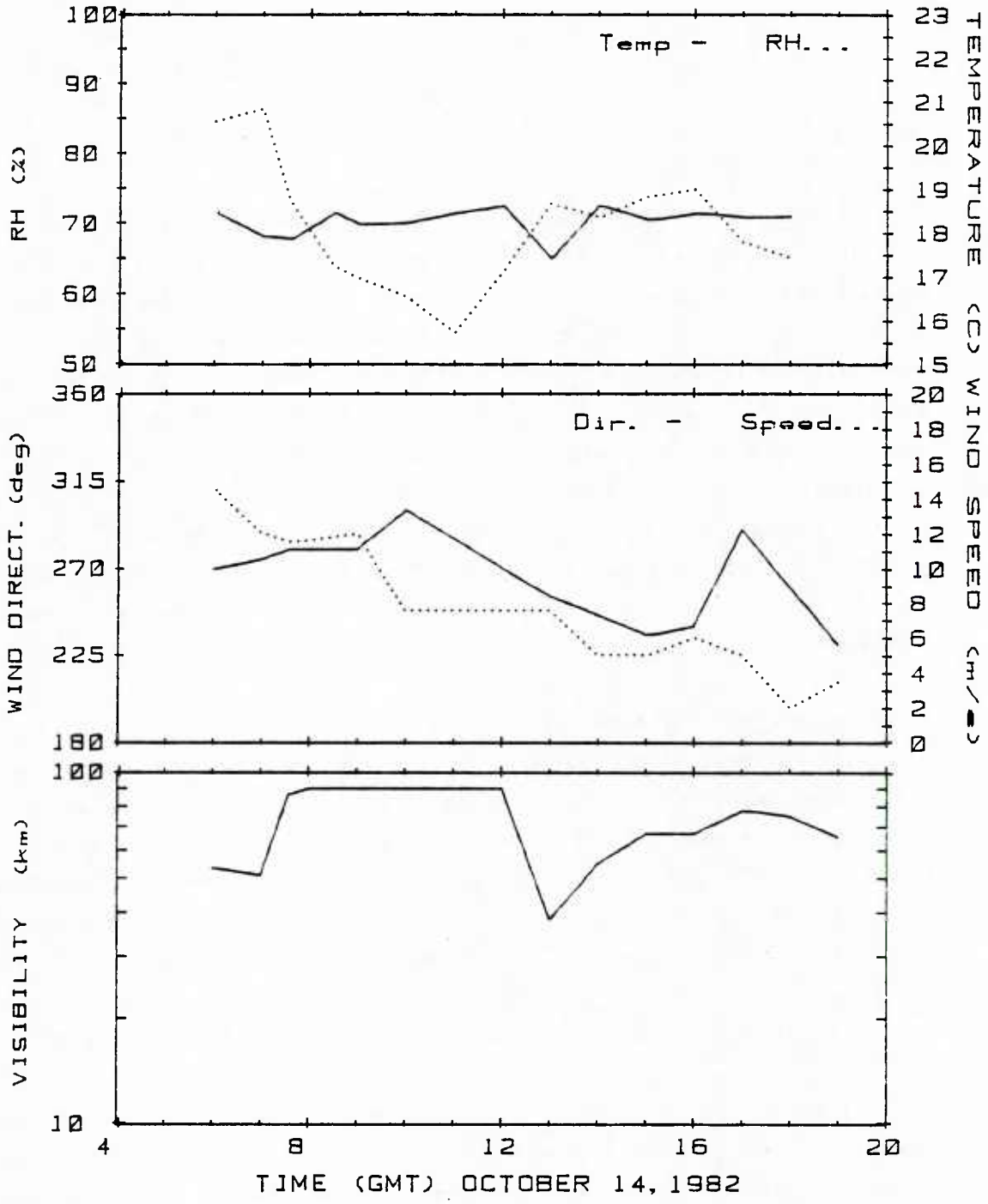

Figure 29: Meteorological Parameters, 14 October 1982

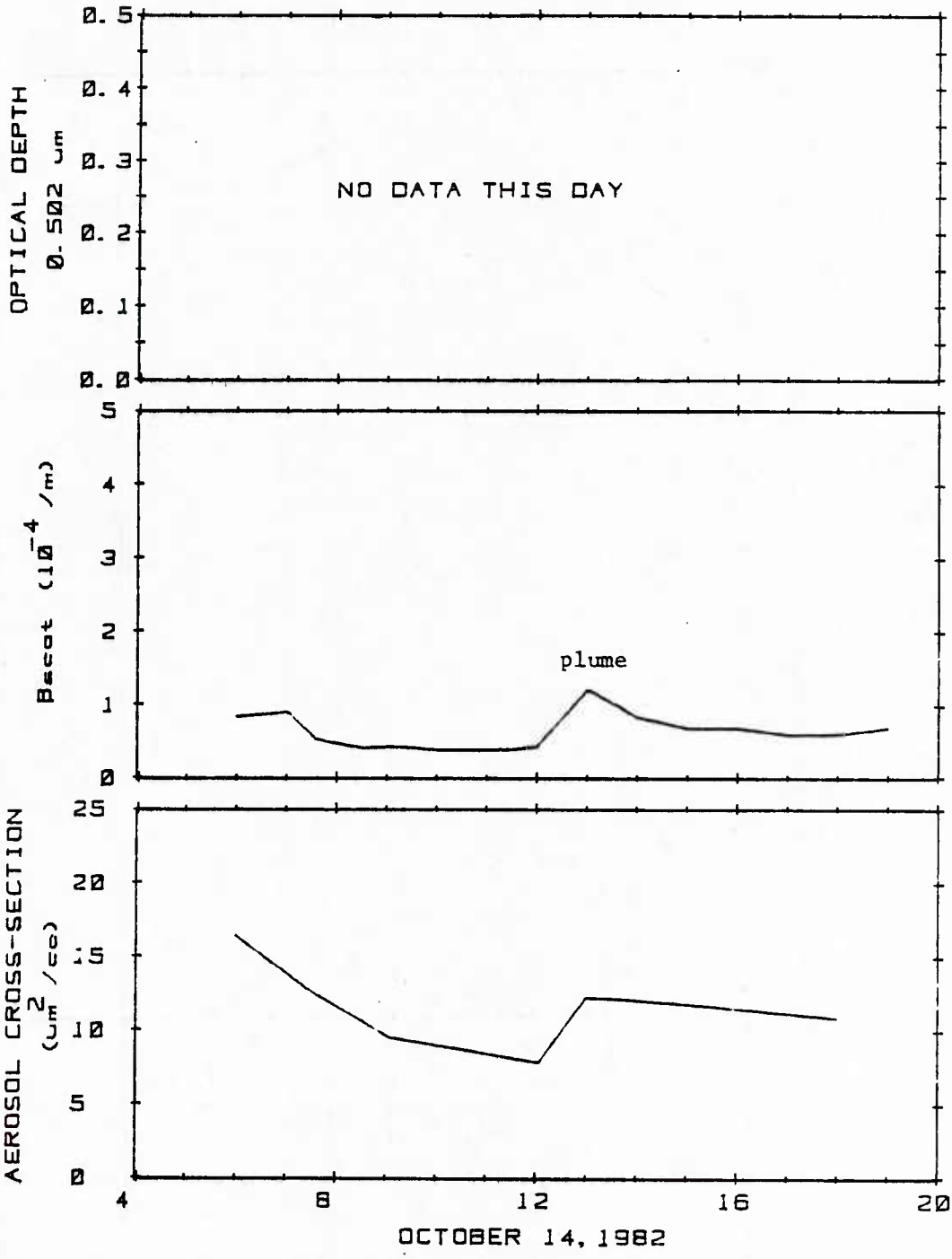

Figure 30: Optical Depth, β_{scat} and Aerosol Cross-section, 14 October 1982

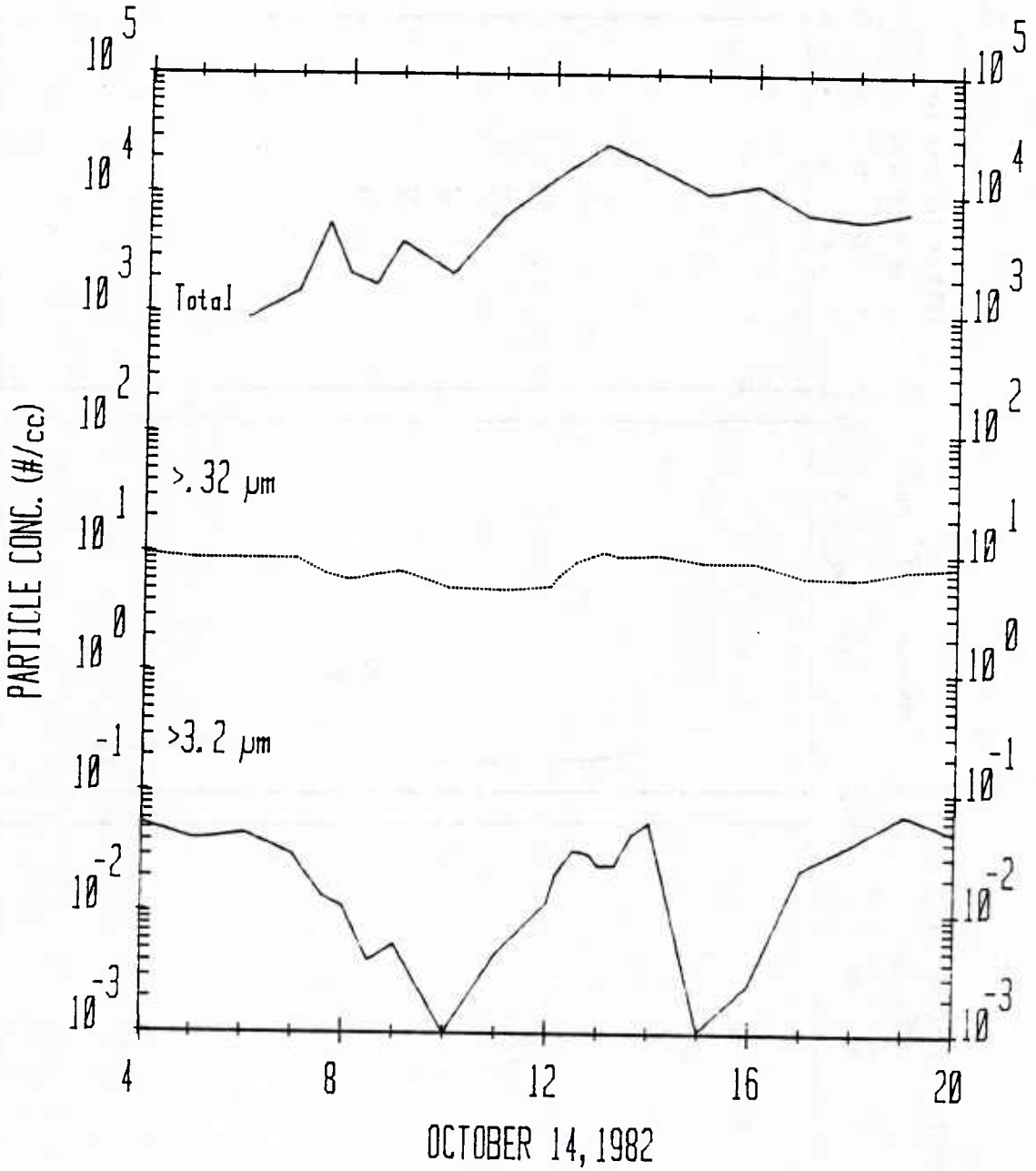

Figure 31: Aerosol Concentrations at Three Size Intervals, 14 October 1982

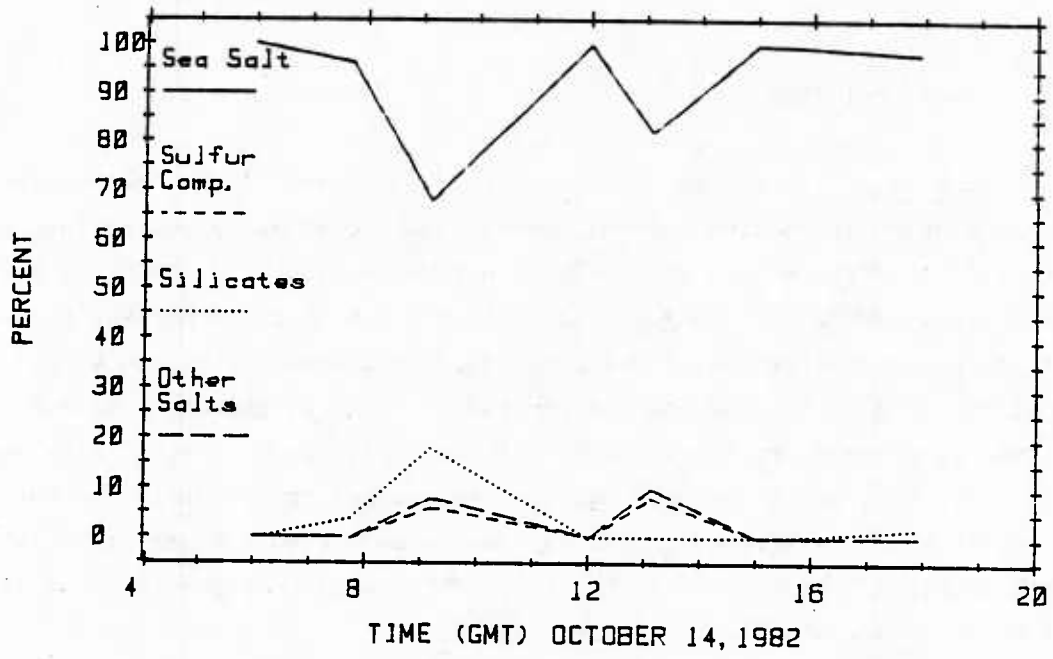

Figure 32: Chemical Classification of Aerosols >0.2 μm dia, 14 October 1982

3.7 15 October 1982

Summary The entire daylight period was spent in the northern half of the Alboran in mooring-recovery operations along the Marbella line, moving from ∿23 km offshore at 0700 to ∿50 km off Marbella by 1700 GMT (See Figure 8b). Light WSW to WNW winds increased from 2-3 m/s in the morning to 4-6 m/s in the late afternoon; cloud cover increased from 0.2 @ 0600 to 0.9 in cirrus by 1200 GMT and for the remainder of the afternoon. The dense cirrus cloud cover precluded meaningful sun photometry. Visibilities were typically 50-60 km through the day, but RH dropped from >80% in the morning to <70 in the late afternoon. We may have encountered a plume again as visibilities dropped (below 35 km after 1700) in late afternoon. The data for this day are provided in Figures 33-36.

While not conclusive, the data suggest that the observed air temperature increase and RH decrease by mid-day may have been a result of the ship crossing the Alboran Front from cold to warm water.

Meteorology The surface trough located over the northern shoreline on the previous day continued to weaken, and the flat pressure gradient kept wind speeds low; whitecaps were not observed this day. The trough line moved southward through about mid-day and then retreated to the north shore by 1800; movement of the troughline was responsible for the wind fluctuations from WNW to WSW. From radiosonde data, boundary layer depths are estimated for Gibralter at 1100 GMT and for the BARTLETT's location at 1230 GMT to be 1200 m and 1380 m, respectively. Rising air temperatures (which may be partly a result of crossing from the cold water of the Alboran Front) helped to reduce relative humidity and keep visibility at high values (see Figure 33) through 1400 GMT. An upper-level trough moved through during the day causing the increase in cirrus cloud cover which prevented meaningful sun photometry for most of the day. The observed decrease in visibility after 1400 may in part be due to a wind shift which placed the Gibraltar area upwind of our position after that time.

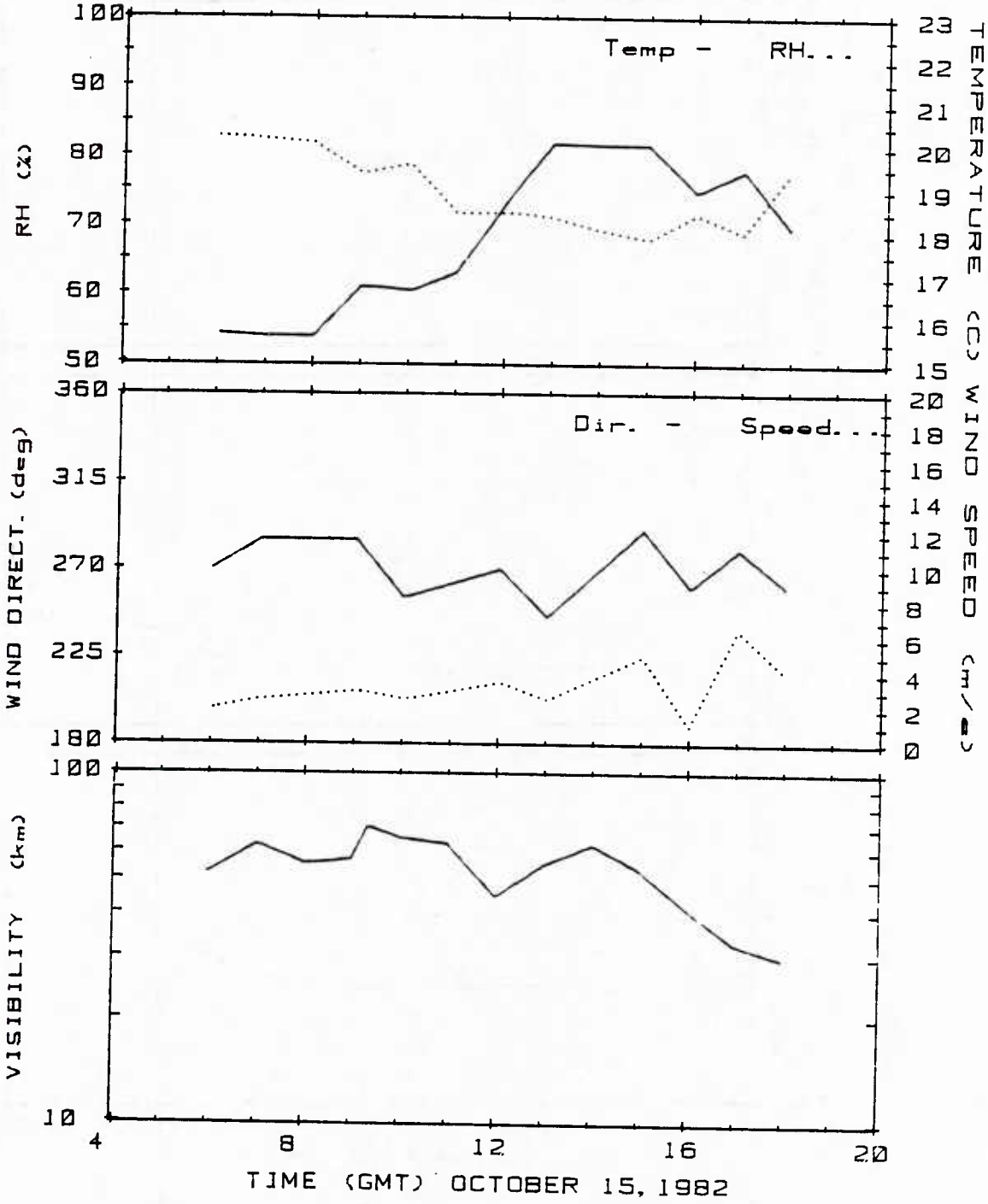

Figure 33: Meteorological Parameters, 15 October 1982

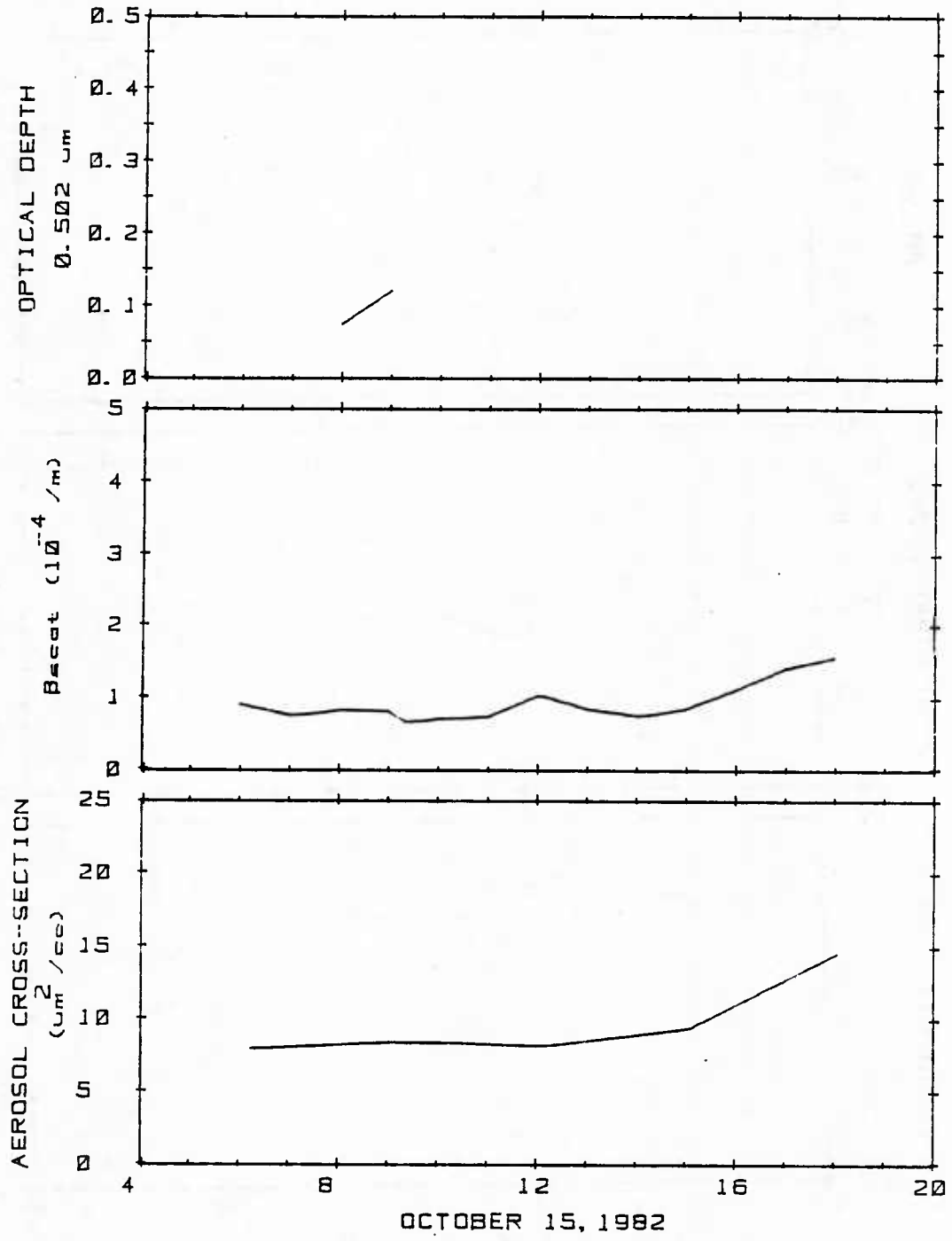

Figure 34: Optical Depth, β_{scat} and Aerosol Cross-section, 15 October 1982

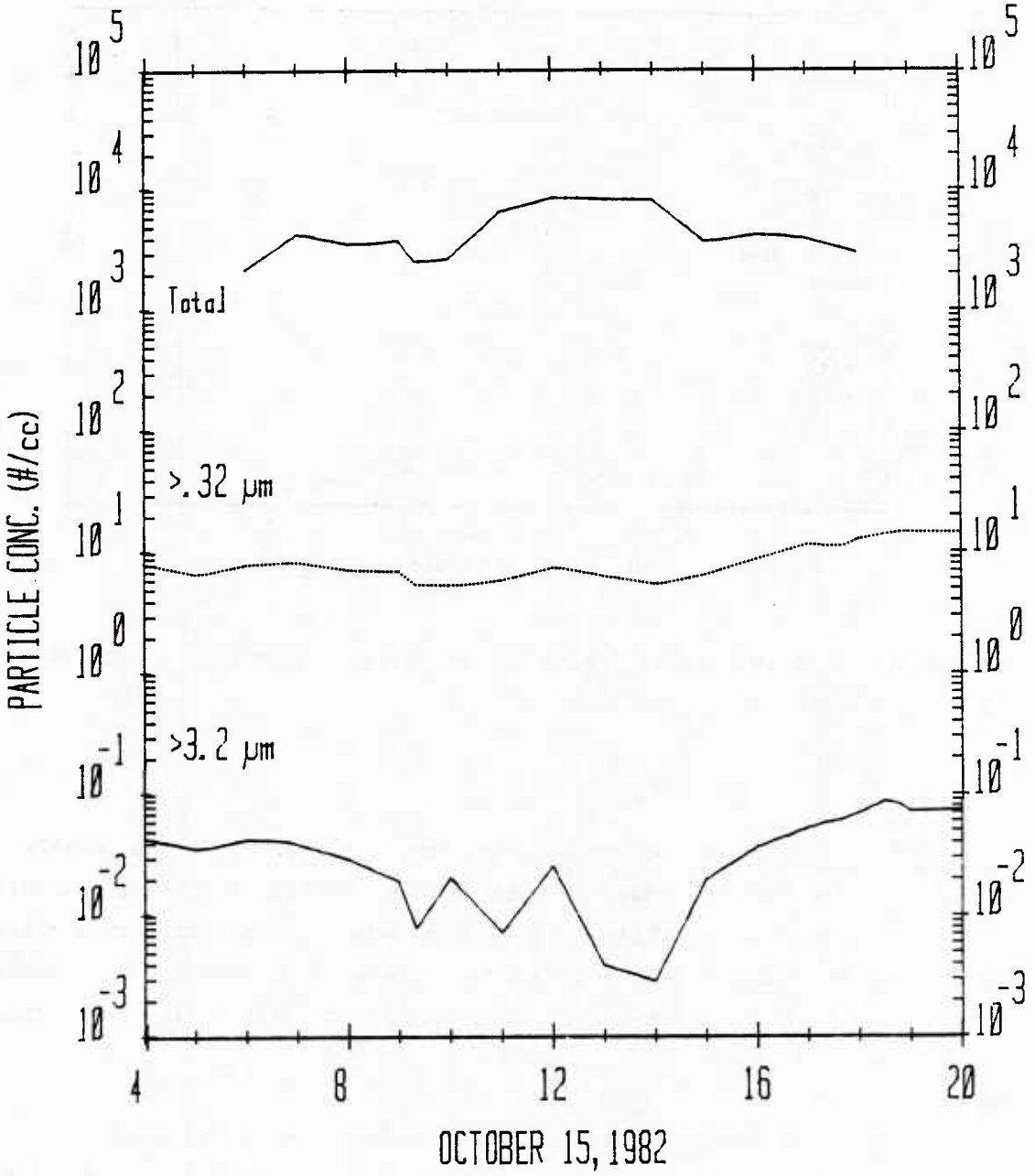

Figure 35: Aerosol Concentrations at Three Size Intervals, 15 October 1982

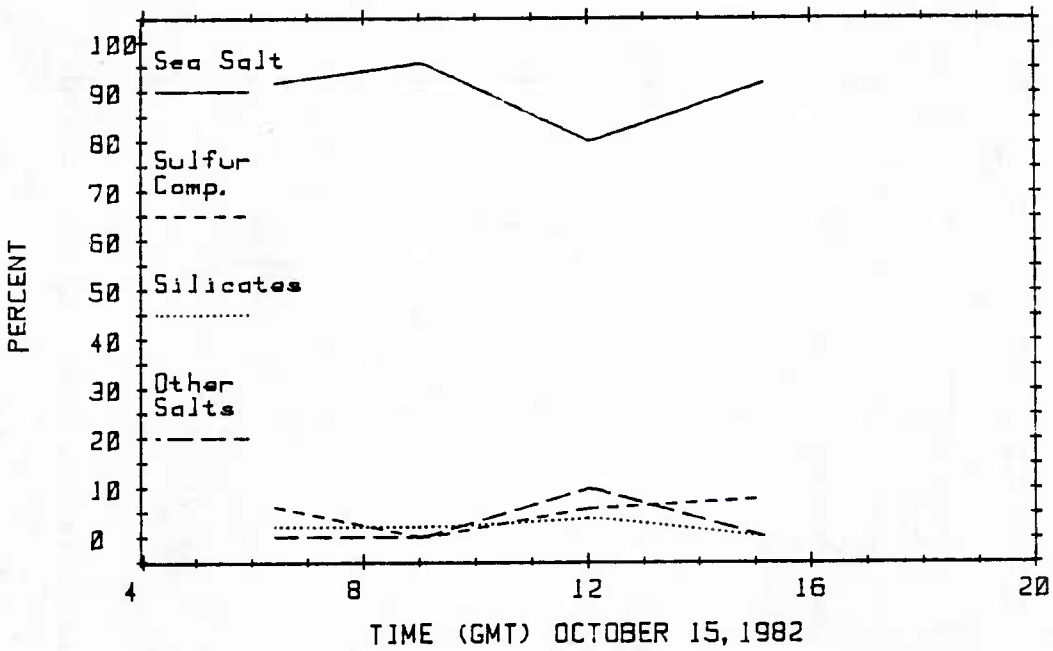

Figure 36: Chemical Classification of Aerosols >0.2 μm dia, 15 October 1982

Aerosols The aerosol records presented in Figures 35 and 36 show that total particle concentrations were highest at mid-day, while concentrations at larger sizes exhibited minima at mid-day. Note that particle concentrations at sizes >0.3 μm and >3.2μ m diameter and aerosol cross-section (Figure 34) increased after 1400, accounting for the visibility restriction noted after that time.

The aerosol chemistry data show unexplainably high NaCℓ content. Since some plumes apparently emanating from the Gibraltar were observed to be composed of NaCℓ aerosols (e.g. see 10 and 16 October), it is reasonable to speculate that the entire area downwind of Gibraltar can be contaminated under such fluctuating wind conditions.

3.8 16 October 1982

Summary The early morning was spent in mid-Alboran near the southern end of the Marbella line, and the remainder of the day was spent approximately retracing the track of the previous day (see Figures 8c and 8d). Beginning at ∿1130 GMT, theBARTLETT made a 4-hr, non-stop track along the Estepona line (mid-way between the Marbella & Gibraltar sections) from 65 km offshore to a point 6 km off the coast by 1520, crossing the Alboran Front at ∿1230 GMT. We then reversed course along the Estepona line, reaching a point ∿30 km offshore by 2000 GMT. Routine observations were made at 1/2 hr intervals during the 4-hr track. Weather during mid-day: sunny (0.1-0.2 cloud cover), winds <3 m/s, RH 77-82% and visibility 30-40 km. Wind speeds increased steadily during the day. Plumes were encountered at ∿1430 and again at ∿1630. Data for this day are plotted in Figures 37-40.

While not conclusive, the data suggest that colder water on the north side of the Gyre was responsible for cooler air temperatures and a shallower boundary layer over the cold water. Again an aerosol plume was found along the Alboran Front over the cold water; material dispersed from this plume may have been responsible for an increase in optical depth during the afternoon.

Meteorology A flat pressure pattern in the early morning and ridging from the Atlantic gave way to a developing trough oriented along the northern shoreline of the Alboran by evening. While boundary-layer depth was estimated to be at ∿2000 m, low-level inversions were located at heights of 490 m and 403 m at 0600 and 1800 GMT, respectively, and at 130 and 40 m, respectively, at those times. The latter low-level inversion was observed on the northern part of the track, presumably over the cold water. An inversion at ∿250 m was observed at Gibraltar at 1100 GMT.

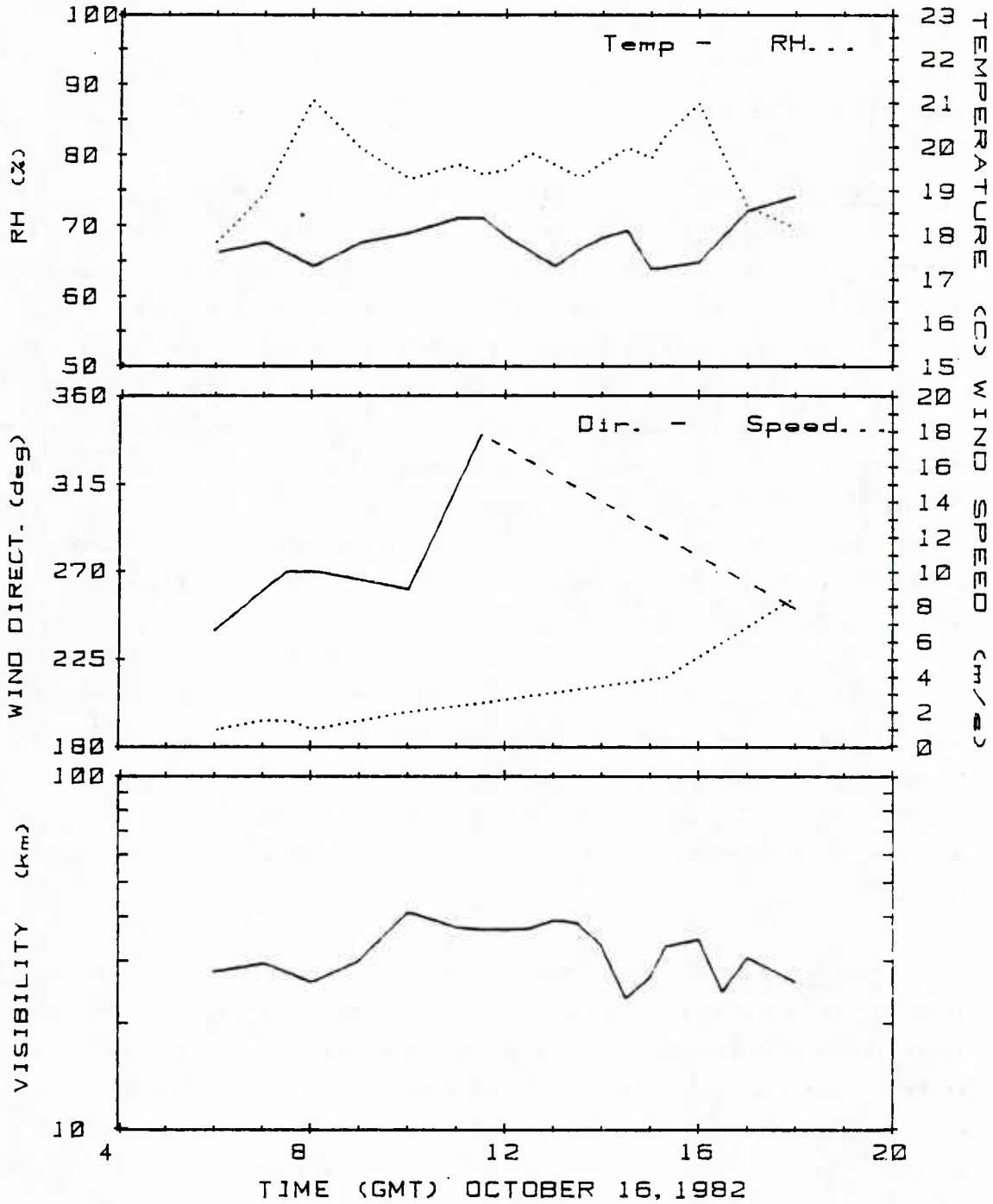

Figure 37: Meteorological Parameters, 16 October 1982

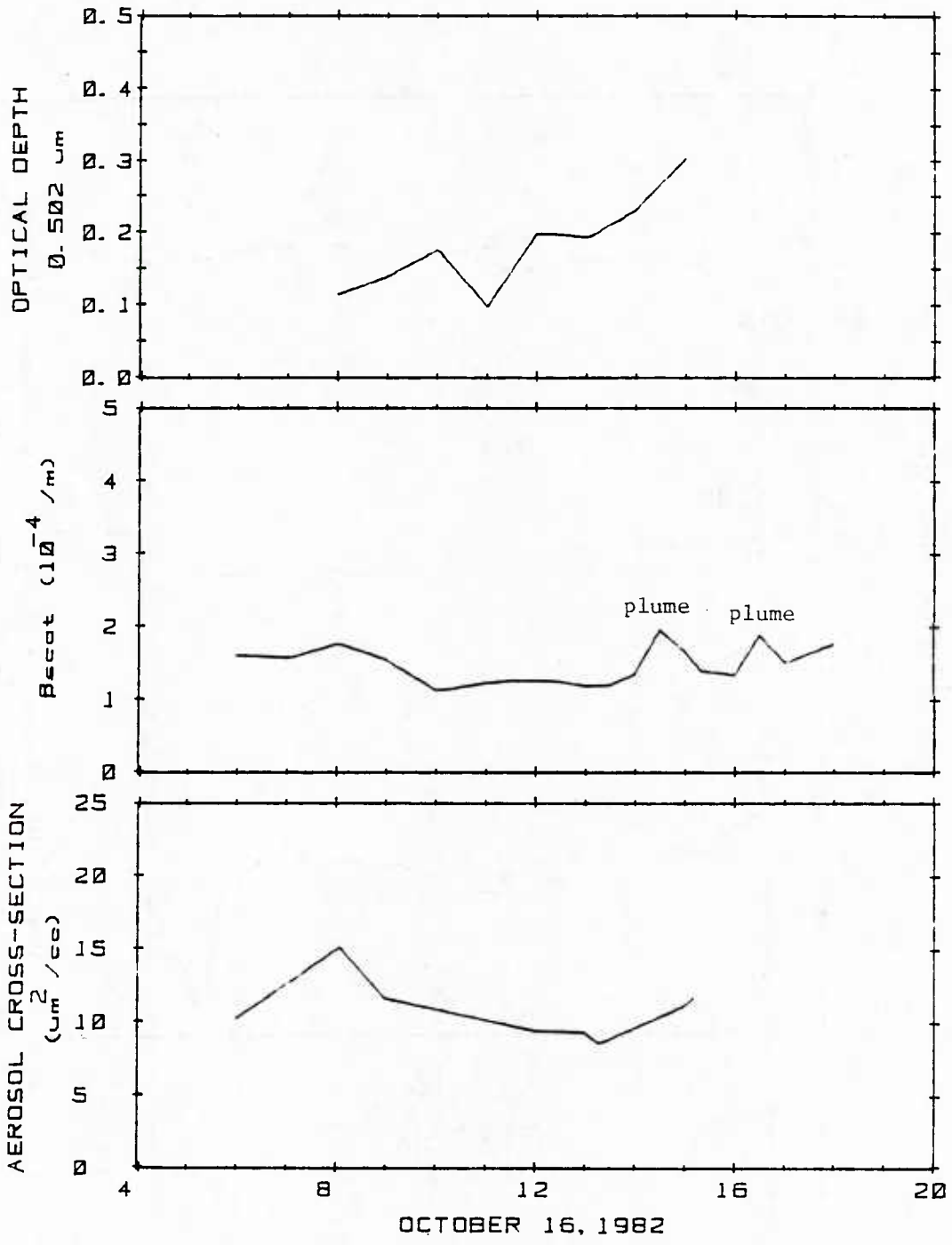

Figure 38: Optical Depth, β_{scat} and Aerosol Cross-section, 16 October 1982

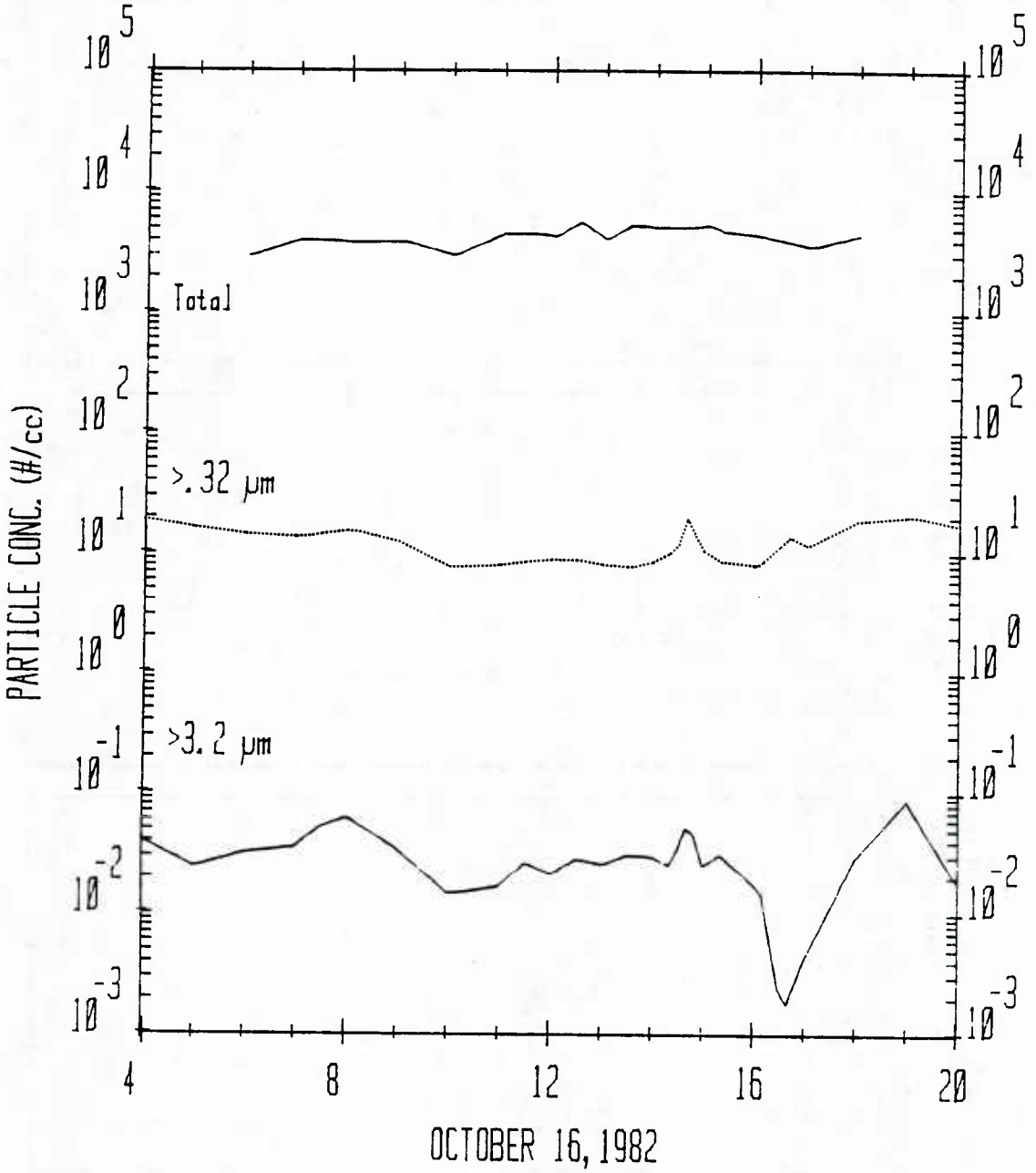

Figure 39: Aerosol Concentrations at Three Size Intervals, 16 October 1982

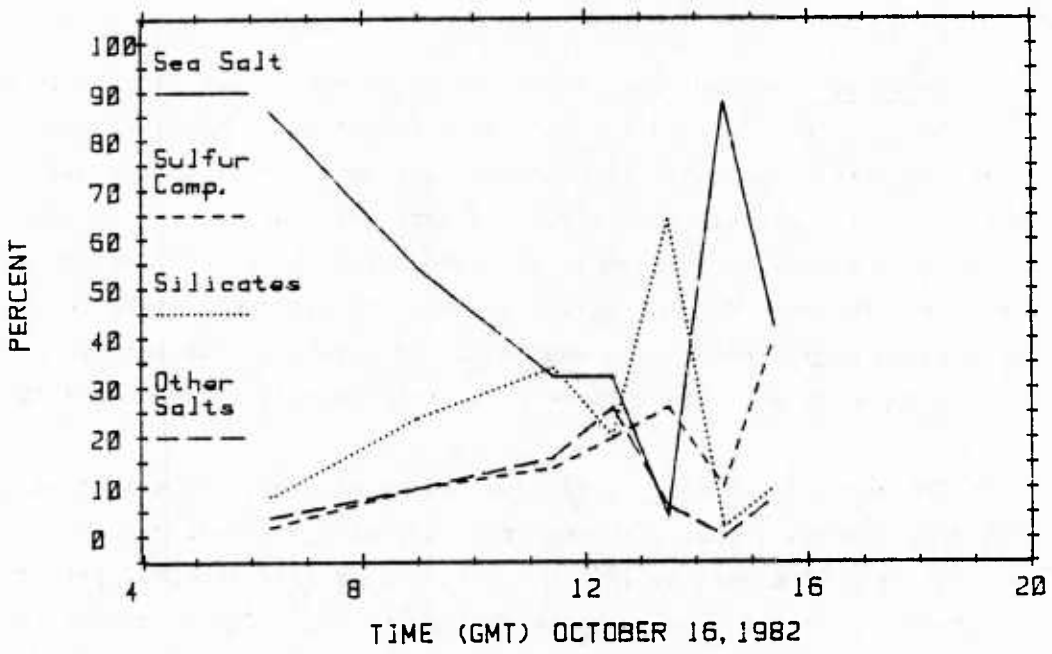

Figure 40: Chemical Classification of Aerosols > 0.2 μm dia, 16 October 1982

In crossing to colder water on the north side of the front, air temperatures decreased temporarily and returned to warmer values farther north. (See Figure 37.) The minimal changes observed across the front may have been due to northwesterly winds advecting cooler air over the warmer water at our early morning location.

The most significant feature of the day was the multiple interception of a plume at 1430 and 1630 on the northerly and southerly legs of the Estepona lines. Visibility was reduced to ∿24 km in both plume encounters. The steady increase in optical depth (Figure 38) during the northward track may be a result of plume material dispersed aloft in the area offshore of Estepona.

Aerosols Aerosol concentrations (Figure 39) were relatively constant throughout the day, except for the plume encounters of late afternoon, and exhibited little variation with change in location over the Gyre. In general, small-particle concentrations were greatest at mid-day, while minima at all size ranges were observed at ∿1000 GMT. The concentrations at sizes > 0.3 μm on average for this day are among the highest observed during the observation period and may be the result of a general contamination (trapped by a low-level inversion) from sources in the Gibraltar area.

The aerosol chemistry data provided in Figure 40 show that aerosol chemistry changed steadily through the day, with the NaCℓ proportion decreasing from 85% at 0715 to ∿5% by 1330 GMT. Increases in silicates (primarily) and sulfates accounted for the drop in NaCℓ particles. The plume observed at 1430 was apparently composed of NaCℓ particles like some of the other plumes encountered in the area; wind data are not available to help determine the specific source area of the plume material.

3.9 17 October 1982

Summary The early morning was spent retracing the Estepona line, continuing the southerly track of previous day and then retracing northward (at 0745) from ∿50 km offshore to ∿20 km offshore. From there, the ship headed to a point ∿10 km due east of Gibraltar, where it drifted until 1600 GMT on 18 October. (See Figure 8d). Encountered a plume twice: at ∿0500-0600 and again at ∿0830 in which visibility was reduced to ∿23 km. Skys remained nearly overcast all day with middle and high cloud and imbedded showers & thundershowers; light precip was observed at the ship at ∿1500. Winds shifted from ∿280° in the morning to SW at ∿4-7 m/s after 1000 GMT. Relative humidity dropped from ∿87% in the morning to ∿83% in the afternoon, while visibility lowered, leveling off at ∿35 km for the afternoon. The data for this day are presented in Figures 41-44.

The data for this day suggest that cold water on the north side of the Alboran Front may have been responsible for reducing air temperature over the Front.

Meteorology The surface trough along the northern shore weakened by mid-day as a weak cold front advanced from the northwest, passing through during the evening between 1800 and 2200 GMT. The shifting wind pattern, light winds of mid-day, and fluctuating temperature, RH and visibility records shown in Figure 41 reflect these events. At 1200, a thunderstorm was clearly visible to the NW in the far distance (over land). A low level inversion was based at 170 m at the BARTLETT's position at 0700 GMT.

The 0800-1000 track probably crossed the Alboran Front, and the drop in air temperature during that period may be due to the sea surface temperature gradient across the Front.

The plume encounters of ∿0530 and 0830 GMT occurred at approximately the same location on the southerly and northerly legs, respectively, of the Estepona line. This location was such that the Gibraltar area was directly

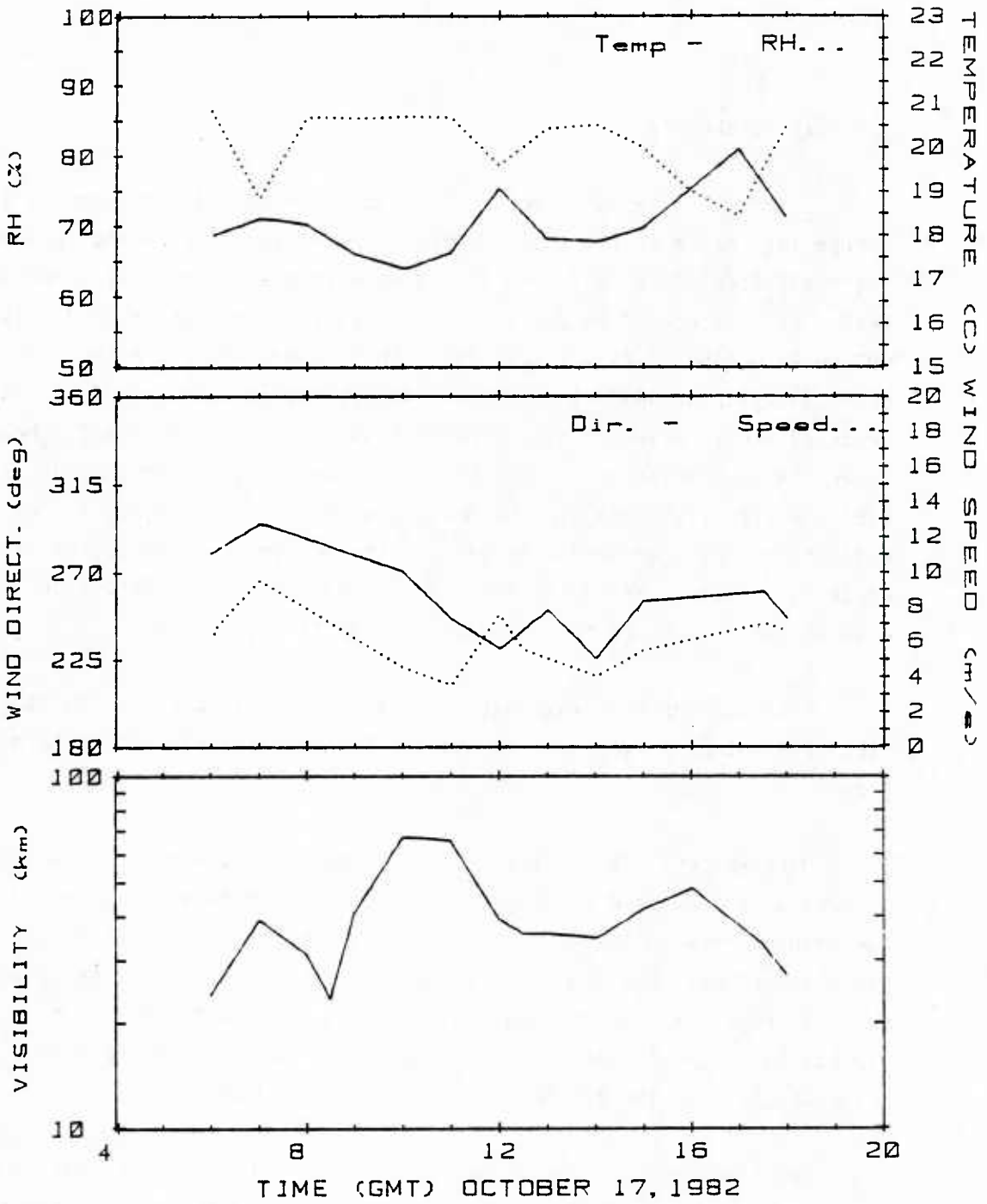

Figure 41: Meteorological Parameters, 17 October 1982

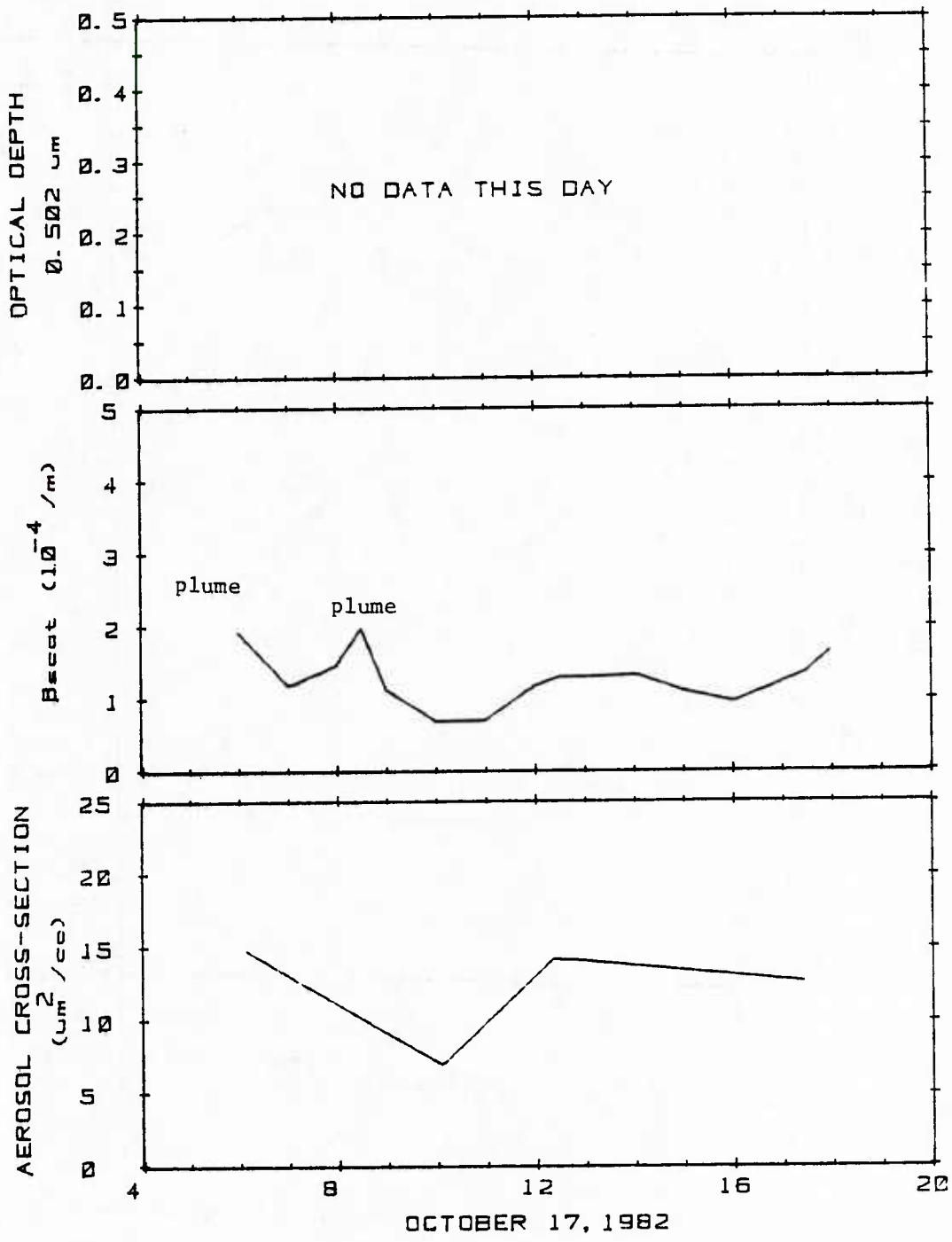

Figure 42: Optical Depth, β_{scat} and Aerosol Cross-section, 17 October 1982

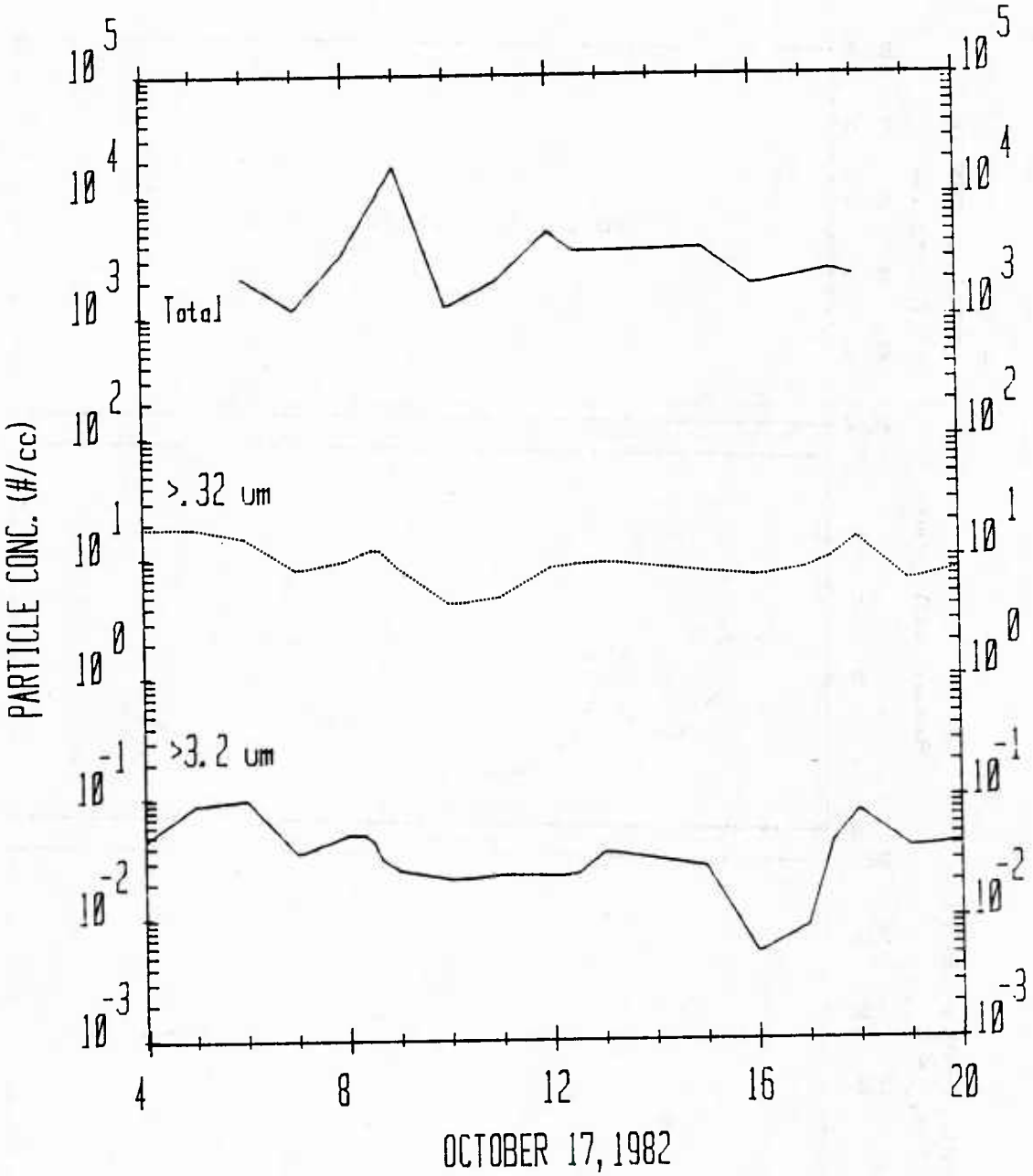

Figure 43: Aerosol Concentrations at Three Size Intervals, 17 October 1982

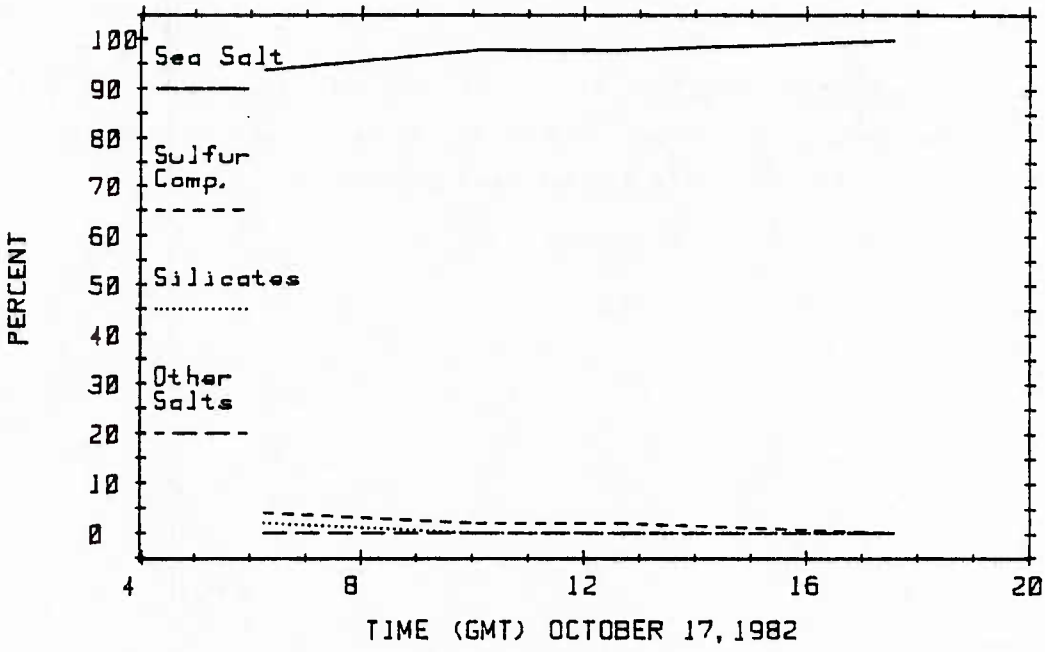

Figure 44: Chemical Classification of Aerosols > 0.2 μm dia, 17 October 1982

upwind and the apparent source of the observed plumes. From the 0900 position the plume was clearly visible (to the eye) coming from the direction of Gibraltar, and the mountains of Morocco could be seen in the background above the plume. The plume was not accompanied by changes in relative humidity or temperature.

Aerosols The plume encounters of 0530 and 0830 (Figure 42) were accompanied by increases in particle concentrations at all sizes (see Figure 43). (The apparent lag in increase at small sizes is probably a result of the lag in the measurement intervals for the Aitken particles.) The improvement in visibility at 1600 GMT and subsequent decrease through 1800 were accompanied, respectively, by decreases and then increases in particle concentrations at larger sizes.

Again aerosol concentrations at sizes > 0.3 μm were among the highest observed during the study and may be a result of contamination of the entire area of the NW corner of the Alboran by industrial sources in the Gibraltar area; low level inversion and general wind directions were appropriate.

Aerosol composition comprised almost entirely NaCℓ ; while no sample was taken directly in a plume, industrial sources (such as produced the plumes observed on other days) may explain this phenomenon.

3.10 18 October 1982

Summary The entire day was spent drifting and maintaining the previous day's position ∿10 km due E of Gibraltar; at 1605 GMT the ship departed, entering the Straits by ∿1800 (see Figure 8d). Near overcast skys with middle cloud, nimbostratus and scattered showers gave way to gusty NW wind, much drier air, improving visibility, and clearing skys (2/10 cloud cover by 1500) after the mid-morning passage of a strong cold front. Whitecaps began to form at 1330 and increased to moderate intensity as winds increased to >10 m/s by 1400. In late afternoon, visibility improved to >80 km as RH dropped to <60%. Four hours of sun photometry were obtained beginning at 1400. The data for this day are plotted in Figures 45-48.

No effects of the Alboran Gyre could be determined because of the ship's stationary position and no known 'gray shade' events occurred in the area.

Meteorology The frontal passage which occurred at ∿1000 GMT was preceded by showers which began at ∿0845; the intermittent shower activity ended by 1100. With the frontal passage, NW winds apparently increased through the mountain gap to the northwest of Gibraltar, producing whitecaps between the ship and the relatively flat area north of Gibraltar; no whitecaps were seen in the lee of or south of the rock over the Straits. During the day air temperatures increased, humidity dropped and visibility improved to 'unlimited'. (See Figure 45).

Aerosol plumes directly off Gibraltar area were advected over the ship at ∿0620, 1015 and 1130. Temporal resolution of the aerosol samples was not sufficient to define the composition of plume aerosols.

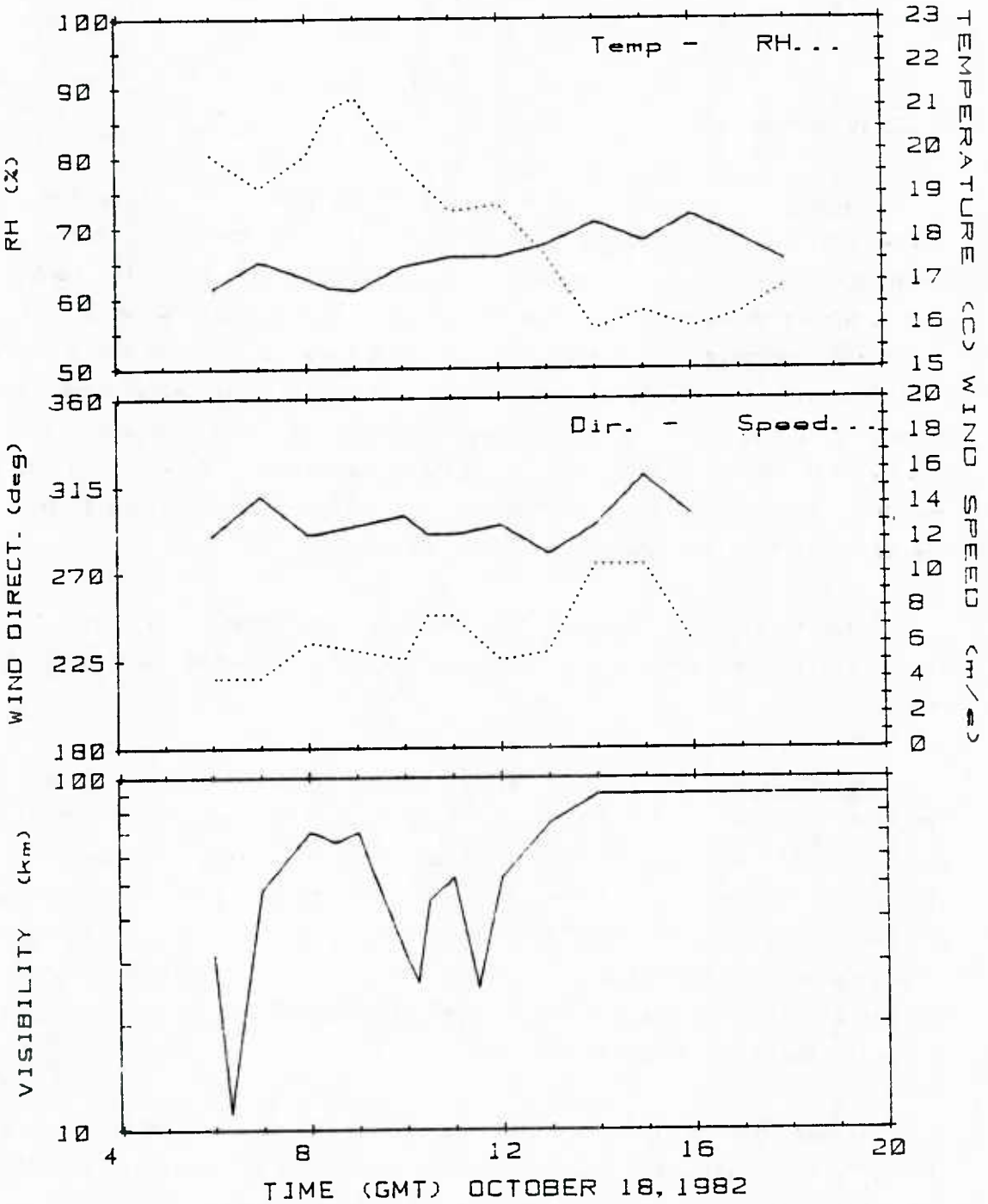

Figure 45: Meteorological Parameters, 18 October 1982

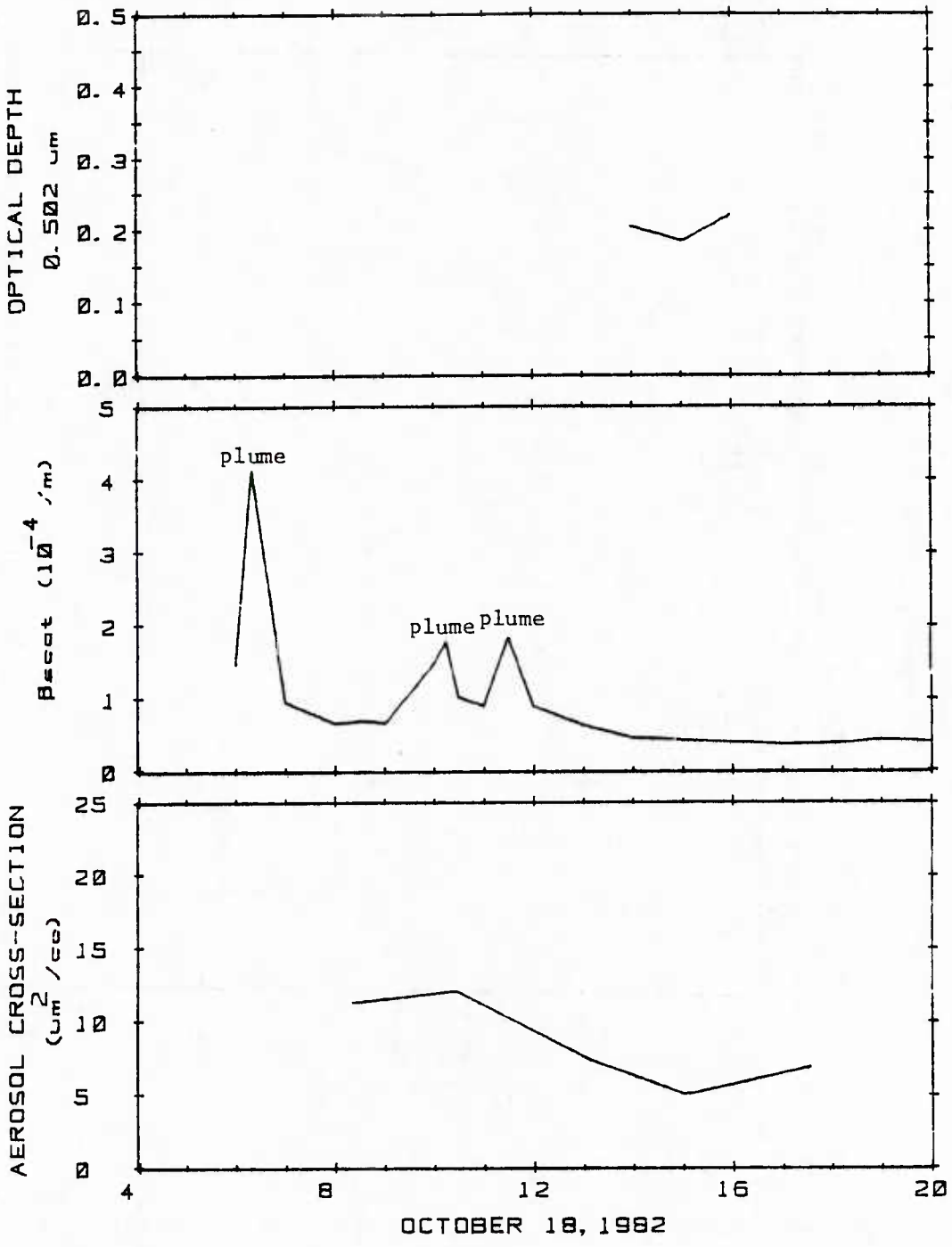

Figure 46: Optical Depth, β_{scat} and Aerosol Cross-section, 18 October 1982

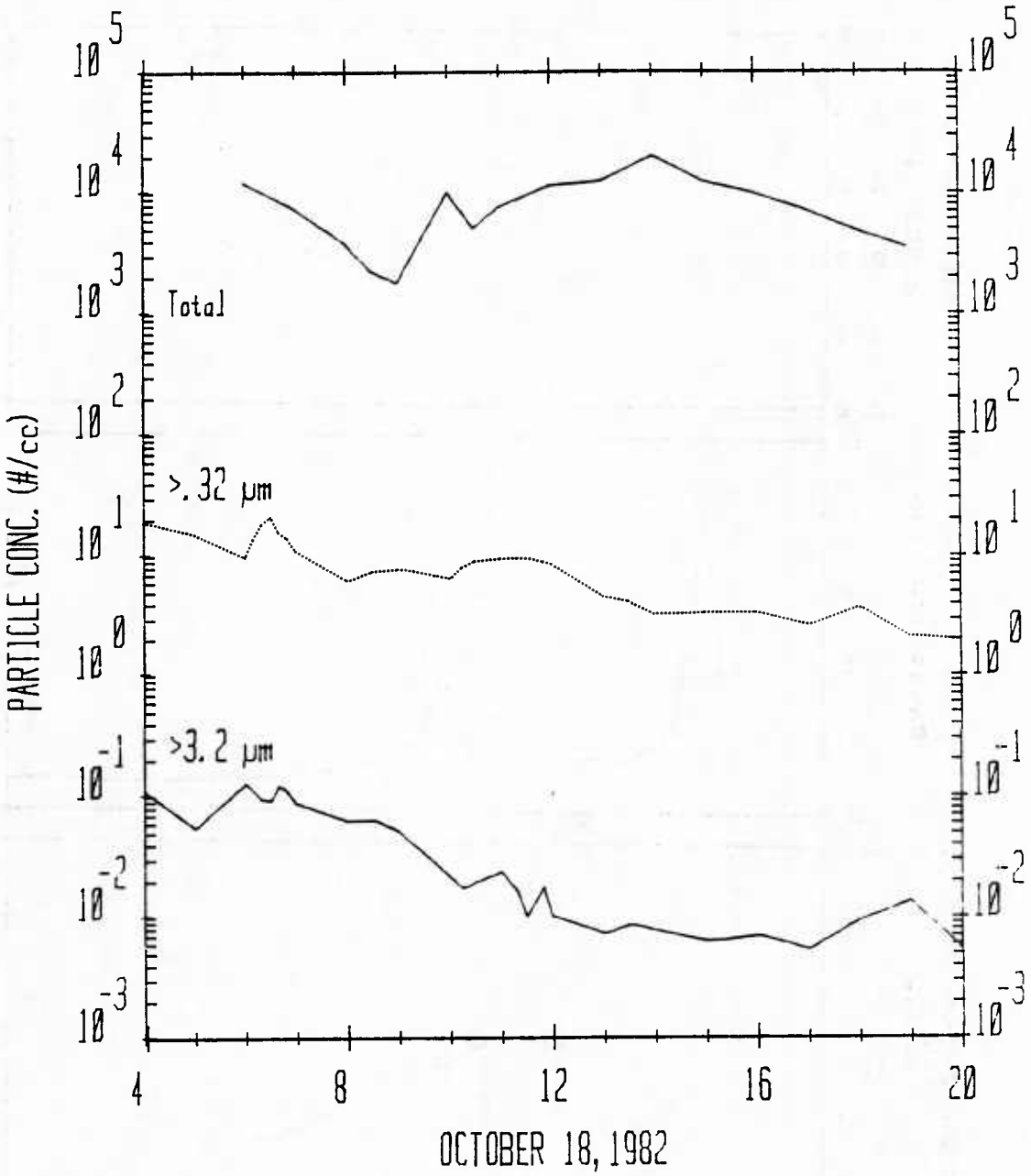

Figure 47: Aerosol Concentrations at Three Size Intervals, 18 October 1982

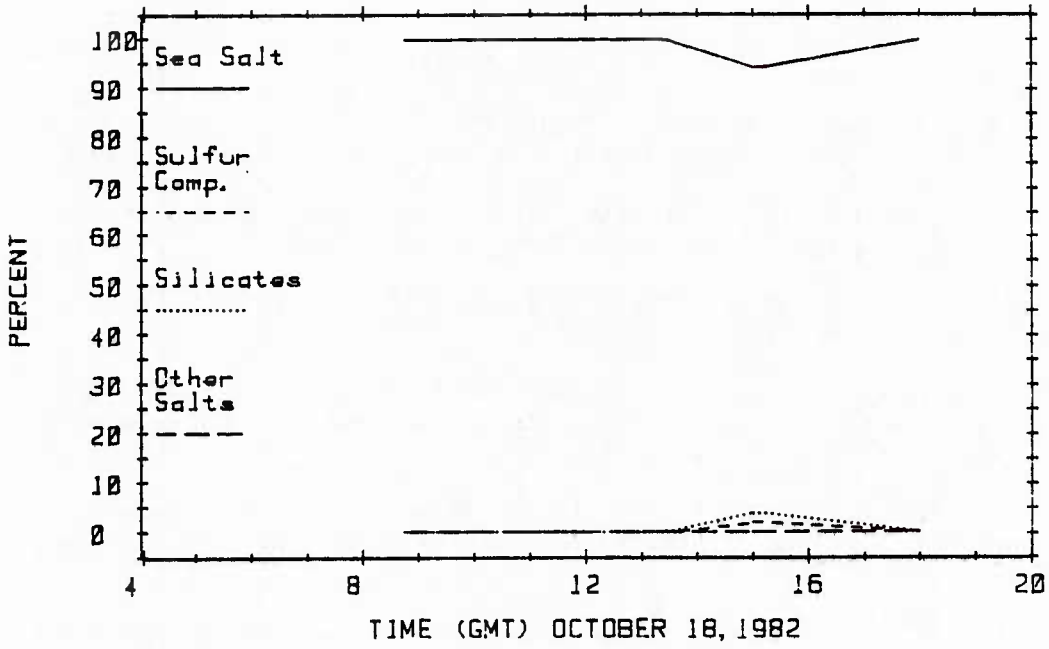

Figure 48: Chemical Classification of Aerosols >0.2 μm dia, 18 October 1982

Aerosols Maximum total particle concentration peaked at 1400 GMT; but concentrations ar larger sizes declined steadily through the day, increasing only in the aforementioned plumes. Large-particle concentrations in the morning were among the highest observed and in the afternoon among the lowest observed during the 10 day field study.

Aerosol composition was again puzzling: nearly all of the sampled aerosols on this day were sea salt (NaCℓ). The chief conclusion to be drawn from the frequent observation of NaCℓ particles and plumes is that local sources of NaCℓ -- either industrial or surf-generated in the Strait -- were apparently responsible for the numerous plumes of NaCℓ particles observed in the NW corner of the Alboran. If the NaCℓ particles are not of industrial origin, they may be of surf origin, generated in the surf-zone of the Strait and carried into the NW Alboran by a low-level jet. With a stable surface layer established by the colder water of the NW Alboran, the particles become trapped at low level and plumes are advected long distances without dispersion.

REFERENCES

1. Fett, R.W. and R.G. Isaacs, 1979: "Concerning Causes of 'Anomalous Gray Shades' in DMSP Visible Imagery," J. Appl. Met., 18, 10, pp 1340-1351.

2. Isaacs, R.G., 1980: "Investigation of the Effect of Low Level Maritime Haze on DMSP VHR and LF Imagery," NEPRF Report No. CR80-06, December, 120 pp.

3. Kinder, T.H., et al, 1982: "Operation Plan, DONDE VA?", NORDA Informal Prospectus, August 1982, 55 pp.

4. LaViolette, P.E. and J.L. Kerling, 1983: "An Analysis of Aircraft Data Collected in the Alboran Sea During Donde Va?, 6 Through 18 October 1982", NORDA Tech Note 222, July 1983, 126 pp.

5. Bergin, M.T. and T.H.Kinder, 1983: "Expendable Bathythermograph Measurements in the Western Alboran Sea, October 1982", NORDA Tech Note 224, August 1983, 96 pp.

6. LaViolette, P.E., 1983: "The Advection of Submesoscale Thermal Features in the Alboran Sea Gyre", NORDA Tech Note 240, Sept 1983, 36 pp.

7. Mack, E.J., U. Katz, and R.J. Pilié, 1976: "The Influence of Continental Aerosols on the Microphysics of Marine Fogs Occurring in Coastal Areas," Proceedings of the First Conference on Coastal Meteorology, 21-23 Sept., Virginia Beach, VA

8. Mack, E.J., U. Katz, C.W. Rogers, D.W.Gaucher, K.R. Piech, C.K. Akers, and R.J. Pilié, 1977: "An Investigation of the Meteorology, Physics, and Chemistry of Marine Boundary Layer Processes," Calspan Report No. CJ-6017-M-1, 122 pp.

9. Katz, U. and E.J. Mack, 1977: "Direct Measurements of Sea Spray Size Spectra at the NCSL Offshore Platform," Calspan Report No. CH-6067-M-1, 95 pp.

10. Mack, E.J. and U. Katz, 1977: "Measurements of Aerosol and Micrometeorological Characteristics of the Marine Boundary Layer in the Gulf of Mexico," Calspan Report, 64 pp.

11. Mack, E.J., R.J. Anderson, C.K. Akers, and T.A. Niziol, 1978: "Aerosol Characteristics of the Marine Boundary Layer of the North Atlantic and Mediterranean During May-June 1977," Calspan Report No. 6232-M-1, 215 pp.

12. Mack, E.J., C.K. Akers and T.A. Niziol, 1980: "Aerosols in the Marine Boundary Layer," Second Conf. on Coastal Meteorology, 30 Jan-1 Feb 1980, Los Angeles.

13. Mack, E.J., B.J. Wattle and J.T. Hanley, 1981: "Fog and Aerosol Characteristics During November 1980 at Meppen, West Germany," Calspan Report 6758-M-1, February, 84 pp.

14. Mack, E.J., J.T. Hanley, R.J. Pilié, C.K. Akers and B.J. Wattle, 1981: "Aerosol Composition in the Marine and Coastal Boundary Layer," Proceedings 25th Annual SPIE Symposium, Vol. 305, San Diego, 27-28 Aug.

15. Wattle, B.J., E.J. Mack and J.T. Hanley, 1983: "Aerosol Characteristics in the Marine Boundary Layer, Charleston (S. Carolina) to Canary Islands to Scotland, March-April 1983--A Data Volume", Calspan Rept. (in press)

16. Mack, E.J. 1983: "Aerosol Characteristics at Coastal Sites in Maine and Florida,"Calspan Rept. (in press)

17.. Hanel, G., 1976: "The Properties of Atmospheric Aerosol Particles as Functions of the Relative Humidity at Thermodynamic Equilibirum with the Surrounding Moist Air," Advances in Geophysics, Vol 19, Ed. H.E. Landsburg & J. VanMieghem, Academic Press, New York, pp 74-171.

APPENDIX A

CALSPAN'S DATA LOG

An hourly observation schedule was maintained aboard the BARTLETT, principally during daylight hours from 0600 to 1900 GMT, 9 through 18 October 1982. Occasionally, special observations were made at half-hour intervals or later into the evening hours. The resultant data set comprised measurements of aerosol concentrations at various sizes, observations and measurements of supporting meteorological variables, and aerosol samples for subsequent chemical and large-particle-concentration analyses as listed in Table 1. All measurements and samples were obtained from the flying bridge area of the BARTLETT at a height of ∿10 m above the sea surface.

The data obtained by Calspan during the Alboran Sea experiment are provided in this section in reduced form, in an 'hourly log' format with minimal interpretation, for objective use by other participants in the field experiment. The data set for each day of Calspan's participation is presented on a single page in the Log which follows. Explanations of the data-columns of the Log and descriptions of the measurement techniques are provided at the end of this section.

DATE: OCTOBER 9, 1982

TIME (GMT)	TOTAL PARTICLE CONC. (#/cc)	ROYCO CONC. >.3 µm (#/cc)	Bscat x0.0001/m	VSBY (km)	WET BULB TEMP (C)	DRY BULB TEMP (C)	RH (%)
7:00	2600	4.64	1.9	23.5	15.3	18.2	74
8:00	3900	5.84	2.4	19.5	15.3	18.1	75
8:45	-	8.50	3.8	12.0	-	-	-
9:00	4500	7.15	2.8	16.5	-	-	-
10:00	2700	5.85	1.8	26.0	15.3	17.4	80
11:00	-	-	-	-	15.3	17.2	82
12:00	5000	5.49	0.8	80.0	16.7	19.3	76
13:00	8000	5.47	0.6	70.0	16.9	19.2	80
14:00	-	6.02	0.8	60.0	16.9	19.4	78
15:00	2700	6.29	0.9	53.0	17.0	18.8	81
16:00	2900	7.89	0.7	65.0	17.1	19.1	82
17:00	4700	8.88	0.7	67.0	17.4	19.8	79
18:00	3400	8.00	0.5	86.5	16.8	19.3	78
19:00	4000	8.98	0.6	78.0	-	-	-

TIME (GMT)	WIND DIRECTION (deg)	WIND SPEED (m/s)	CLOUD COVER FRACTION	SUN PHOTOMETRY 0.4-1.1µ λ (ly/min)	SUN PHOTOMETRY 0.502µ λ (0.01 ly/min)	CLOUD COVER	Drop Sample (O) or Casella (X)
6:25	*270	9.0					
7:00	*265	8.5	0.35	0.27	0.17	Ci St	
8:00	*275	5.0	0.90	-	-	Ci overcast	
9:00	*210	2.5	0.90	-	-	Ci overcast	O X
10:00	*305	3.5	0.90	-	-	Ci overcast	
11:00	*305	3.5	0.90	-	-	-	
12:00	*260	6.0	0.90	-	-	Alto cu & St	O X
13:00	*280	8.0	0.90	-	-	-	
14:00	*235	5.0	0.90	-	-	-	
15:00	*240	7.5	1.00	-	-	-	O X
16:00	*255	10.0	1.00	-	-	-	
17:00	*260	9.5	0.90	-	-	-	
18:00	*275	7.0	0.60	-	-	-	X
19:00	-	-	-	-	-	-	

DATE: OCTOBER 10, 1982

TIME (GMT)	TOTAL PARTICLE CONC. (#/cc)	ROYCO CONC. >.3 μm (#/cc)	Bscat x0.0001/m	VSBY (km)	WET BULB TEMP (C)	DRY BULB TEMP (C)	RH (%)
6:00	1050	3.83	0.6	70.0	17.7	18.9	90
7:00	1800	4.30	0.8	55.0	18.1	18.9	92
8:00	2900	3.82	0.8	60.0	16.3	17.4	89
8:23	-	6.50	1.3	35.5	-	-	-
8:33	11000	6.30	2.8	16.5	-	-	-
8:45	30000	6.10	1.2	39.0	-	-	-
9:00	16500	4.38	0.9	52.0	15.8	18.3	77
10:00	26000	5.92	0.9	48.0	16.4	18.2	93
11:00	7000	7.21	0.8	60.0	16.4	18.2	84
12:00	5200	5.31	0.8	60.0	16.6	18.3	84
13:00	13000	8.92	0.9	48.0	16.3	18.8	32
14:00	7500	5.79	0.7	65.0	17.1	19.7	78
15:00	3400	6.49	0.9	48.0	17.5	19.4	83
16:00	1700	4.59	0.8	60.0	16.1	20.4	64
17:00	1400	8.05	1.0	47.5	16.4	20.0	69
18:00	2500	5.64	0.7	65.0	15.3	19.3	72
19:00	1200	8.70	0.9	48.0	-	-	-
20:00	2700	7.67	1.0	44.5	-	-	-
21:30	5400	14.08	1.8	26.0	-	-	-
22:00	3300	6.02	1.1	43.5	15.9	19.6	66

TIME (GMT)	WIND DIRECTION (deg)	WIND SPEED (m/s)	CLOUD COVER FRACTION	SUN PHOTOMETRY 0.4-1.1μ λ (ly/min)	0.502μ λ (0.01 ly/min)	CLOUD COVER	Drop Sample (O) or Casella (X)
6:00	-	-	0.70	-	-	-	X
7:00	*235	4.5	0.20	0.13	0.08	Ci	
8:00	*275	4.5	0.10	0.62	0.55	Ci	
8:23	-	-	-	-	-	-	O X
8:33	-	-	-	0.75	0.73	(in plume)	
8:45	-	-	-	-	-	-	O
9:00	*280	0.5	0.10	0.82	0.75	Ci	X
10:00	-	-	0.10	0.89	0.90	fair wx cu	
11:00	*230	6.0	0.20	0.91	0.96	fair wx cu	
12:00	*240	10.5	0.10	0.94	1.01	fair wx cu	O X
13:00	*295	10.0	0.10	0.93	1.01	fair wx cu	
14:00	*250	10.0	~0.10	0.90	0.96	fair wx cu	
15:00	*270	10.0	0.00	0.83	0.90	clear	O X
16:00	-	-	0.00	0.67	0.63	thin Ci to NW	
17:00	*270	12.5	<0.10	0.32	0.23	Ci to NW horizon	
18:00	*280	11.5	<0.10	-	-	-	O X
19:00	-	-	0.00	-	-	-	
20:00	-	-	0.00	-	-	-	
21:30	-	-	0.00	-	-	-	X
22:00	-	-	0.00	-	-	-	

DATE: OCTOBER 11, 1982

TIME (GMT)	TOTAL PARTICLE CONC. (#/cc)	ROYCO CONC. >.3 µm (#/cc)	Bscat x0.0001/m	VSBY (km)	WET BULB TEMP (C)	DRY BULB TEMP (C)	RH (%)
6:00	4400	4.17	0.9	48.0	18.6	19.7	73
7:00	1800	4.62	0.9	52.0	16.5	19.7	72
8:00	1500	3.56	0.8	60.0	16.8	20.0	73
9:00	1700	3.27	0.8	60.0	17.7	21.5	68
10:00	1800	4.08	0.9	50.5	17.7	21.3	70
11:00	1800	2.58	0.8	57.0	18.1	21.1	74
12:00	1700	2.54	0.7	65.0	17.8	21.3	71
13:00	-	2.30	0.7	67.0	-	-	-
14:00	1800	3.64	0.7	65.0	17.3	21.8	66
15:00	2300	6.52	1.0	45.0	17.4	20.6	73
16:00	2800	7.29	1.2	37.0	18.1	21.7	70
17:00	2800	7.28	1.5	31.0	18.3	20.7	79
18:00	3000	8.18	1.8	25.0	17.9	19.8	83
19:00	2800	9.30	1.9	23.5	17.9	20.1	80

TIME (GMT)	WIND DIRECTION (deg)	WIND SPEED (m/s)	CLOUD COVER FRACTION	SUN PHOTOMETRY 0.4-1.1u λ (ly/min)	0.502u λ (0.01 ly/min)	CLOUD COVER	Drop Sample (O) or Casella (X)
6:00	-	-	0.00	-	-	clear, no clouds	O X
7:00	*305	2.0	0.00	0.26	0.12	clear, no clouds	
8:00	-	0.0	0.00	0.64	0.57	clear, no clouds	X
9:00	-	0.0	0.00	0.79	0.80	clear, no clouds	O X
10:00	* 70	1.0	0.00	0.87	0.91	clear, no clouds	
11:00	* 60	1.0	0.00	0.92	0.96	clear, no clouds	
12:00	-	0.0	0.00	0.94	1.01	clear, no clouds	O X
13:00	-	0.0	0.00	0.92	0.98	clear, no clouds	
14:00	-	0.0	0.00	0.89	0.91	clear, no clouds	
15:00	-	0.0	0.00	0.79	0.76	clear, no clouds	O X
16:00	-	0.0	0.10	0.62	0.50	Ci to West	
17:00	-	0.0	0.50	0.14	0.08	thin Ci, lt sfc haze	
18:00	-	0.0	0.20	-	-	Ci to East	O X
19:00	-	0.0	0.00	-	-	-	

DATE: OCTOBER 12, 1982

TIME (GMT)	TOTAL PARTICLE CONC. (#/cc)	ROYCO CONC. >.3 μm (#/cc)	Bscat x0.0001/m	VSBY (km)	WET BULB TEMP (C)	DRY BULB TEMP (C)	RH (%)
6:00	3400	19.64	2.3	20.0	15.4	17.1	84
7:00	3200	12.26	1.8	26.0	15.7	16.7	89
8:00	2900	5.14	1.0	45.0	15.4	16.8	86
9:00	4300	7.60	1.0	47.5	15.1	17.3	79
10:00	3300	5.27	0.8	60.0	16.6	19.0	79
11:00	4700	20.84	3.2	14.5	16.0	18.4	79
12:00	4500	9.81	1.2	38.0	17.9	20.1	80
12:18	3600	9.09	1.2	38.0	-	-	-
13:00	3400	8.25	1.2	37.0	17.9	21.2	72
14:00	3800	8.24	1.1	43.5	18.4	21.7	72
15:00	3400	4.99	0.7	62.5	18.9	22.3	73
16:00	-	5.04	-	-	19.3	21.7	81
17:00	-	-	-	-	18.9	21.3	81
17:15	2700	5.76	0.9	50.5	-	-	-
18:20	2800	8.53	1.1	41.0	18.3	21.3	76

TIME (GMT)	WIND DIRECTION (deg)	WIND SPEED (m/s)	CLOUD COVER FRACTION	SUN PHOTOMETRY 0.4-1.1μ λ (ly/min)	SUN PHOTOMETRY 0.502μ λ (0.01 ly/min)	CLOUD COVER	Drop Sample (O) or Casella (X)
3:44	*270	2.0					
6:00	-	-	0.30	-	-	-	O X
7:00	-	-	0.30	0.24	0.11	-	
8:00	*	0.0	0.35	0.69	0.53	-	
9:00	-	-	0.35	0.84	0.76	-	O X
10:00	-	-	0.50	0.84	0.78	-	
11:00	-	-	0.70	0.93	1.00	thin Ci (in plume)	O X
12:00	-	-	0.75	0.93	0.90	thin Ci	
12:18	-	-	0.85	-	-	-	O X
13:00	-	-	0.90	0.92	0.86	thin Ci	
14:00	-	-	0.85	0.87	0.81	thin Ci	
15:00	-	-	0.85	0.83	0.76	Ci	O X
16:00	-	-	0.90	0.62	0.50	Ci	
17:00	-	-	0.85	0.23	0.11	Ci	
17:15	-	-	-	-	-	-	
18:20	-	-	0.80	-	-	-	

DATE: OCTOBER 13, 1982

TIME (GMT)	TOTAL PARTICLE CONC. (#/cc)	ROYCO CONC. >.3 μm (#/cc)	Bscat x0.0001/m	VSBY (km)	WET BULB TEMP (C)	DRY BULB TEMP (C)	RH (%)
6:00	3000	11.25	1.3	34.5	16.6	18.3	80
7:00	1300	12.23	1.4	32.5	16.7	19.1	79
8:00	2800	11.43	1.3	35.5	17.0	18.9	82
8:30	4300	10.55	1.2	37.0	-	-	-
9:00	3500	10.71	1.3	34.5	16.7	19.4	75
10:00	4000	8.63	1.2	39.0	16.7	19.5	75
11:00	4000	9.29	1.2	38.0	16.8	19.2	78
12:00	5400	10.33	1.4	33.0	16.7	20.0	71
13:00	6600	9.49	1.2	37.0	16.6	19.7	73
14:00	10000	9.49	1.3	36.5	16.2	20.1	67
15:00	9500	10.50	1.1	43.5	16.7	20.3	69
16:00	-	10.78	0.9	52.0	16.7	20.4	69
17:00	-	-	-	-	16.7	20.2	71
17:30	8100	9.46	0.9	53.0	-	-	-
18:00	-	9.75	0.9	52.0	16.6	19.7	73
18:45	8000	10.66	0.9	50.5	-	-	-
20:00	-	10.70	0.9	51.7	-	-	-
21:30	-	13.60	1.0	47.4	-	-	-
22:30	-	14.70	1.0	44.7	-	-	-
23:30	-	14.10	1.1	43.4	-	-	-

TIME (GMT)	WIND DIRECTION (deg)	WIND SPEED (m/s)	CLOUD COVER FRACTION	SUN PHOTOMETRY 0.4-1.1μ λ (ly/min)	SUN PHOTOMETRY 0.502μ λ (0.01 ly/min)	CLOUD COVER	Drop Sample (O) or Casella (X)
6:00	*265	10.0	0.85	-	-	-	O X
7:00	-	-	0.80	0.44	0.30	Ci & Ci St	
8:00	*245	6.0	0.70	0.78	0.67	Ci	
8:30	265	13.5	0.65	-	-	-	O X
9:00	*265	12.5	0.55	0.92	0.85	Ci	
10:00	*270	13.0	0.45	0.96	0.93	Ci	
11:00	*280	13.0	0.30	0.96	0.93	Ci	
12:00	*270	13.0	0.20	1.22	1.00	Ci	O X
13:00	*270	14.0	0.10	0.99	0.98	Ci	
14:00	270	14.5	<0.10	0.96	0.95	Ci to NE	
15:00	270	14.5	<0.10	0.92	0.83	Ci to N & E	O X
16:00	-	-	<0.10	0.77	-	Ci to N & E	
17:00	-	-	-	-	-	-	
17:30	270	17.5	0.00	-	-	-	O X
18:00	-	-	-	-	-	-	
18:45	270	15.5	-	-	-	-	

DATE: OCTOBER 14, 1982

TIME (GMT)	TOTAL PARTICLE CONC. (#/cc)	ROYCO CONC. >.3 μm (#/cc)	Bscat x0.0001/m	VSBY (km)	WET BULB TEMP (C)	DRY BULB TEMP (C)	RH (%)
6:00	900	3.75	0.9	53.0	16.8	19.4	85
7:00	1550	3.84	0.9	50.5	16.4	17.9	86
7:35	5600	6.56	0.5	86.5	14.9	17.8	74
8:00	2100	5.91	0.5	97.5	-	-	-
8:30	1700	6.59	0.4	111.5	14.3	18.4	65
9:00	3900	7.08	0.4	104.0	13.9	18.2	61
10:00	2100	5.07	0.4	120.0	13.6	18.2	59
11:00	6500	4.91	0.4	120.0	13.2	18.4	51
12:00	13500	5.95	0.4	104.0	14.4	18.6	63
13:00	26000	10.30	1.3	36.0	14.4	17.4	71
14:00	16500	9.89	0.8	55.0	15.3	18.6	72
15:00	10000	8.41	0.7	67.0	15.4	18.3	75
16:00	12000	8.48	0.7	67.0	15.7	18.4	75
17:00	6800	6.35	0.6	78.0	14.7	18.3	68
18:00	6000	6.24	0.6	74.5	14.4	18.4	66
19:00	7300	7.54	0.7	65.0	-	-	-

TIME (GMT)	WIND DIRECTION (deg)	WIND SPEED (m/s)	CLOUD COVER FRACTION	SUN PHOTOMETRY 0.4-1.1μ λ (ly/min)	SUN PHOTOMETRY 0.502μ λ (0.01 ly/min)	CLOUD COVER	Drop Sample (O) or Casella (X)
6:00	270	14.5	>0.90	-	-	-	O X
7:00	275	12.0	1.00	-	-	heavier to W & N	
7:35	280	11.5	1.00	-	-	-	O X
8:00	-	-	1.00	-	-	-	
8:30	-	-	1.00	-	-	-	
9:00	280	12.0	1.00	-	-	-	O X
10:00	300	7.5	>0.90	-	-	clearing to N	
11:00	-	-	0.90	-	-	-	
12:00	-	-	0.90	-	-	-	O X
13:00	255	7.5	0.85	0.84	0.81	thin Ci St	O X
14:00	245	5.0	0.75	0.84	0.78	Ci St (broken)	
15:00	235	5.0	0.80	0.87	0.78	Ci St (broken)	O X
16:00	240	6.0	0.90	-	-	thickening Ci	
17:00	290	5.0	0.90	-	-	-	
18:00	-	2.0	1.00	-	-	-	O X
19:00	230	3.5	-	-	-	-	

DATE: OCTOBER 15, 1982

TIME (GMT)	TOTAL PARTICLE CONC. (#/cc)	ROYCO CONC. >.3 µm (#/cc)	Bscat x0.0001/m	VSBY (km)	WET BULB TEMP (C)	DRY BULB TEMP (C)	RH (%)
6:00	3200	7.64	0.9	52.0	13.9	15.7	83
7:00	4300	-	0.7	62.5	13.8	15.6	83
8:00	3500	7.06	0.8	55.0	13.8	15.6	83
9:00	3800	6.89	0.8	57.0	14.4	16.8	80
9:20	2500	5.75	0.6	70.0	-	-	-
10:00	2700	5.28	0.7	65.0	14.4	16.7	80
11:00	6600	5.91	0.7	62.5	14.1	17.1	72
12:00	8500	7.48	1.0	44.5	15.5	18.7	72
13:00	9100	6.24	0.8	55.0	16.7	20.1	71
14:00	8000	5.36	0.7	62.5	16.4	20.1	70
15:00	3650	6.54	0.9	53.0	16.3	20.1	68
16:00	4200	8.72	1.1	41.0	15.7	18.9	72
17:00	3800	11.48	1.4	32.5	15.8	19.4	69
18:00	2900	12.65	1.6	29.5	15.7	18.1	78

TIME (GMT)	WIND DIRECTION (deg)	WIND SPEED (m/s)	CLOUD COVER FRACTION	SUN PHOTOMETRY 0.4-1.1µ λ (ly/min)	0.502µ λ (0.01 ly/min)	CLOUD COVER	Drop Sample (O) or Casella (X)
1:20	*320	4.5					
3:10	*280	1.5					
6:00	270	2.0	0.20	-	-	-	O X
7:00	285	2.5	0.20	0.23	0.11	Ci	
8:00	-	-	0.25	0.64	0.51	Ci	
9:00	285	3.0	0.40	0.79	0.70	thin Ci	O X
9:20	-	-	0.65	-	-	-	
10:00	255	2.5	0.75	0.82	0.76	thin Ci	
11:00	-	-	0.80	0.77	0.75	thin Ci	
12:00	270	3.5	0.75	0.94	0.91	thick & thin Ci	O X
13:00	245	2.5	0.85	0.77	0.73	thicker Ci	
14:00	-	-	0.90	0.53	0.50	thick Ci	
15:00	290	5.0	0.90	-	-	-	O X
16:00	290	6.0	0.90	-	-	-	
17:00	280	6.5	0.90	-	-	-	
18:00	260	4.0	0.75	-	-	-	O
21:26	* 90	4.0					

DATE: OCTOBER 16, 1982

TIME (GMT)	TOTAL PARTICLE CONC. (#/cc)	ROYCO CONC. >.3 μm (#/cc)	Bscat x0.0001/m	VSBY (km)	WET BULB TEMP (C)	DRY BULB TEMP (C)	RH (%)
6:00	2900	13.87	1.3	28.0	14.1	17.6	68
7:00	3950	13.24	1.6	29.5	15.1	17.8	74
8:00	3700	15.29	1.8	26.0	16.0	17.3	88
9:00	3800	12.06	1.5	30.0	15.8	17.8	82
10:00	2900	7.56	1.1	41.0	15.5	18.1	77
11:00	4500	8.04	1.2	37.0	16.1	18.4	80
11:30	4500	9.01	1.3	36.5	15.9	18.4	77
12:00	4200	8.94	1.3	36.5	15.6	17.9	78
12:30	5600	8.70	1.2	37.0	15.5	17.6	80
13:00	4000	7.92	1.2	39.0	15.0	17.3	79
13:30	5300	7.67	1.2	38.0	15.2	17.7	77
14:00	5000	8.70	1.4	33.0	15.7	17.9	79
14:30	5000	12.06	1.9	23.5	16.1	18.1	82
15:00	5300	10.36	1.7	27.0	15.1	17.2	79
15:20	4600	7.87	1.4	33.0	15.5	17.3	84
16:00	4300	7.89	1.3	34.5	16.1	17.4	87
17:00	3500	11.55	1.5	30.5	15.5	18.6	72
18:00	4500	17.59	1.8	26.0	15.4	18.9	69

TIME (GMT)	WIND DIRECTION (deg)	WIND SPEED (m/s)	CLOUD COVER FRACTION	SUN PHOTOMETRY 0.4-1.1μ λ (1ly/min)	0.502μ λ (.01 ly/min)	CLOUD COVER	Drop Sample (O) or Casella (X)
0:15	*320	2.5					
3:00	*300	1.5					
6:00	240	1.0	0.20	-	-	-	O
7:00	260	1.5	0.10	0.18	0.08	Ci	
8:00	270	1.0	0.10	0.53	0.43	Ci; lt haze	O
9:00	-	-	0.10	0.72	0.67	Ci	O X
10:00	260	2.0	0.10	0.82	0.78	Ci	
11:00	-	-	0.15	0.87	0.96	Ci	
11:30	340	2.5	0.15	-	-	-	O X
12:00	-	-	0.20	0.89	0.85	Ci	
12:30	-	-	0.20	-	-	-	O X
13:00	-	-	0.20	0.89	0.85	Ci & Alto St	
13:30	-	-	0.20	-	-	-	O X
14:00	-	-	0.10	0.82	0.78	Ci	
14:30	-	-	<0.10	-	-	-	O X
15:00	-	-	<0.10	0.70	0.58	Ci (in plume)	
15:20	80	4.0	<0.10	-	-	-	O X
16:00	-	-	0.10	0.16	0.18	Ci St	
17:00	-	-	0.15	-	-	-	
18:00	250	8.5	0.20	-	-	-	
21:50	*270	9.0					

DATE: OCTOBER 17, 1982

TIME (GMT)	TOTAL PARTICLE CONC. (#/cc)	ROYCO CONC. >.3 µm (#/cc)	Bscat x0.0001/m	VSBY (km)	WET BULB TEMP (C)	DRY BULB TEMP (C)	RH (%)
6:00	8100	14.70	1.9	24.0	16.6	18.0	87
7:00	1150	8.10	1.2	39.0	15.5	18.4	75
8:00	3400	9.83	1.3	31.0	16.7	18.2	87
9:00	17500	8.36	1.1	41.0	16.0	17.6	86
10:00	1200	4.54	0.7	67.0	15.7	17.2	87
11:00	2000	4.80	0.7	65.0	16.1	17.6	85
12:00	5000	8.40	1.2	39.0	16.7	19.1	79
12:30	3400	8.91	1.3	35.5	-	-	-
13:00	-	9.16	1.3	35.5	16.2	17.9	83
14:00	-	-	1.3	34.5	16.2	17.8	83
15:00	3700	7.46	1.1	42.0	16.1	18.2	82
16:00	1800	6.91	0.9	48.0	16.2	19.1	75
17:00	2700	8.12	1.1	43.5	16.6	19.9	71
17:30	2400	9.89	1.4	33.0	-	-	-
18:00	2100	13.57	1.7	27.0	16.7	18.4	85

TIME (GMT)	WIND DIRECTION (deg)	WIND SPEED (m/s)	CLOUD COVER FRACTION	SUN PHOTOMETRY 0.4-1.1µ λ (ly/min)	SUN PHOTOMETRY 0.502µ λ (0.01 ly/min)	CLOUD COVER	Drop Sample (O) or Casella (X)
1:05	280	7.5					
6:00	280	6.5	>0.90	-	-	overcast	O X
7:00	295	9.5	1.00	-	-	-	
8:00	-	-	1.00	-	-	-	
9:00	-	-	0.90	-	-	-	
10:00	270	4.5	0.90	-	-	-	O X
11:00	245	3.5	0.70	-	-	-	
12:00	230	7.5	0.70	-	-	Thunderstorm to NW	
12:30	240	5.5	>0.90	-	-	-	O X
13:00	250	5.0	>0.90	-	-	Nimbostratus to W	
14:00	225	4.0	1.00	-	-	-	
15:00	255	5.5	>0.90	-	-	lt shower	
16:00	-	-	>0.90	-	-	-	
17:30	260	7.0	1.00	-	-	Nimbostratus	O X
18:00	245	6.5	1.00	-	-	-	

DATE: OCTOBER 18, 1982

TIME (GMT)	TOTAL PARTICLE CONC. (#/cc)	ROYCO CONC. >.3 µm (#/cc)	Bscat x0.0001/m	VSBY (km)	WET BULB TEMP (C)	DRY BULB TEMP (C)	RH (%)
6:00	12000	13.25	1.5	31.0	14.9	16.8	81
6:20	-	20.16	4.1	11.2	-	-	-
7:00	7250	10.27	0.9	48.0	14.9	17.4	76
8:00	3700	6.14	0.6	70.0	15.0	17.1	82
8:30	2200	7.47	0.7	65.0	15.5	16.8	87
9:00	1750	7.77	0.6	70.0	15.6	16.8	89
10:00	10000	8.35	1.5	31.0	15.2	17.3	79
10:30	5000	9.02	1.0	45.0	-	-	-
11:00	7600	9.49	0.9	52.0	14.6	17.6	72
12:00	11500	8.25	0.9	52.0	14.7	17.6	74
13:00	12500	4.50	0.6	74.5	14.1	17.8	66
14:00	20000	3.21	0.4	104.0	13.2	18.3	55
15:00	12000	3.36	0.4	111.5	13.2	17.9	58
16:00	9600	3.30	0.4	120.0	13.4	18.5	56
17:00	7000	2.59	0.4	130.0	13.2	18.0	58
18:00	4700	3.71	0.4	120.0	13.2	17.4	62
19:00	3400	4.09	0.4	104.0	-	-	-
20:00	7000	3.09	0.4	120.0	-	-	-
21:00	2400	3.22	0.2	195.0	-	-	-

TIME (GMT)	WIND DIRECTION (deg)	WIND SPEED (m/s)	CLOUD COVER FRACTION	SUN PHOTOMETRY 0.4-1.1µ λ (ly/min)	SUN PHOTOMETRY 0.502µ λ (0.01 ly/min)	CLOUD COVER	Drop Sample (O) or Casella (X)
6:00	290	4.0	0.85	-	-	-	
7:00	310	4.0	0.85	-	-	-	
8:00	290	6.0	0.90	-	-	showers to WSW	
8:30	-	-	>0.90	-	-	-	O X
9:00	-	-	>0.90	-	-	lt shower	
10:00	300	5.0	>0.90	-	-	-	
10:30	290	7.5	1.00	-	-	-	O X
11:00	290	7.5	>0.90	-	-	-	
12:00	295	5.0	>0.90	-	-	-	
13:00	280	5.5	0.80	-	-	-	O X
14:00	295	10.5	0.45	0.83	0.80	fair wt cu; Alto St	
15:00	320	10.5	0.20	0.78	0.73	clouds on horizon	O X
16:00	300	6.0	0.20	0.59	0.50	Ci to E, cu to W	
17:00	-	-	0.20	0.17	0.08	-	
18:00	-	-	0.10	-	-	-	O X
19:00	-	-	-	-	-	-	
20:00	-	-	-	-	-	-	
21:00	-	-	-	-	-	-	

-- Explanation of the Data Log --

Column 1, top half of page: TIME: all measurements provided in the Log were obtained over a 5-10 min interval centered about the indicated time (GMT).

Column 2, top half: TOTAL PARTICLE CONCENTRATION, in units of number per cm^3, was measured on-the-hour with a Gardner Small Particle Detector. This simple but reliable device provides an estimate of particle concentrations in the size range $\sim$0.003 to $\sim$1.0 μm diameter. The measurement provides a sensitive determination of the timing of airmass changes, encounters with aerosol plumes, and a measure of the continentality of the aerosol population. (Previous studies by Calspan have shown that aerosol concentrations in excess of $\sim$500 cm^{-3} in the marine boundary layer are indicative of continental/anthropogenic contributions to the aerosol population.) Additional data were obtained with Calspan-loaned equipment by NEPRF personnel aboard the NAUCRATES; cross-calibration for the two instruments suggests that the NAUCRATES data should be reduced by $\sim$33% for comparison with the BARTLETT data.

Column 3, top half: ROYCO PARTICLE CONCENTRATIONS at diameters >0.32 μm in units of number per cm^3. The device was run continuously, providing consecutive 10 min counts of the aerosol size spectra in 5 size channels: for sizes >0.32 μm, >0.56 μm, >1.78 μm, >3.16 μm and >5.62 μm diameter. The data for all 5 channels were recorded continuously on a strip-chart printer and are available for further analyses; only the on-the-hour total number concentration data (>0.32 μm dia) are provided in the log.

Column 4, top half: B_{scat}, aerosol scattering coefficient in units of $10^{-4} m^{-1}$ as measured by an MRI Nephelometer. The data were recorded continuously on strip chart, with only the 'instantaneous', on-the-hour 10-min average values reported in the Log.

Column 5, top half: VSBY, atmospheric visibility in units of kilometers, calculated from the MRI Nephelometer scattering coefficient data according to the manufacturer's assumptions and calibration.

The Nephelometer assumes that, in the absence of absorption, scattering coefficient (B_{scat}) is equivalent to extinction coefficient (β) - - a reasonable assumption at visible wavelength in the atmosphere.

Extinction (β) can be related to visual range, V, through Koschmieder's expression

$$V = -\ln \varepsilon/\beta$$

where ε is the threshold contrast. Values of ε ranging from 0.01 to 0.06 have been proposed by a number of authors, however, the MRI device assumes $\varepsilon = 0.01$ and the relationship for visibility restriction due to aerosol scattering reduces to

$$V = 4.605/\beta$$

Columns 6, 7 and 8, top half of page: WET BULB TEMPERATURE (°C) and DRY BULB TEMPERATURE (°C) were measured hourly with a calibrated standard sling psychrometer, and RH (relative humidity) was read from psychrometric tables.

Columns 2 and 3, bottom half of page: WIND DIRECTION (degrees-mag.) and SPEED (meters/sec) were observed from the ship's anemometer system and converted to actual winds by factoring in ship's speed and heading. These data are ∿1-2 min 'eyeball' averages. The data marked by an asterisk (*) in the first half of the cruise were taken by LSU-CSI personnel and are included here for completeness.

Column 4, bottom half: CLOUD COVER FRACTION, in tenths of the sky covered by cloud, was estimated hourly. Additional information on cloud type and general weather is provided in Column 7.

Columns 5 and 6, bottom half: SUN PHOTOMETRY in langleys/min for two wavelength intervals: for the 0.4 to 1.1 μ wavelength response interval of the silicon chip and for a 5 nm wide interval centered at 0.502 μ wavelength. The measurements were made with a modified and calibrated UDT Mod 40 Optometer. Optical depth calculations were performed for the 0.502 μband according to the method of Volz and are listed in Appendix B, Section 1.

Caution is advised in using either the sun photometry data or optical depth estimates for surface level correlations due to contamination of the data by cirrus cloud cover. Clearest skys occurred on 10 and 11 Oct. and on the afternoon of 13 Oct. While data are provided for 12 and 15 Oct., these days were characterized by a near overcast in thin cirrus.

Column 8, bottom half: an '0' in this column signifies when a DROPLET SAMPLE (large particles) was taken with a Calspan-fabricated drop sampler which employs gelatin replication. We have used this device for more than 15 years to provide reliable drop size distributions (i.e., ∿ 3.0 to >50 μm dia) in fog and sea spray. When run at high speed to maximize collection efficiencies and for extended periods (i.e., tens of seconds), the device provides reliable data on the size spectra of larger aqueous aerosols found in the high RH marine boundary layer. During the Alboran Sea Experiment, these samples were obtained at ∿3-hr intervals.

A major drawback associated with this device is the labor-intensive data acquisition and reduction required to produce size spectra. However, the aerosol size range covered by this instrument is very important, and a reliable measurement is difficult to obtain otherwise. The drop sampler and Royco, together, provide a measurement of aerosol size spectra over the range of 0.3-50 μm.

A total of 51 droplet samples were reduced and mated with appropriate Royco data to provide size spectra (0.3-20 μm dia) which are presented in Appendix B, Section 2. From these aerosol size spectra, we generated values of particle concentration, cross-sectional area and volume data which are provided in tabular form in the Appendix. We also attempted Mie scattering approximations for comparison with measured scattering coefficient; the results of these comparisons, presented in Appendix B-3, suggest that aerosols of sizes smaller than we measured (<0.32 μm) contributed substantially (perhaps as much as 25-75% of the scattering) to the observed visibilities. A result not unreasonable in the highly 'continentalized' air masses encountered on the cruise.

Column 8, bottom half of page: CASELLA; an 'X' in this column signifies that an aerosol sample was collected for later chemical analyses. These samples were typically collected over ∿20 min sampling periods via Casella cascade impactor for identification of individual particles by scanning electron microscopy (SEM) and energy dispersive x-ray analysis (EDXA). This technique has been used for years in our studies of boundary layer aerosols and provides

a simple means for classifying individual particles (>0.2 μm dia) and identifying airmass aerosol source regions. These samples were obtained at ∿3 hr intervals, keyed to drop sample collections and to changes in meteorological circumstances. Additional collections of aerosols via a Casella impactor were obtained from aboard the NAUCRATES by NEPRF personnel.

A total of 54 of these samples from the BARTLETT were analyzed, and the data reduced to provide two forms of chemical classification: (1) Particles were classified according to their over all chemical make-up into 6 categories -- Organics, NaCℓ (Sea Salt), NaCℓ + other salts, Silicates, Sulfates, and other salts; (2) the total element distribution of the aerosol population. The fraction of the aerosol population at sizes >0.2 μm dia was then determined. Similarly, 7 samples obtained from the Naucrates were reduced. These data are provided in tabular form in Appendix B, Section 4.

Appendix B

REDUCED DATA

B-1 Optical Depth Computations

B-2 Aerosol Size Spectra; and Number, Cross-section and Volume Concentrations

B-3 Extinction Estimates based on Aerosol Size Spectra

B-4 Aerosol Chemistry

B-5 Summary Discussion of the Alboran Gyre

B-1 Optical Depth Computations

During the Alboran Sea Experiment, sun photometry data were acquired at hourly intervals, when possible, from aboard the USNS BARTLETT. Data were obtained for two wavelength intervals: 0.4 to 1.1 μ and for a 5 nm wide band centered at 0.502 μ λ. For a narrow wavelength band, such as prescribed by the 0.502 μ filter, aerosol optical thickness can be computed from sun photometer measurements by:

$$\tau_A = \frac{1}{M} (\ln I_o - \ln I - \ln F - (\tau_R + \tau_o) KM \frac{p}{p_o})$$

(From Volz: Sun Photometer Instructions)

τ_A = aerosol optical depth at M = 1

M = sec z where z is the solar zenith angle

I_o = solar radiation at top of earth's atmosphere and at mean solar distance

I = observed solar radiation

F = correction factor for distance to sun at observation time relative to mean solar distance

τ_R = Rayleigh optical thickness (scattering by atmospheric gases) at standard pressure, p_o = 1013 mb.

τ_o = Ozone optical thickness (gaseous absorption) at standard pressure

p = observed surface pressure

K = correction factor to τ_R and τ_o when M >1 (supplied by Volz)

From Hoyt, D.V. (J. Appl. Met. 16 p. 432, 1977):

τ_R = .1402 for October and 30°N.

From Voltz (I bid)

τ_o = .0092

From: Thekaekara, M.P., R. Kruger, C.H. Duncan, 1969:

Solar Irradiance Measurements from a Research Aircraft, Applied Optics, 8, No. 8 p. 1713-1732, August.

I_o = .0139598 Langleys/minute/5 nanometers.

These values are consistent with those for the same part of the world and the same time of year which are published in Atmospheric Turbidity and Precipitation Chemistry Data for World - 1973 National Climatic Center, Asheville, N.C. One word of warning, the computation technique outlined above does not work well for large zenith angles; therefore optical depths for times before 0900 and after 1500 should be treated with extreme caution.

OCTOBER	TIME (GMT)	0.502 μm (0.01 ly/min)	Optical Depth
9	7:00	0.17	0.074
10	7:00	0.08	0.155
10	8:00	0.55	0.124
10	8:33	0.73	0.114
10	9:00	0.75	0.144
10	10:00	0.90	0.129
10	11:00	0.96	0.118
10	12:00	1.01	0.092
10	13:00	1.01	0.088
10	14:00	0.96	0.100
10	15:00	0.90	0.098
10	16:00	0.63	0.161
10	17:00	0.23	0.255
11	7:00	0.12	0.104
11	8:00	0.57	0.115
11	9:00	0.80	0.114
11	10:00	0.91	0.117
11	11:00	0.96	0.118
11	12:00	1.01	0.092
11	13:00	0.98	0.114
11	14:00	0.91	0.134
11	15:00	0.76	0.189
11	16:00	0.50	0.254
11	17:00	0.08	0.497

OCTOBER	TIME (GMT)	0.502 μm (0.01 ly/min)	Optical Depth
12	7:00	0.11	0.116
12	8:00	0.53	0.133
12	9:00	0.76	0.135
12	10:00	0.78	0.218
12	11:00	1.00	0.093
12	12:00	0.90	0.185
12	13:00	0.86	0.209
12	14:00	0.81	0.212
12	15:00	0.76	0.189
12	16:00	0.50	0.254
12	17:00	0.11	0.414
13	7:00	0.30	0.011
13	8:00	0.67	0.067
13	9:00	0.85	0.085
13	10:00	0.93	0.106
13	11:00	0.93	0.142
13	12:00	1.00	0.105
13	13:00	0.98	0.114
13	14:00	0.95	0.112
13	15:00	0.83	0.141
14	13:00	0.81	0.218
14	14:00	0.78	0.218
14	15:00	0.78	0.151
15	7:00	0.11	0.072
15	8:00	0.51	0.075
15	9:00	0.70	0.122
15	10:00	0.76	0.189
15	11:00	0.75	0.260
15	12:00	0.91	0.145
15	13:00	0.73	0.292
15	14:00	0.50	0.501
16	7:00	0.08	0.097
16	8:00	0.43	0.115
16	9:00	0.67	0.140
16	10:00	0.78	0.177
16	11:00	0.96	0.096
16	12:00	0.85	0.199
16	13:00	0.85	0.193
16	14:00	0.76	0.232
16	15:00	0.58	0.304
16	16:00	0.18	0.579
18	14:00	0.80	0.203
18	15:00	0.73	0.184
18	16:00	0.50	0.221
18	17:00	0.08	0.349

B-2 Aerosol Size Spectra; and Number, Cross-section & Volume Concentrations

A total of 51 droplet samples (particles >2 μm diameter) were reduced and mated with appropriate Royco data to provide size spectra (0.3-20 μm dia) which are presented here. (Each spectrum annotated with the attendant measured total (Aitken) particle concentration.) From these aerosol size spectra, we generated values of particle concentration, cross-sectional area and volume data which are provided at the end of this section in tabular form. (We performed Mie scattering approximations for comparison with measured scattering coefficient. The results of these comparisons, presented in Appendix B-3, suggest that aerosols of sizes smaller than we measured (<0.32 μm) contributed substantially (perhaps as much as 50-80% of the scattering) to be observed visibilities. A result not unreasonable in view of the high Aitken counts of the highly 'continentalized' air masses encountered on the cruise.)

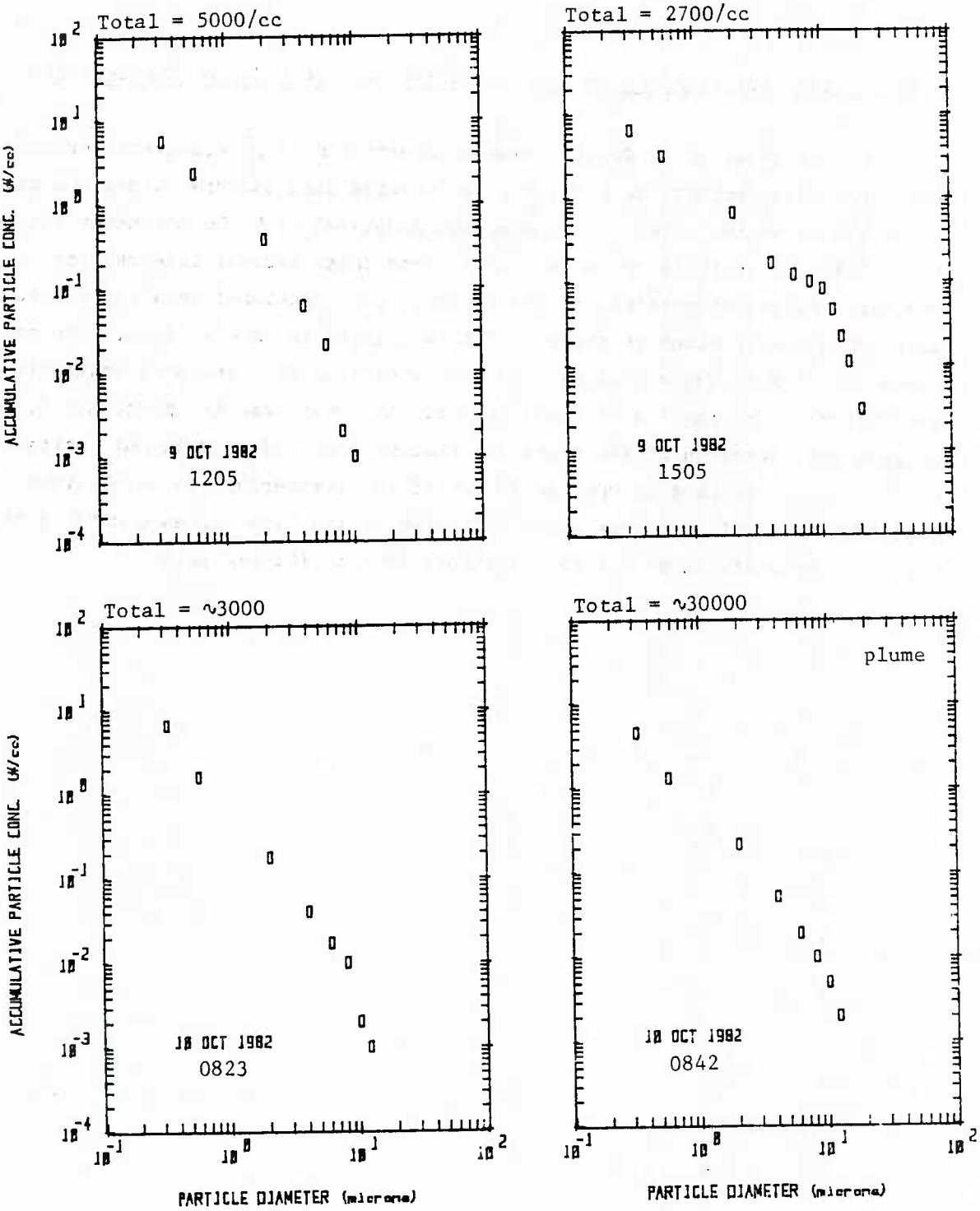
Total = 5000/cc
9 OCT 1982
1205
Total = 2700/cc
9 OCT 1982
1505
Total = ∿3000
10 OCT 1982
0823
Total = ∿30000
plume
10 OCT 1982
0842
ACCUMULATIVE PARTICLE CONC. (#/cc)
PARTICLE DIAMETER (microns)

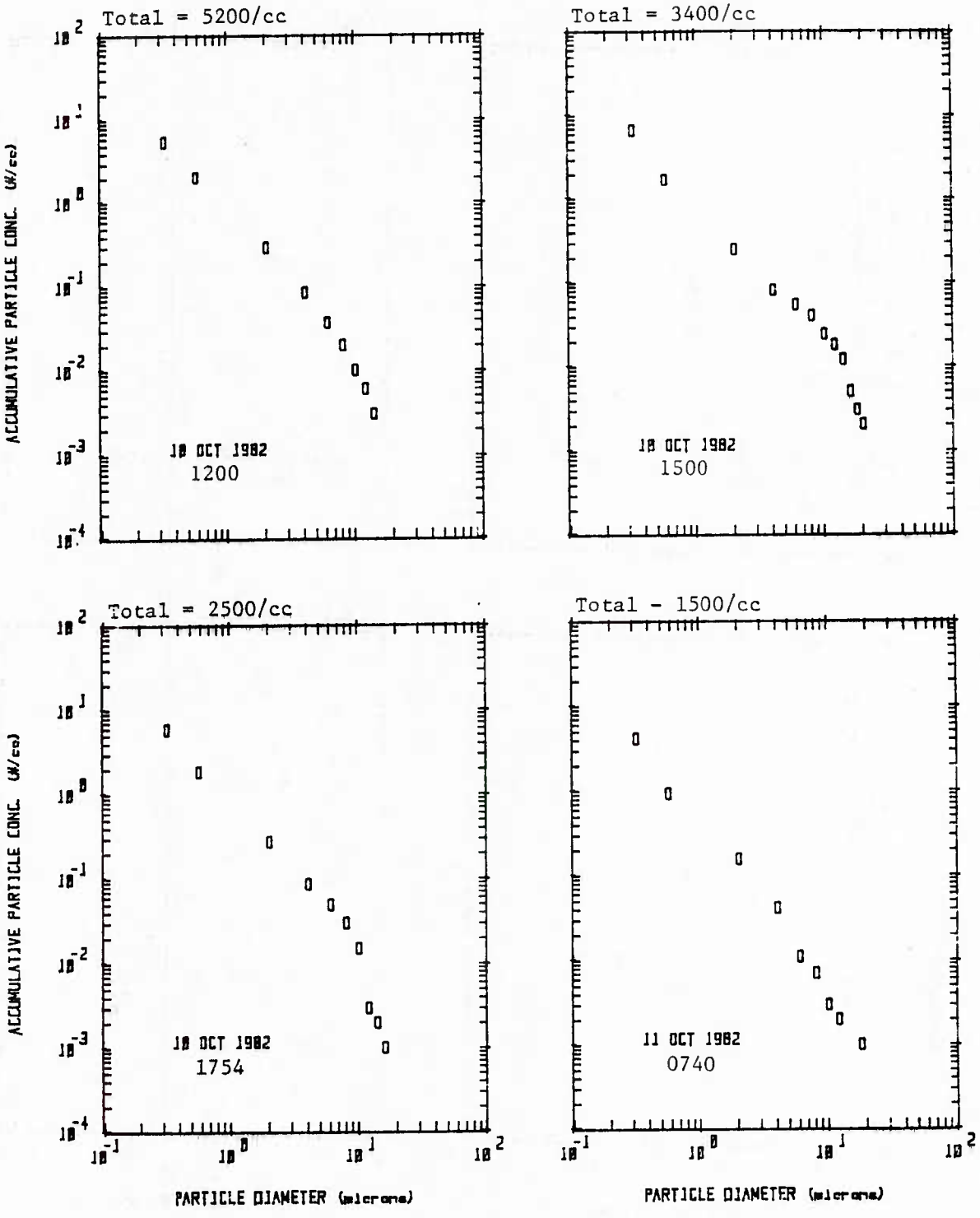
Total = 5200/cc
18 OCT 1982
1200
Total = 3400/cc
18 OCT 1982
1500
Total = 2500/cc
18 OCT 1982
1754
Total - 1500/cc
11 OCT 1982
0740
ACCUMULATIVE PARTICLE CONC. (#/cc)
PARTICLE DIAMETER (microns)

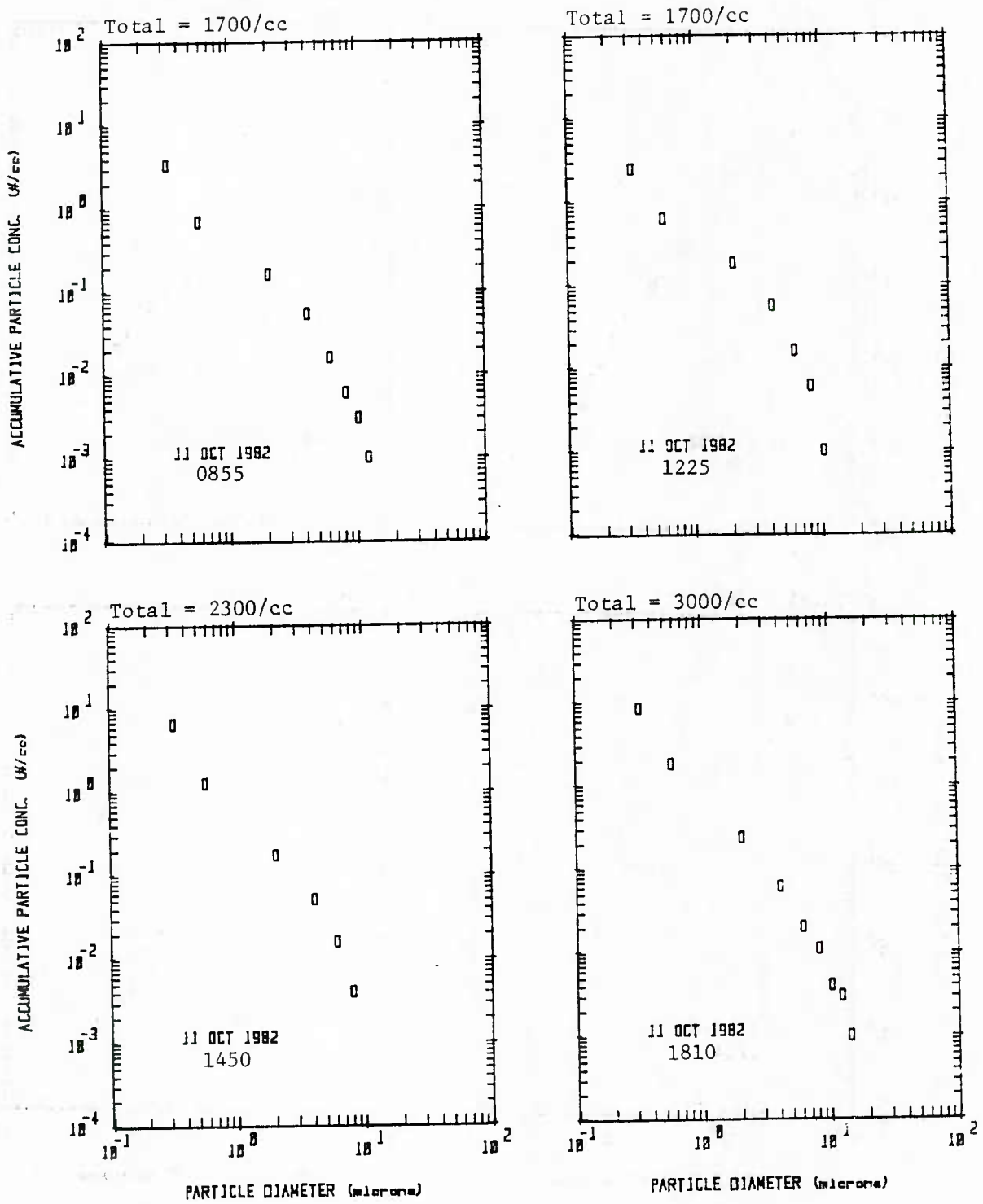
Total = 1700/cc
11 OCT 1982
0855
Total = 1700/cc
11 OCT 1982
1225
Total = 2300/cc
11 OCT 1982
1450
Total = 3000/cc
11 OCT 1982
1810
ACCUMULATIVE PARTICLE CONC. (#/cc)
PARTICLE DIAMETER (microns)

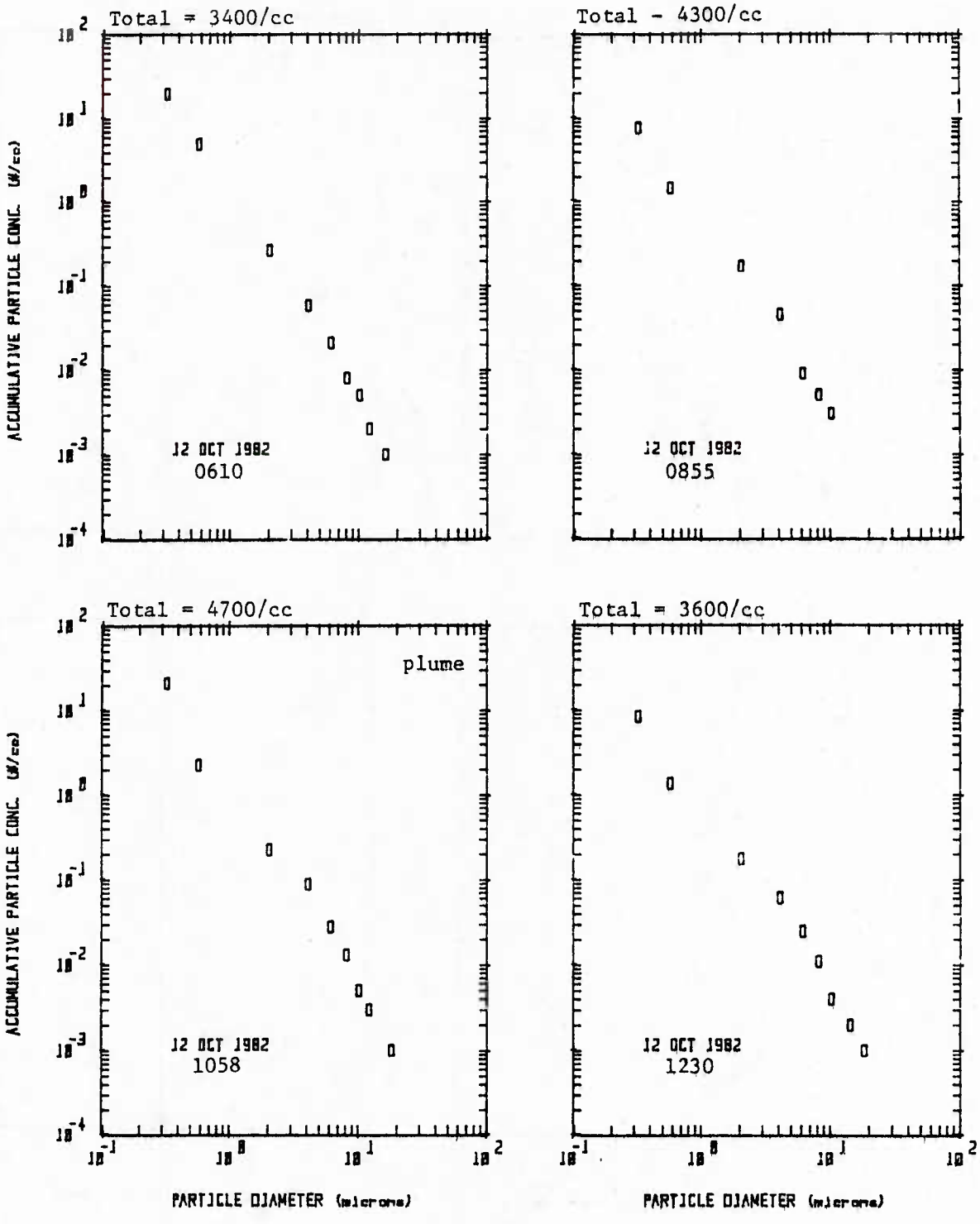
Total = 3400/cc
12 OCT 1982
0610
Total - 4300/cc
12 OCT 1982
0855
Total = 4700/cc
plume
12 OCT 1982
1058
Total = 3600/cc
12 OCT 1982
1230
ACCUMULATIVE PARTICLE CONC. (#/cc)
PARTICLE DIAMETER (microns)

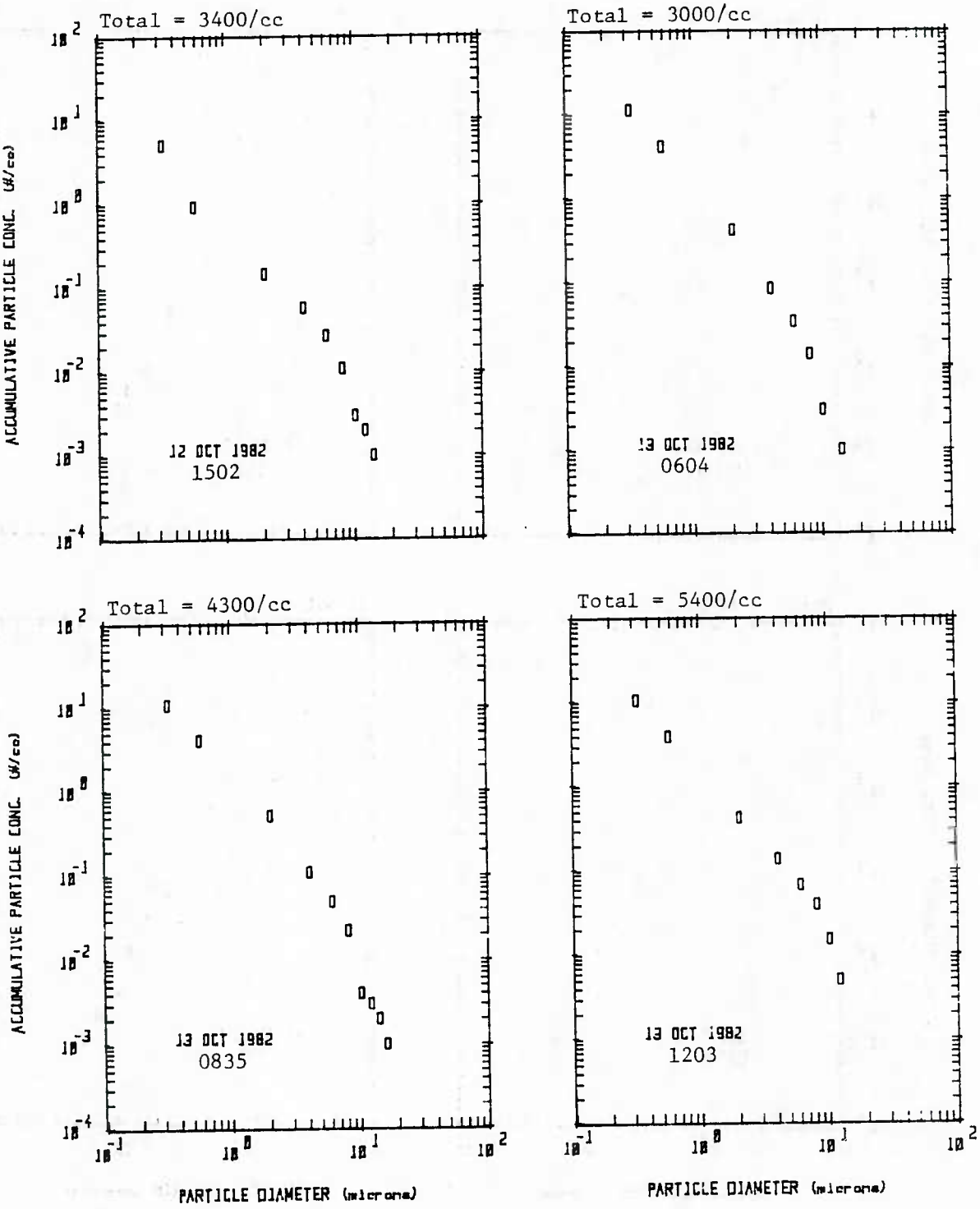
Total = 3400/cc
12 OCT 1982
1502
Total = 3000/cc
13 OCT 1982
0604
Total = 4300/cc
13 OCT 1982
0835
Total = 5400/cc
13 OCT 1982
1203
ACCUMULATIVE PARTICLE CONC. (#/cc)
PARTICLE DIAMETER (microns)

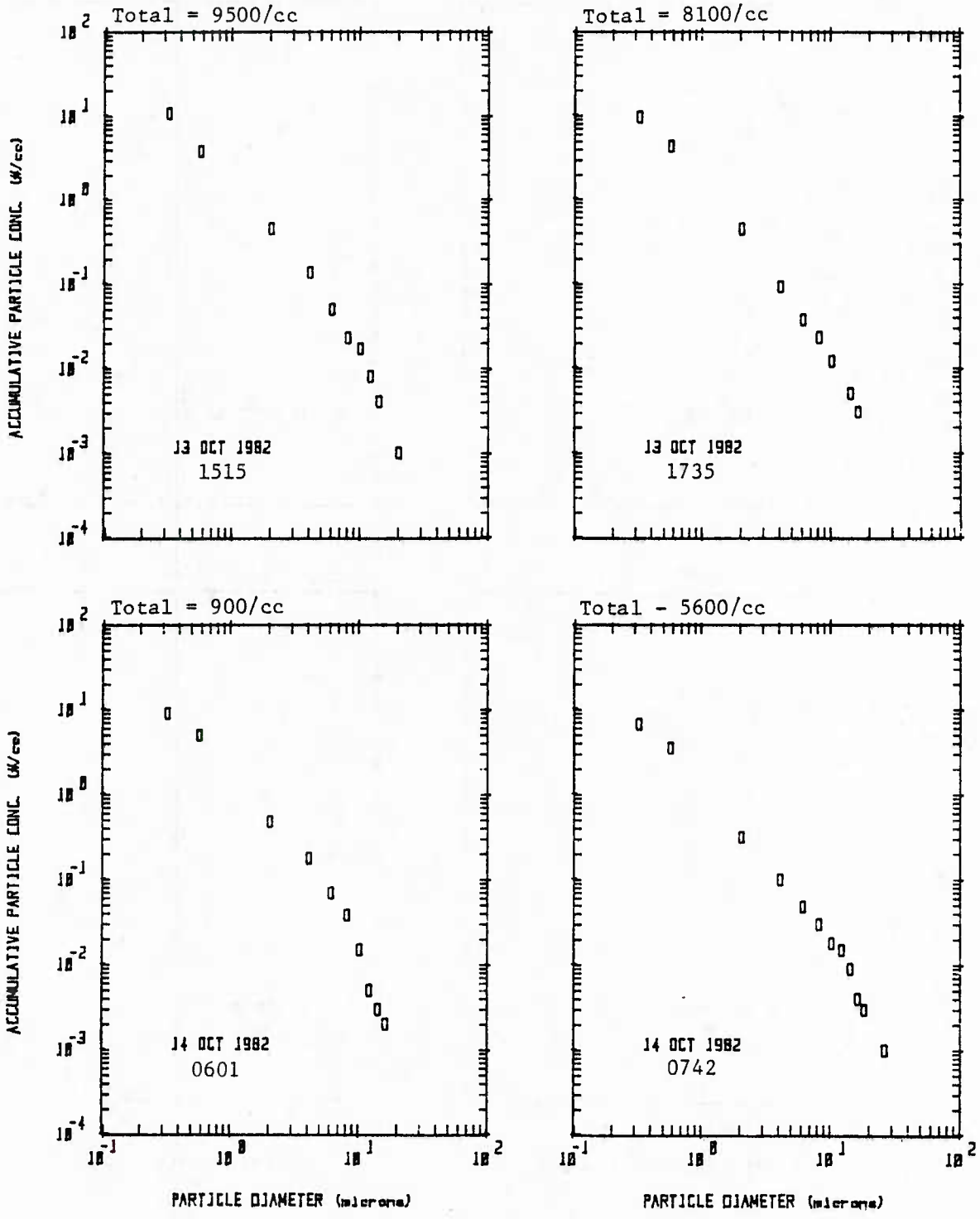
Total = 9500/cc
13 OCT 1982
1515
Total = 8100/cc
13 OCT 1982
1735
Total = 900/cc
14 OCT 1982
0601
Total - 5600/cc
14 OCT 1982
0742
ACCUMULATIVE PARTICLE CONC. (#/cc)
PARTICLE DIAMETER (microns)

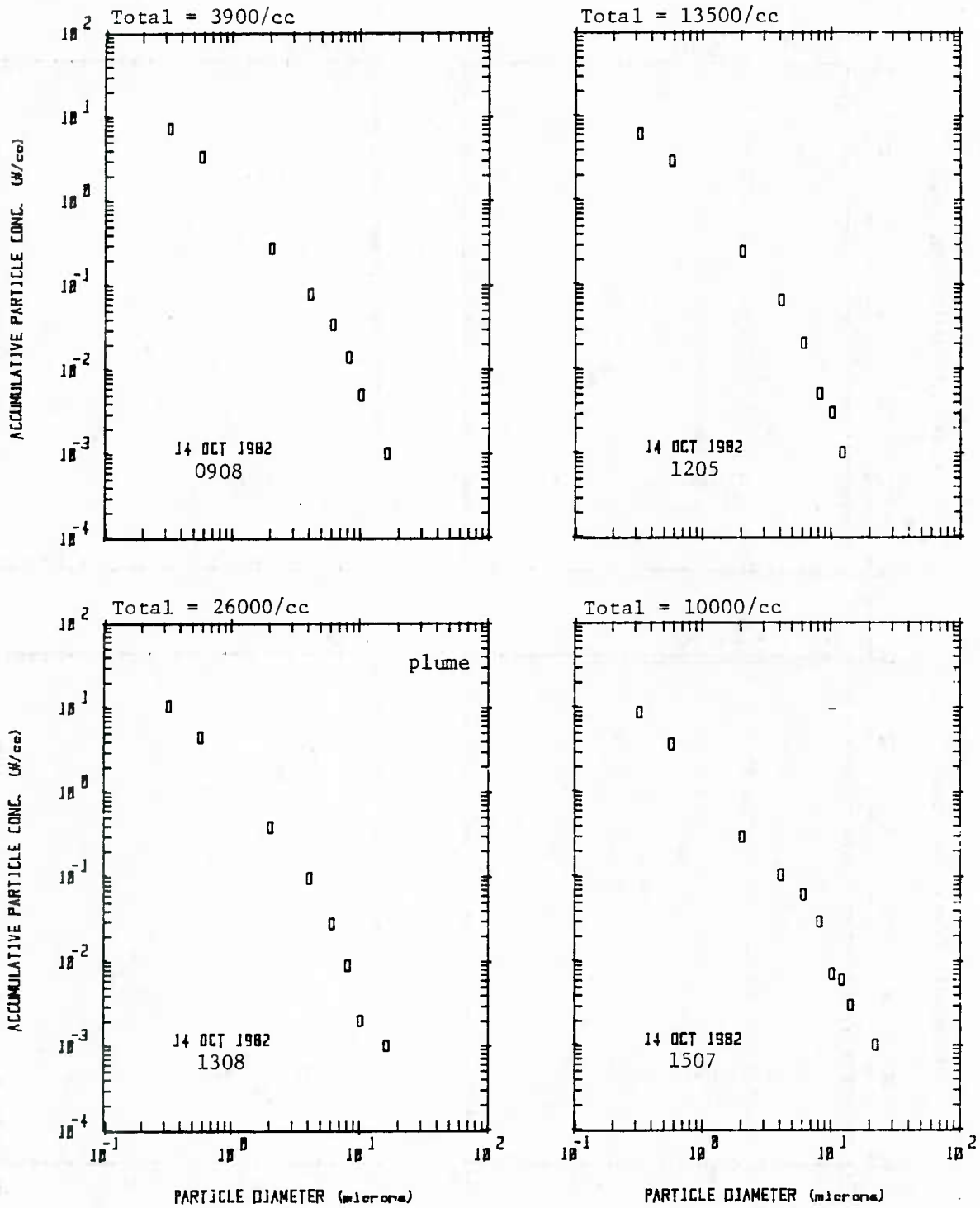
Total = 3900/cc
14 OCT 1982
0908
Total = 13500/cc
14 OCT 1982
1205
Total = 26000/cc
plume
14 OCT 1982
1308
Total = 10000/cc
14 OCT 1982
1507
ACCUMULATIVE PARTICLE CONC. (#/cc)
PARTICLE DIAMETER (microns)

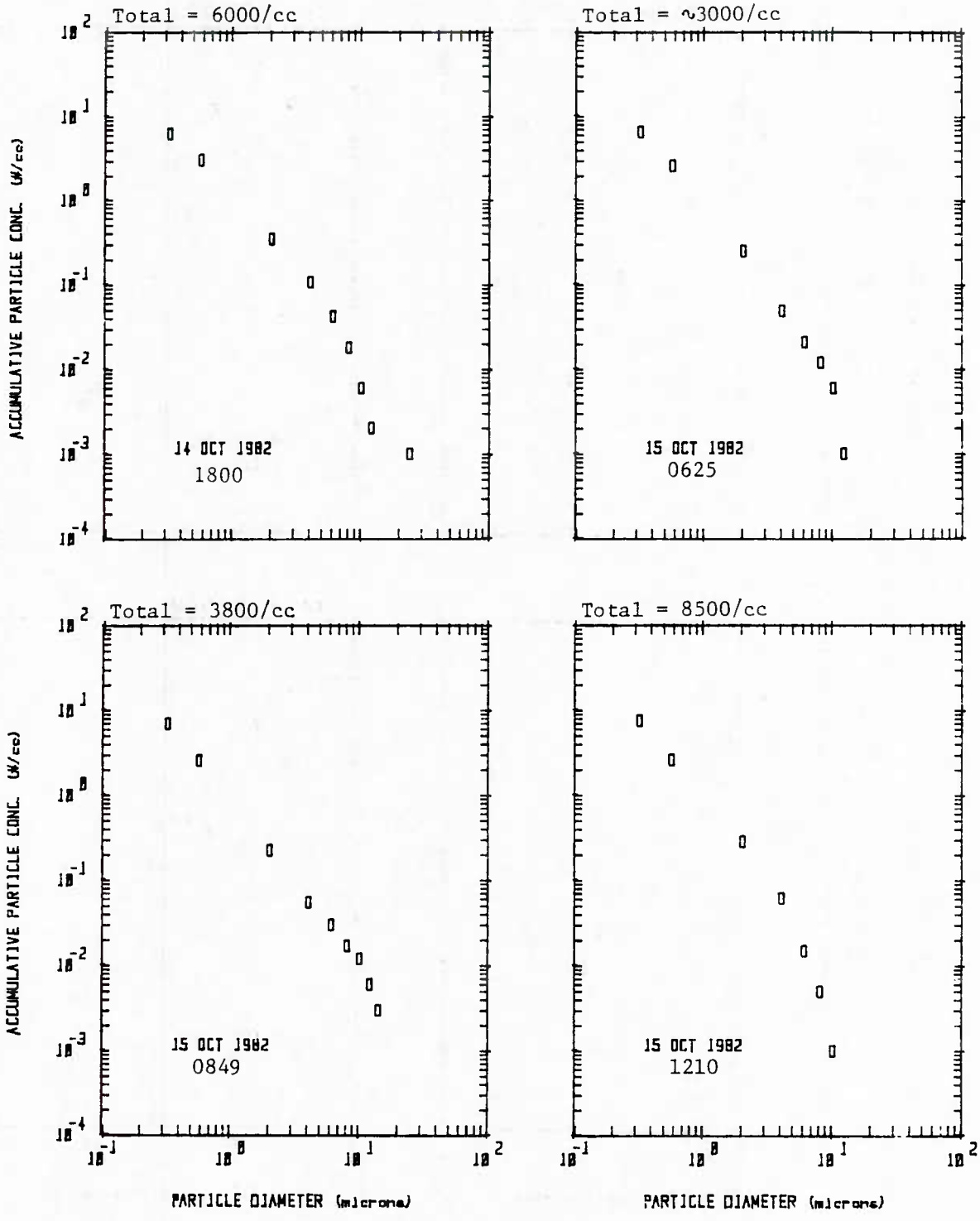
Total = 6000/cc
Total = ∿3000/cc
Total = 3800/cc
Total = 8500/cc
ACCUMULATIVE PARTICLE CONC. (#/cc)
14 OCT 1982
1800
15 OCT 1982
0625
15 OCT 1982
0849
15 OCT 1982
1210
PARTICLE DIAMETER (microns)

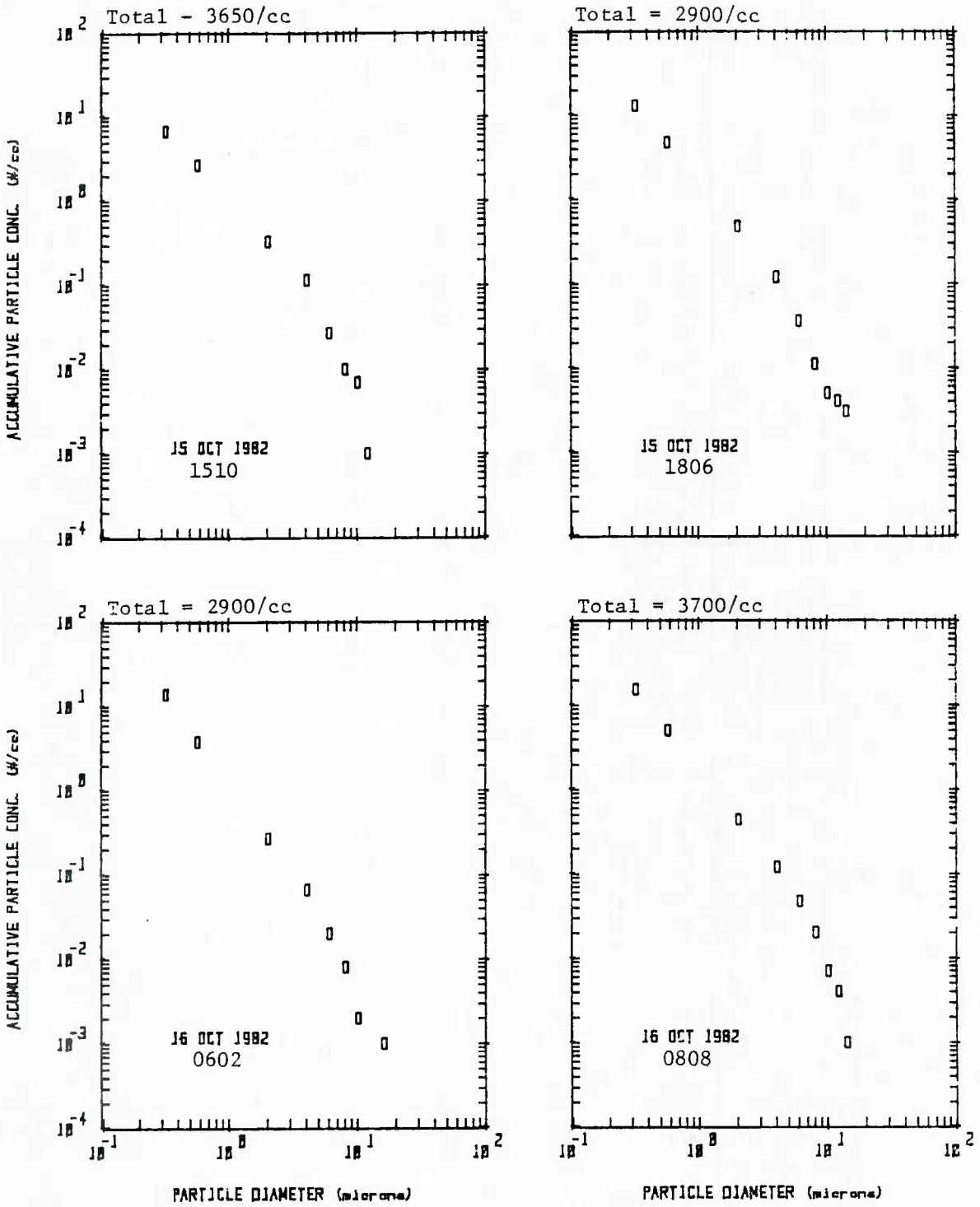
Total = 3650/cc
15 OCT 1982
1510
Total = 2900/cc
15 OCT 1982
1806
Total = 2900/cc
16 OCT 1982
0602
Total = 3700/cc
16 OCT 1982
0808
ACCUMULATIVE PARTICLE CONC. (#/cc)
PARTICLE DIAMETER (microns)

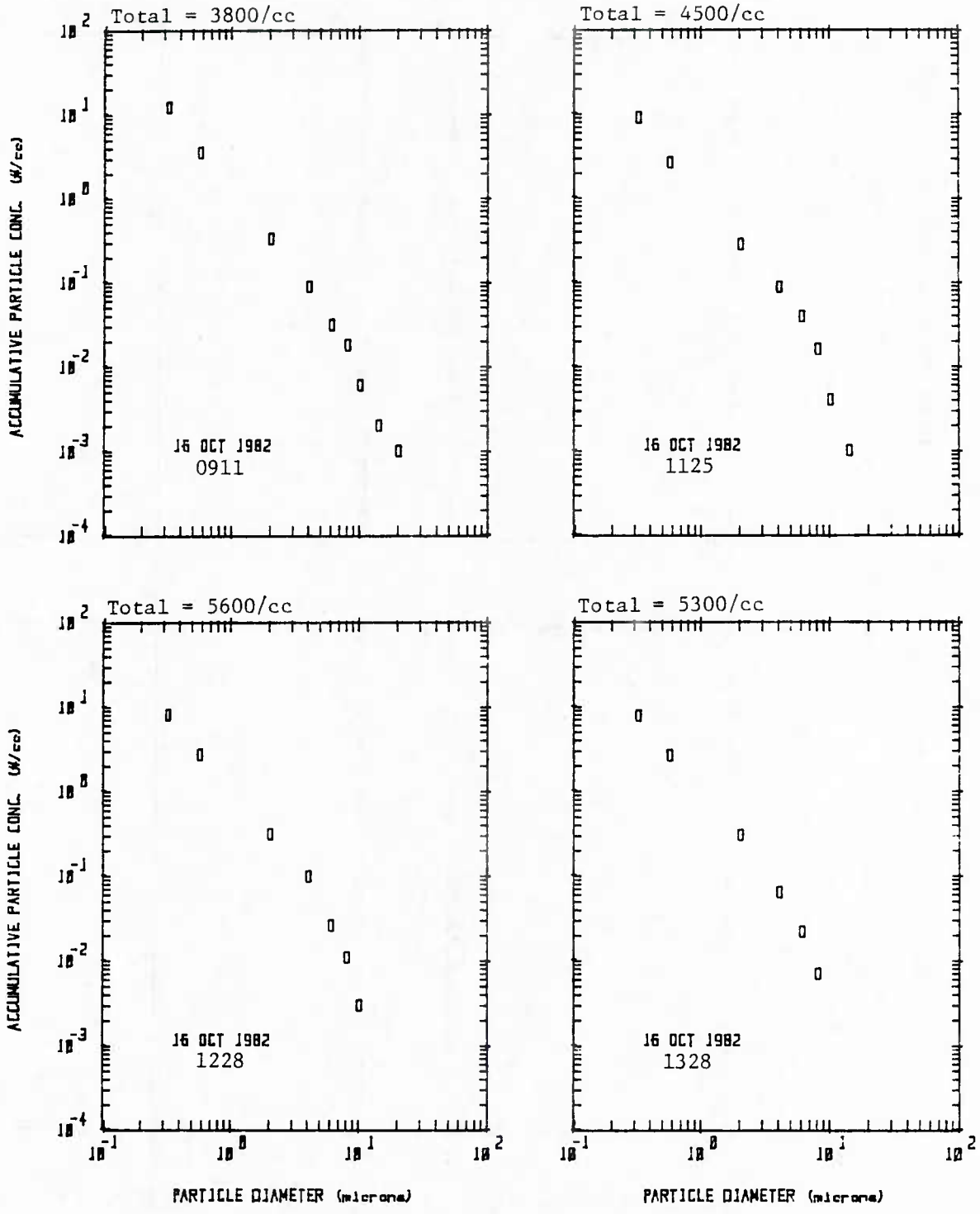
Total = 3800/cc
16 OCT 1982
0911
Total = 4500/cc
16 OCT 1982
1125
Total = 5600/cc
16 OCT 1982
1228
Total = 5300/cc
16 OCT 1982
1328
ACCUMULATIVE PARTICLE CONC. (#/cc)
PARTICLE DIAMETER (microns)

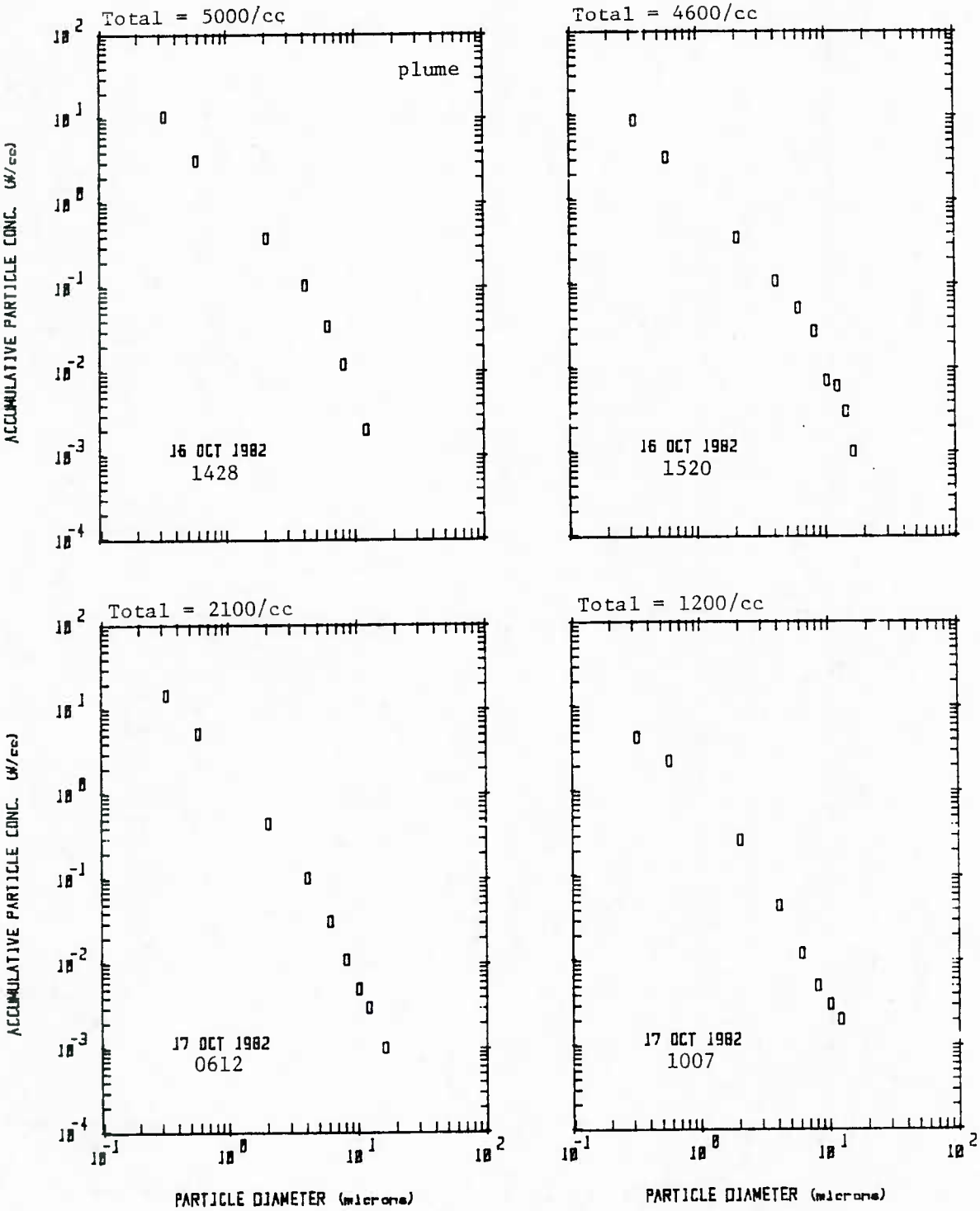
Total = 5000/cc
plume
16 OCT 1982
1428
Total = 4600/cc
16 OCT 1982
1520
Total = 2100/cc
17 OCT 1982
0612
Total = 1200/cc
17 OCT 1982
1007
ACCUMULATIVE PARTICLE CONC. (#/cc)
PARTICLE DIAMETER (microns)

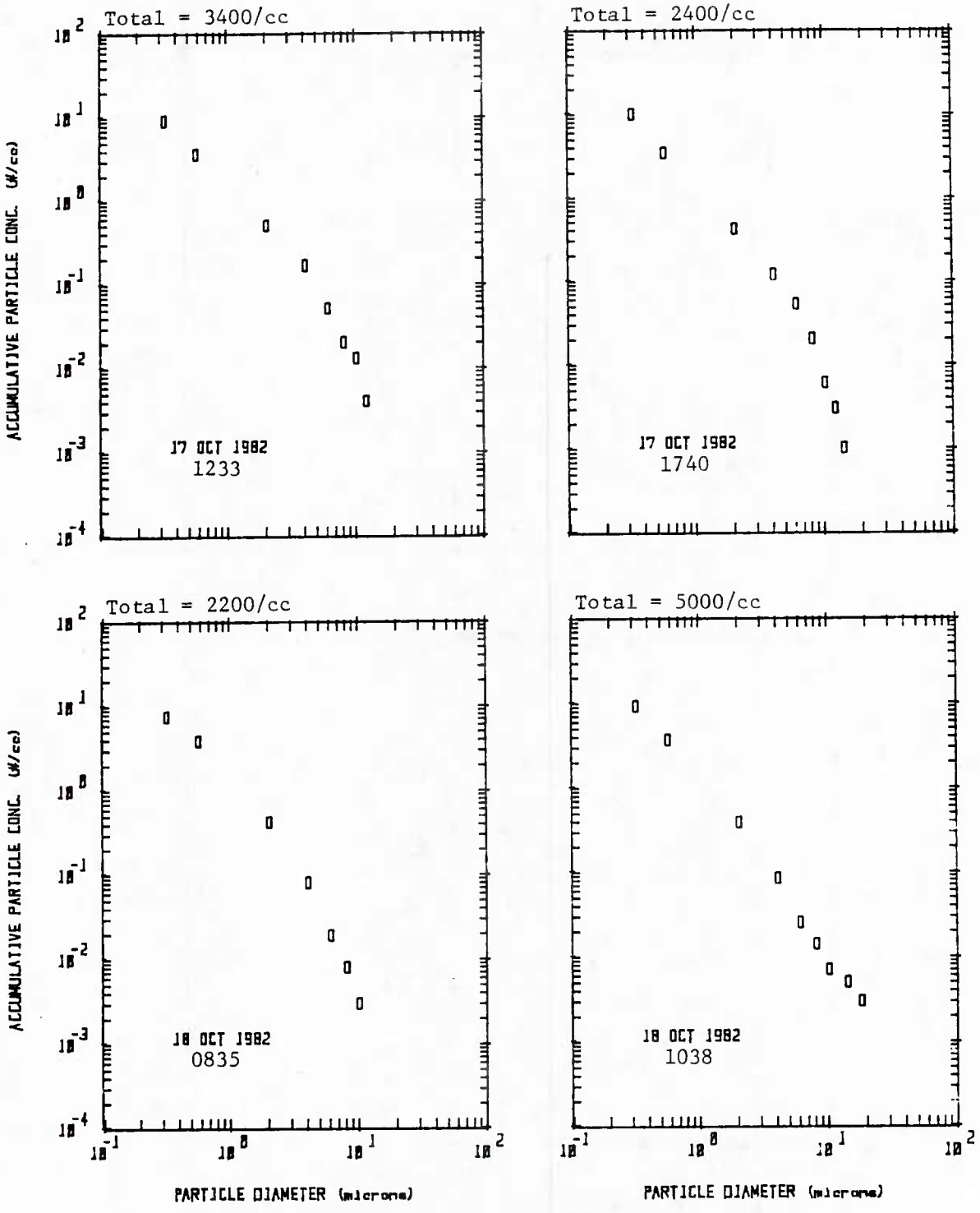
Total = 3400/cc
17 OCT 1982
1233
Total = 2400/cc
17 OCT 1982
1740
Total = 2200/cc
18 OCT 1982
0835
Total = 5000/cc
18 OCT 1982
1038
ACCUMULATIVE PARTICLE CONC. (#/cc)
PARTICLE DIAMETER (microns)

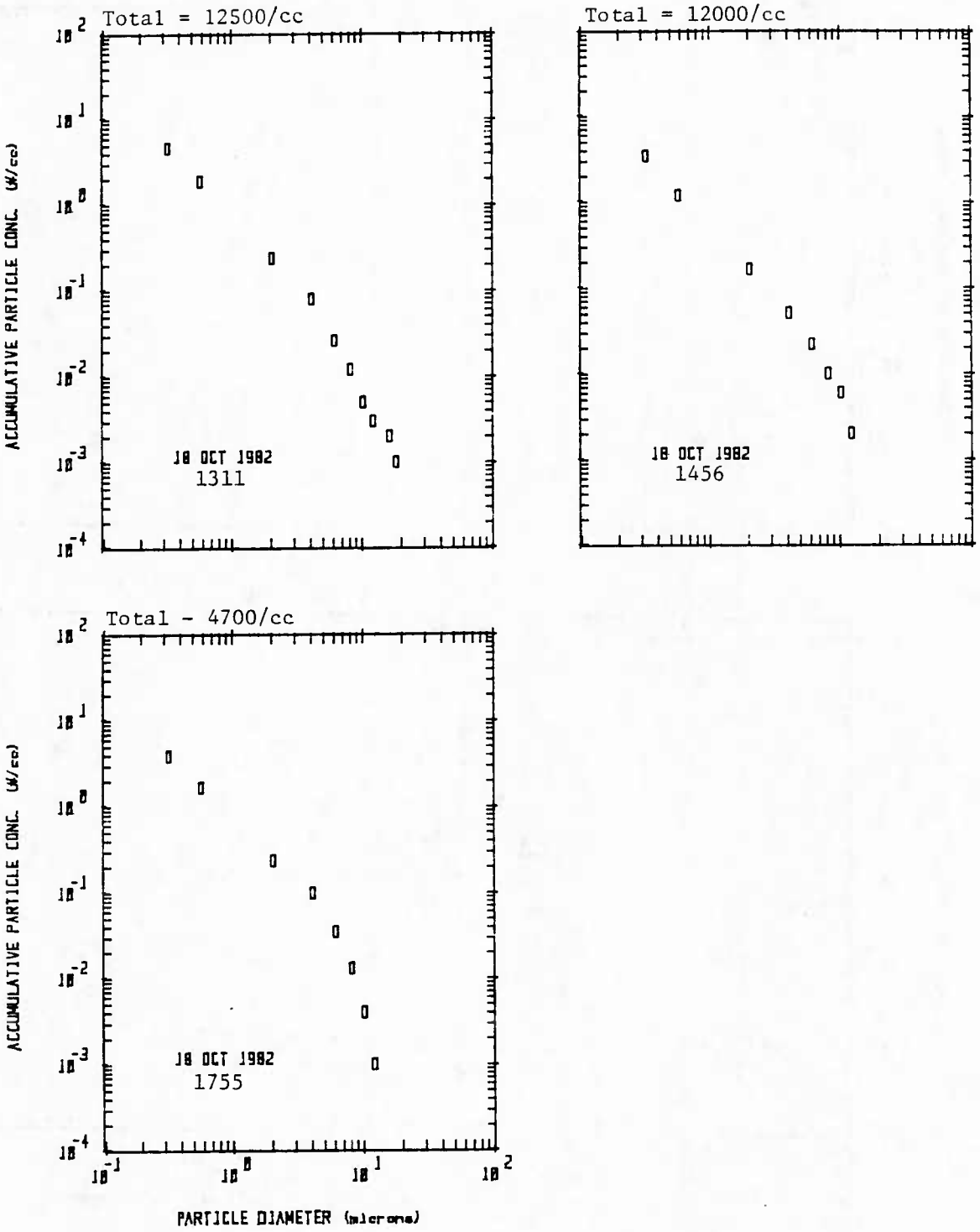
Total = 12500/cc
18 OCT 1982
1311
Total = 12000/cc
18 OCT 1982
1456
Total - 4700/cc
18 OCT 1982
1755
ACCUMULATIVE PARTICLE CONC. (#/cc)
PARTICLE DIAMETER (microns)

PARTICLE CONCENTRATION AS A FUNCTION OF SIZE (NUMBER PER CC)

		NUMBER CONCENTRATION AT SIZES > THAN INDICATED DIAMETER					
OCTOBER	GMT	>0.32um	>0.56um	>2.0um	>6.0um	>10.0um	>20.0um
9	12:03	6.03	2.678	0.7120	0.0210	0.0010	0.0000
9	15:03	7.00	3.697	1.1711	0.1220	0.0820	0.0030
10	8:14	5.72	1.731	0.3149	0.0170	0.0020	0.0000
10	9:00	4.73	1.489	0.3835	0.0190	0.0050	0.0000
10	12:00	5.72	2.266	0.5090	0.0370	0.0100	0.0000
10	15:00	6.85	1.373	0.4200	0.0540	0.0240	0.0020
10	17:32	5.99	2.045	0.4620	0.0490	0.0150	0.0000
11	7:24	4.24	1.043	0.2704	0.0110	0.0030	0.0000
11	9:00	3.51	0.815	0.2732	0.0160	0.0030	0.0000
11	13:00	2.58	0.757	0.3130	0.0160	0.0010	0.0000
11	15:00	6.73	1.402	0.2991	0.0160	0.0000	0.0000
11	18:06	8.67	2.011	0.4130	0.0200	0.0040	0.0000
12	6:06	19.82	5.210	0.4768	0.0210	0.0050	0.0000
12	9:00	7.81	1.584	0.2979	0.0090	0.0030	0.0000
12	11:00	21.15	2.391	0.3640	0.0280	0.0050	0.0000
12	13:00	8.49	1.480	0.2892	0.0250	0.0040	0.0000
12	15:00	5.18	1.021	0.2371	0.0270	0.0030	0.0000
13	6:02	11.59	4.475	0.7552	0.0340	0.0030	0.0000
13	9:00	11.26	4.519	0.9184	0.0490	0.0040	0.0000
13	12:00	10.85	4.179	0.7020	0.0670	0.0150	0.0000
13	15:00	11.02	4.123	0.7594	0.0500	0.0170	0.0010
13	17:21	9.97	4.724	0.7950	0.0370	0.0120	0.0000
14	6:01	9.30	5.295	0.7774	0.0690	0.0150	0.0000
14	7:25	6.91	3.714	0.5296	0.0480	0.0180	0.0010
14	9:05	7.44	3.518	0.4678	0.0340	0.0050	0.0000
14	12:03	6.24	3.084	0.4226	0.0200	0.0030	0.0000
14	13:00	10.73	4.779	0.6717	0.0290	0.0020	0.0000
14	15:00	8.84	3.808	0.4744	0.0610	0.0070	0.0010
14	18:00	6.56	3.332	0.5822	0.0420	0.0060	0.0010
15	6:15	6.81	2.859	0.4537	0.0210	0.0060	0.0000
15	9:00	7.14	2.733	0.3940	0.0300	0.0120	0.0000
15	12:00	7.80	2.842	0.5085	0.0150	0.0010	0.0000
15	15:06	6.90	2.871	0.5403	0.0270	0.0070	0.0000
15	18:04	13.11	5.063	0.8289	0.0360	0.0050	0.0000
16	6:01	14.11	3.990	0.4643	0.0200	0.0020	0.0000
16	8:05	15.70	5.301	0.7476	0.0470	0.0070	0.0000
16	9:00	12.38	3.303	0.5742	0.0310	0.0080	0.0010
16	12:00	9.24	2.872	0.4730	0.0390	0.0040	0.0000
16	13:00	8.25	2.940	0.5283	0.0260	0.0030	0.0000
16	13:17	8.02	2.873	0.5432	0.0220	0.0090	0.0000
16	15:00	10.90	3.436	0.6494	0.0340	0.0020	0.0000
16	15:12	8.86	3.395	0.5936	0.0510	0.0070	0.0000
17	6:07	15.06	5.523	0.7946	0.0310	0.0050	0.0000
17	10:04	4.48	2.472	0.4783	0.0120	0.0030	0.0000
17	12:20	9.49	3.965	0.8223	0.0510	0.0130	0.0000
17	17:24	10.34	3.737	0.7004	0.0520	0.0060	0.0000
18	8:21	7.86	4.173	0.7620	0.0190	0.0030	0.0000
18	10:23	9.49	3.959	0.6914	0.0250	0.0070	0.0000
18	13:07	4.78	2.052	0.3973	0.0260	0.0050	0.0000
18	15:00	3.57	1.310	0.2784	0.0220	0.0060	0.0000
18	17:33	3.99	1.806	0.3720	0.0350	0.0040	0.0000

AEROSOL CROSS-SECTION AS A FUNCTION OF SIZE (SQUARE MICRONS PER CC)

		AEROSOL CROSS-SECTION AT SIZES > THAN INDICATED DIAMETER					
OCTOBER	GMT	>0.32um	>0.56um	>2.0um	>6.0um	>10.0um	>20.0um
9	12:03	8.95	8.440	6.2395	0.8899	0.0950	0.0000
9	15:03	24.68	24.179	21.4160	13.3973	11.4056	1.0391
10	8:14	5.71	4.950	3.4010	1.0061	0.2278	0.0000
10	9:00	5.91	5.415	4.2061	1.2150	0.5506	0.0000
10	12:00	8.98	8.460	6.5387	2.5989	1.3085	0.0000
10	15:00	10.86	10.106	8.5171	5.5905	4.0338	0.6927
10	17:32	9.08	8.478	6.7469	3.3623	1.6768	0.0000
11	7:24	4.46	3.977	3.1320	0.9217	0.5133	0.0000
11	9:00	4.21	3.799	3.2063	0.8985	0.3238	0.0000
11	13:00	4.17	3.897	3.4123	0.7980	0.0950	0.0000
11	15:00	5.17	4.364	3.1583	0.7172	0.0009	0.0000
11	18:06	7.38	6.369	4.6221	1.3289	0.5372	0.0000
12	6:06	12.43	10.199	5.0230	1.3361	0.6450	0.0000
12	9:00	5.41	4.467	3.0609	0.5663	0.2851	0.0000
12	11:00	10.04	7.194	4.9675	1.8257	0.7395	0.0000
12	13:00	6.34	5.269	3.9672	1.6348	0.6507	0.0000
12	15:00	4.89	4.261	3.4040	1.5292	0.4045	0.0000
13	6:02	12.71	11.630	7.5626	1.8364	0.3669	0.0000
13	9:00	14.69	13.666	9.7276	2.9157	0.6315	0.0000
13	12:00	14.40	13.388	9.5866	4.2184	1.6140	0.0000
13	15:00	14.52	13.471	9.7918	3.6840	2.2632	0.3464
13	17:21	14.08	13.284	9.9874	2.9335	1.6997	0.0000
14	6:01	16.40	15.785	10.8547	4.5027	1.8465	0.0000
14	7:25	12.81	12.329	8.8467	4.7890	3.3329	0.5738
14	9:05	9.50	8.905	5.5689	1.9497	0.6074	0.0000
14	12:03	7.83	7.349	4.4386	1.0273	0.3228	0.0000
14	13:00	12.30	11.396	6.9036	1.4988	0.3223	0.0000
14	15:00	11.75	10.990	7.3443	3.8941	1.2630	0.4158
14	18:00	10.84	10.347	7.3401	2.6922	1.0052	0.4916
15	6:15	7.98	7.377	4.7465	1.3360	0.6079	0.0000
15	9:00	8.43	7.761	5.2038	2.3169	1.4985	0.0000
15	12:00	8.12	7.365	4.8132	0.7343	0.0950	0.0000
15	15:06	9.44	8.831	6.2820	1.5480	0.7029	0.0000
15	18:04	14.60	13.580	8.7496	2.1017	0.7579	0.0000
16	6:01	10.29	8.753	4.8972	1.1658	0.3223	0.0000
16	8:05	15.14	13.562	8.5829	2.7261	0.8600	0.0000
16	9:00	11.57	10.267	6.7363	2.1676	0.9039	0.3464
16	12:00	9.39	8.418	5.7943	2.1105	0.4619	0.0000
16	13:00	9.28	8.477	5.8391	1.3713	0.2851	0.0000
16	13:17	8.56	7.783	5.2342	1.0226	0.0000	0.0000
16	15:00	11.16	10.039	6.9903	1.7484	0.2656	0.0000
16	15:12	11.70	10.872	7.8090	3.2696	1.0736	0.0000
17	8:07	14.74	13.294	8.1239	1.8341	0.6827	0.0000
17	10:04	6.94	6.636	4.4555	0.7571	0.3805	0.0000
17	12:20	14.21	13.372	9.9344	3.0946	1.3862	0.0000
17	17:24	12.59	11.582	8.2621	2.8494	0.7273	0.0000
18	8:21	11.35	10.788	7.0576	1.0265	0.2851	0.0000
18	10:23	12.13	11.289	7.7153	2.2631	1.3944	0.0000
18	13:07	7.35	6.931	5.1206	1.8176	0.8335	0.0000
18	15:00	5.01	4.867	3.5387	1.3619	0.6456	0.0000
18	17:33	6.94	6.604	5.0360	1.8370	0.4178	0.0000

AEROSOL VOLUME AS A FUNCTION OF SIZE
(CUBIC MICRONS PER CC)

		AEROSOL VOLUME AT SIZES > THAN INDICATED DIAMETER					
OCTOBER	GMT	>0.32um	>0.56um	>2.0um	>6.0um	>10.0um	>30.0um
9	12:03	18.20	18.055	16.3635	4.4909	0.6969	0.0000
9	15:03	137.70	137.551	135.3782	118.0841	107.2624	14.5471
10	8:14	12.99	12.768	11.5500	6.1580	1.8473	0.0000
10	9:00	15.86	15.713	14.7623	7.9163	4.3914	0.0000
10	12:00	29.21	29.058	27.5466	18.4103	11.5401	0.0000
10	15:00	58.54	58.320	57.0697	50.5035	41.8879	8.8991
10	17:32	32.27	32.090	30.7285	22.9907	13.8529	0.0000
11	7:24	13.72	13.575	12.9101	7.7041	5.4589	0.0000
11	9:00	11.71	11.588	11.1219	5.4852	2.5442	0.0000
11	13:00	11.17	11.085	10.7034	4.4014	0.6969	0.0000
11	15:00	10.68	10.439	9.4902	3.6917	0.0098	0.0000
11	18:06	18.38	18.087	16.7127	9.0530	4.7647	0.0000
12	6:06	22.36	21.710	17.6374	9.2951	5.8153	0.0000
12	9:00	10.89	10.611	9.5043	3.5725	2.0907	0.0000
12	11:00	23.50	22.662	20.9185	13.0378	7.2902	0.0000
12	13:00	18.91	18.600	17.5759	11.9423	6.7561	0.0000
12	15:00	14.96	14.777	14.1027	9.5415	3.8144	0.0000
13	6:02	27.23	26.914	23.7141	10.9527	3.1621	0.0000
13	9:00	36.73	36.425	33.3275	17.9066	6.1868	0.0000
13	12:00	42.77	42.470	39.4793	26.9104	12.7209	0.0000
13	15:00	45.86	45.557	42.6626	28.1695	21.0302	4.8490
13	17:21	40.00	39.762	36.3824	22.8442	16.1311	0.0000
14	6:01	50.09	49.912	46.0337	30.5284	16.1818	0.0000
14	7:25	58.08	57.938	55.1990	45.7222	37.9091	10.3254
14	9:05	23.58	23.405	20.7807	12.3902	5.3630	0.0000
14	12:03	16.43	16.292	14.0022	6.0015	2.5442	0.0000
14	13:00	25.75	25.480	21.8461	9.3565	3.2723	0.0000
14	15:00	39.30	39.076	36.2084	28.2084	14.0639	8.3755
14	18:00	34.56	34.418	32.0526	21.0291	12.1384	8.1925
15	6:15	18.34	18.165	16.0957	8.5415	4.6349	0.0000
15	9:00	25.81	25.617	23.6054	17.1772	12.9339	0.0000
15	12:00	15.64	15.415	13.4078	4.0197	0.6969	0.0000
15	15:06	23.49	23.307	21.3019	9.5390	5.3318	0.0000
15	18:04	33.40	33.040	29.3974	13.9288	7.1487	0.0000
16	6:01	19.90	19.444	16.4107	7.7176	3.2703	0.0000
16	8:05	35.10	34.636	30.7186	17.1201	7.3089	0.0000
16	9:00	30.14	29.760	26.9823	16.3263	9.4111	3.8490
16	12:00	23.57	23.284	21.2206	12.5701	3.8590	0.0000
16	13:00	21.00	20.760	18.6349	7.8383	2.0907	0.0000
16	13:17	17.12	16.893	14.8387	5.3658	0.0000	0.0000
16	15:00	25.14	24.810	22.4121	10.0695	2.3014	0.0000
16	15:12	35.40	35.154	32.7439	22.1990	10.2547	0.0000
17	6:07	31.08	30.657	26.5892	12.1508	6.2687	0.0000
17	10:04	15.06	14.868	13.2526	5.0182	2.9976	0.0000
17	12:20	38.92	38.673	35.9695	19.1129	10.8736	0.0000
17	17:24	32.71	32.415	29.8026	17.2494	6.1586	0.0000
18	8:21	22.76	22.595	19.3601	5.9748	2.0907	0.0000
18	10:23	35.86	35.613	32.8024	20.3534	15.7059	0.0000
18	13:07	23.46	23.340	21.9157	13.8960	8.7097	0.0000
18	15:00	14.87	14.771	13.8831	8.7703	5.0893	0.0000
18	17:33	20.06	19.961	18.7270	10.6275	3.2411	0.0000

B-3: Extinction Estimates Based on Aerosol Size Spectra

Particle Scattering Cross-Section

Calculations of particle scattering cross-section were made using the Deirmendjian[1] approximation to the total Mie series. The approximation defines the particle scattering cross-section, k, for non-adsorbing spheres

$$k = G\left(2 - \frac{4 \sin Z}{Z} + 4\,\frac{(1-\cos Z)}{Z^2}\right) \qquad (1)$$

$$Z = \frac{4\pi r}{\lambda}(n-1) \qquad (2)$$

where r = particle radius

λ = wavelengh of incident radiation

n = real index of refraction

G = Deirmendjian's modification.

Depending on the value of Z, G has the following forms:

$$Z \leq 4.08: \quad G = \frac{5(n-1)^2}{4.08n} + \frac{Z}{5(n-1)} \qquad a)$$

$$4.08 < Z \leq 5(n-1): \quad G = 1 + (n-1)\,\frac{4.08}{Z+n} \qquad b) \qquad (3)$$

$$Z > 5(n-1): \quad G = 1 + (n-1)\,\frac{Z}{4.08n} \qquad c)$$

A plot of the cross-section from the Diermendjian formulation compared to the Mie series is shown in Fig B-3.1 for λ = .474 um and n = 1.33.

---

[1] Deirmendjian, D., 1969: Electromagnetic Scattering on Spherical Polydispersions, American Elsevier Publishing Co., Inc., New York.

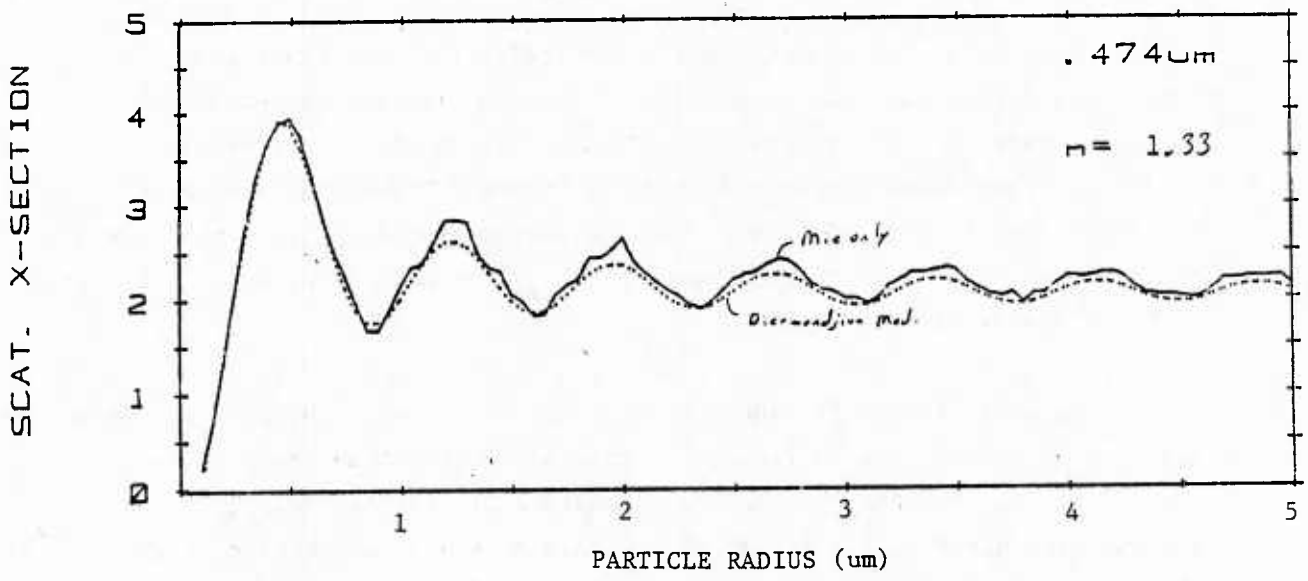

Figure B-3.1 SCATTERING CROSS-SECTION VS. PARTICLE RADIUS

Using the above approximation a mean scattering cross-section was computed for each sampling interval of radius for which we had number concentrations of particles. The values obtained were:

$\lambda = 0.474$
$n = 1.37$

Radius interval (um)	Mean k	# of values in the mean
.05 - .158	0.311	116
.158- .281	1.914	58
.281- .890	3.026	116
1.0 - 2.0	2.263	70
2.0 - 3.0	2.072	41
3.0 - 4.0	2.081	29
4.0 - 5.0	2.052	23
5.0 - 6.0	2.037	19
6.0 - 7.0	2.044	16
7.0 - 8.0	2.022	14
8.0 - 9.0	2.037	12
9.0 -10.0	2.016	11
10.0 -11.0	2.028	10
11.0 -12.0	2.015	9
12.0 -13.0	2.018	9
13.0 -14.0	2.018	8
14.0 -15.0	2.015	7

Comparison of Calculated vs Measured β_{scat}

Based on the foregoing, extinction coefficient (or scattering coefficient, β_{scat}) was computed for 0.474 μm λlight and indices of refraction (η) 1.33 (pure water), 1.37 (saturated NaCℓ solution) and 1.50 (dry NaCℓ). The results of these computations are shown in Figure B-3.2 where calculated β_{scat} for each index of refraction is plotted against measured β_{scat}. Immediately apparent from the Figure is that computed β_{scat} matched measured β_{scat} for only 4 to 5 of the 51 size spectra.

The computations for index of refraction 1.37 are tabulated in the accompanying list. From left to right, the columns in the table show (1) date and time of the size spectra (plotted in Appendix B-2), (2) Aerosol β_{scat} computed from the size spectra, (3) Aerosol β_{scat} plus molecular scattering (0.23×10^{-4}/m), (4) measured β_{scat} (MRI Nephelometer), (5) the difference between measured and computed β_{scat}, and (6) the % of measured β_{scat} accounted-for by molecular scattering and the aerosol at sizes >0.32 μm diameter. This presentation shows that the measured size distribution (at sizes only >0.32 μm diameter) could, in general, account for only a fraction of the measured β_{scat}. The far right-hand column shows that this fraction ranged from 13 to 104% of the measured value but was typically in the range 25-75%; further, approximately 50% of the size spectra data sets could account for only 25-40% of their respective measured β_{scat} values.

Figure B-3.3 provides some insight into the reasons for the apparent discrepancy between measured and computed β_{scat}. The figure shows the accumulative average daily size spectra for the period 9 through 17 October for sizes >0.32 μm diameter. Superimposed on this figure are the average Aitken counts for the respective days (plotted at the 10^{-2} μm size value) and estimations of the slope of the size spectra between 0.01 and 0.32 μm based on previous observations in coastal Europe. It is clear that substantial numbers of particles must have been present at optically effective sizes; e.g., below 0.32 μm number concentrations at 0.1 μm size, on average, could have been two orders of magnitude or more greater than those measured at >0.32 μm sizes. Reference to the Mie theory discussion shows that such high number concentrations in the 0.1 to 0.32 μm

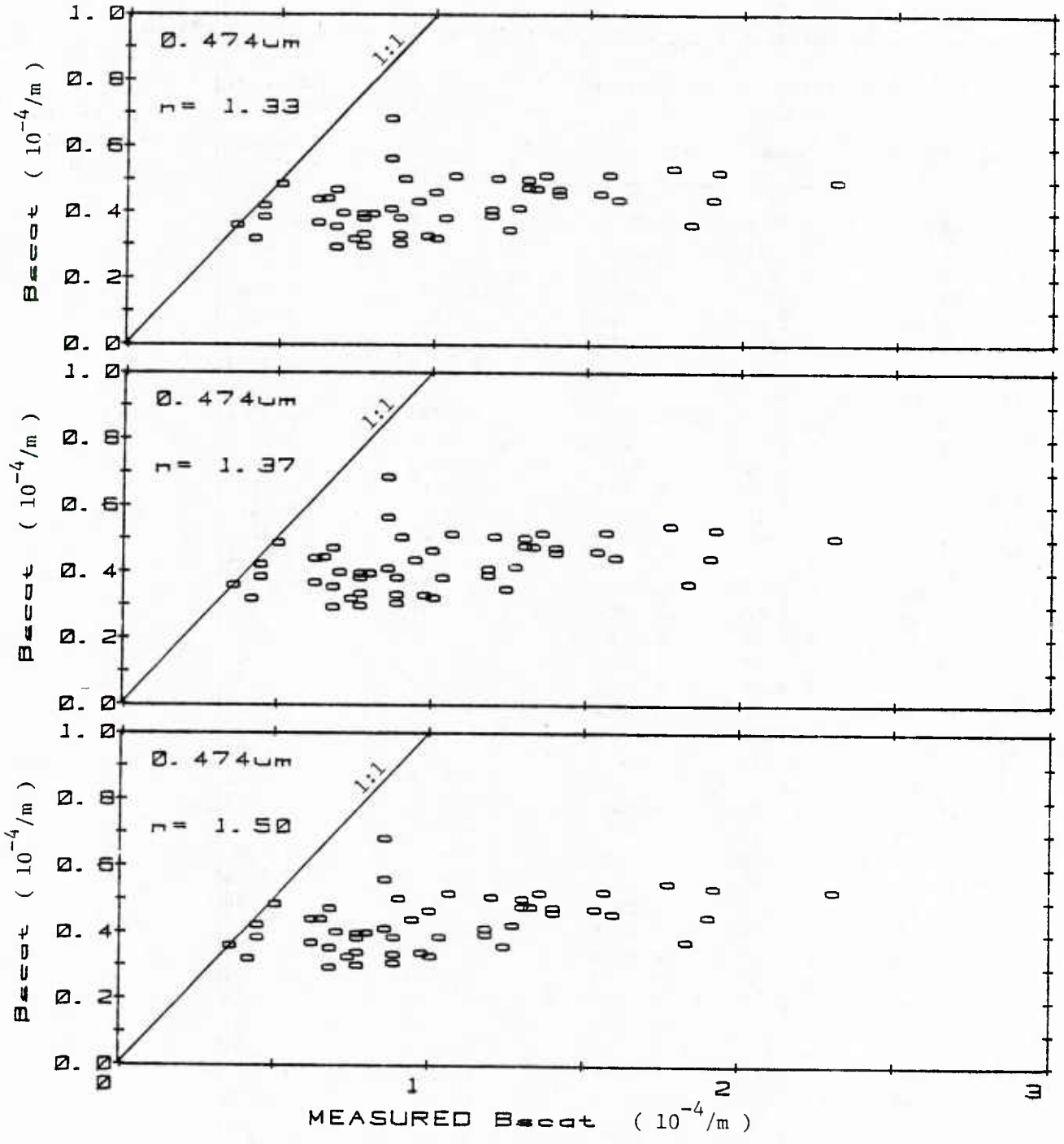

Figure B-3.2

Comparison of Measured B_{scat} with B_{scat} Calculated from Aerosol Size Spectra >0.32 um Diameter for Three Indices of Refraction and Visible Wavelength Light.

Comparison of Measured β_{scat} with that Computed for $\eta = 1.37$ @ 0.474 μm λ

OCTOBER	(GMT)	Computed Aerosol β_{scat} (10^{-4}/m)	Computed β_{scat} (Aerosol + 0.23) (10^{-4}/m)	Measured β_{scat} (10^{-4}/m)	Difference Meas.-Comp. β_{scat} (10^{-4}/m)	% β_{scat} Accounted for By Aerosol >0.3μm dia
9	12:05	0.1610	0.3910	0.7670	0.3760	51%
9	15:05	0.4806	0.7106	0.8555	0.1449	83
10	8:23	0.1081	0.3381	0.7670	0.4289	44
10	9:00	0.1097	0.3397	0.8850	0.5453	38
10	12:00	0.1727	0.4027	0.7670	0.3643	53
10	15:00	0.2128	0.4428	0.9440	0.5012	47
10	17:54	0.1767	0.4067	0.9735	0.5668	42
11	7:40	0.0827	0.3127	0.8850	0.5723	25
11	9:00	0.0769	0.3069	0.7670	0.4601	40
11	13:00	0.0744	0.3044	0.6785	0.3741	45
11	15:00	0.0954	0.3254	1.0030	0.6776	32
11	18:10	0.1380	0.3680	1.8290	1.4610	20
12	6:10	0.2510	0.4810	2.3010	1.8200	21
12	9:00	0.1012	0.3312	0.9735	0.6423	34
12	11:00	0.1859	0.4159	3.1360	2.7677	13
12	13:00	0.1196	0.3496	1.2390	0.8894	28
12	15:00	0.0924	0.3224	0.7375	0.4151	44
13	6:04	0.2456	0.4756	1.3275	0.8519	36
13	9:00	0.2790	0.5090	1.3275	0.8185	38
13	12:00	0.2871	0.5171	1.3570	0.8399	38
13	15:00	0.2850	0.5150	1.0620	0.5470	48
13	17:35	0.2772	0.5072	0.9000	0.3928	56
14	6:01	0.3368	0.5668	0.8555	0.2887	66
14	7:42	0.2501	0.4801	0.9145	0.4344	53
14	9.08	0.1933	0.4233	0.4425	0.0192	96
14	12:05	0.1584	0.3884	0.4425	0.0541	88
14	13:00	0.2462	0.4762	1.2095	0.7333	39
14	15:00	0.2405	0.4705	0.6785	0.2080	69
14	18:00	0.2154	0.4454	0.6195	0.1741	72
15	6:25	0.1570	0.3870	0.8850	0.4980	44
15	9:00	0.1686	0.3986	0.7965	0.3979	50
15	12:00	0.1554	0.3854	1.0325	0.6471	37
15	15:10	0.1863	0.4163	0.8555	0.4392	49
15	18:06	0.2849	0.5149	1.5635	1.0486	33
16	6:02	0.2049	0.4349	1.5930	1.1581	27
16	8:08	0.3003	0.5303	1.7700	1.2397	30
16	9:00	0.2275	0.4575	1.5340	1.0765	30
16	12:00	0.1834	0.4134	1.3685	0.8551	33
16	13:00	0.1811	0.4111	1.1800	0.7689	35
16	13:28	0.1623	0.3923	1.1800	0.7877	33
16	15:00	0.2134	0.4434	1.6520	1.2086	27
16	15:20	0.2300	0.4600	1.6520	1.1920	28
17	6:12	0.2910	0.5210	1.9175	1.3965	27
17	10:07	0.1330	0.3630	0.6785	0.3155	54
17	12:33	0.2775	0.5075	1.3000	0.7925	39
17	17:40	0.2436	0.4736	1.4000	0.9264	34
18	8:35	0.2197	0.4497	0.6490	0.1993	69
18	10:38	0.2366	0.4666	1.4750	1.0084	32
18	13:11	0.1446	0.3746	0.6195	0.2449	60
18	15:00	0.0972	0.3272	0.4130	0.0858	79
18	17:55	0.1374	0.3674	0.3510	-0.0134	104

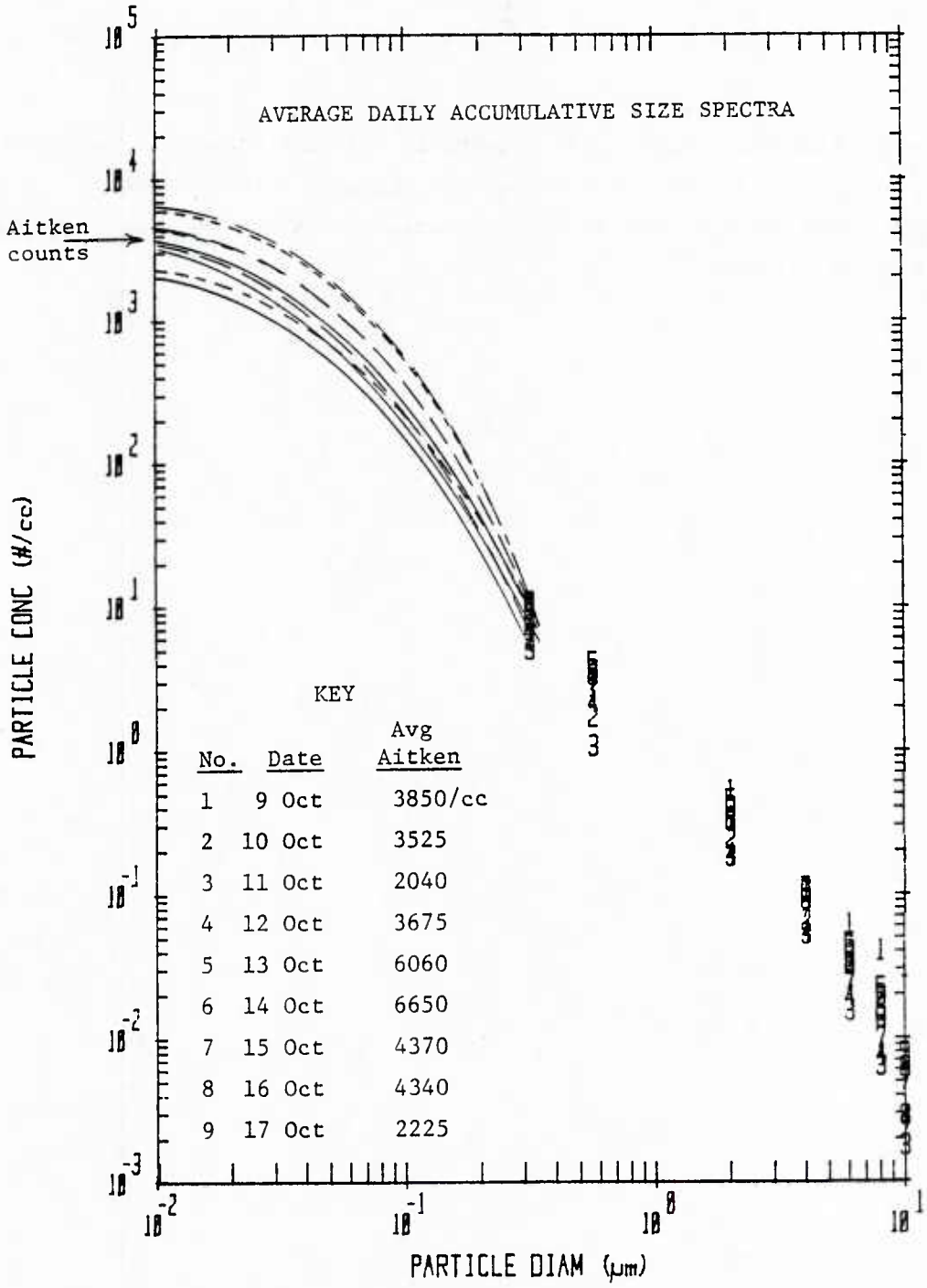

Figure B-3.3

Extrapolation of Aerosol Size Spectra (Royco/Drop-Sampler) to Sizes Below 0.32 μm Diameter Based on Aitken Nuclei Concentrations and Observations from Prior Measurement Programs (References 11, 15, 16).

diameter interval could easily account in most instances for the 'missing' aerosol β_{scat}. It is therefore recommended that future measurements of aerosol size spectra intended for extinction computations include the size range down to 0.05 μm diameter.

B-4 Aerosol Chemistry

During the Alboran Sea Experiment, aerosol samples were collected from the Flying Bridge area of the BARTLETT via a Casella cascade impactor. (Additional samples were obtained by NEPRF personnel from aboard the Naucrates.) Subsequently, the samples were returned to Calspan for analysis via scanning electron microscopy (SEM) and elemental energy dispersive x-ray analysis (EDXA). The combination of these two techniques allowed (1) visualization of individual impacted particles where size measurements could be obtained and (2) determination of elemental composition of particles with specific identification of elements from sodium (atomic number 11) and greater in atomic number. Detector sensitivity limits analyses to particles of size >0.2 μm diameter. The analysis equipment, procedures and output are discussed in detail elsewhere (e.g. Reference 11).

This technique has been used for years in our studies of boundary layer aerosols and provides a simple means for classifying individual particles (>0.2 μm diameter) and identifying airmass aerosol source regions. The Casella samples were obtained over ∿20 min sampling periods at ∿3 hr intervals, keyed to drop sample collections and to changes in meteorological circumstances.

A total of 54 of these samples from the BARTLETT were analyzed, and the data reduced to provide two forms of chemical classification: (1) the total element distribution of the aerosol population; and (2) classified according to their over all chemical make-up into 6 categories -- Organics, NaCℓ (Sea Salt), NaCℓ + other salts, Silicates, Sulfates, and other salts. For each sample, 50 or 100 particles were individually analyzed. The fraction of the aerosol population at sizes >0.2 μm dia was then determined for each classification scheme. Similarly, 7 of the 12 samples obtained from aboard the Naucrates were reduced. These data are provided in tabular form in this Appendix.

Chemical Analyses by Element Distribution

Each particle, individually analyzed, produced EDXA spectra indicating the presence of various elements. The data, so obtained, were summarized for each of the 50 to 100 particles analyzed for each sample and tabulated in Table B-4.1. Inthe table, the date, the center-time for each 20-minute sample, and the number of particles counted for each sample are shown in the three left-hand columns. In the 10 columns to the right, the percent of those particles which contained Aℓ, Mg, Ca, Na, Cℓ , S, P, K, Fe and Si, respectively, are indicated. (Naucrates data are provided at the end of the table.)

Chemical Classification by Particle Type

As was the case for our previous studies of natural aerosol composition, it was found that individual particles could be grouped into six categories according to total elemental composition:

(1) those with atomic numbers lower than Na--probably organics;
(2) NaCℓ only--sea salt;
(3) NaCℓ - mixed with minor amounts of other inorganic salts;
(4) Si-containing compounds--flyash and soil particulates;
(5) S-containing compounds -- chiefly ammonium sulfate;
(6) inorganic salts without NaCℓ -- Calcite, gypsum, minerals.

As for Table B-4.1, the data grouped according to particle type are tabulated in Table B-4.2. These same data are plotted in Figure 5 (Section 2) and in the chemistry figures provided in Section 3. (In the text of this report the NaCℓ and NaCℓ -Mixed categories were lumped together; the Organic category was not plotted because very few of that particle-type were observed.)

Table B-4.1

ELEMENTAL CLASSIFICATION

BARTLETT DATA

			% Particles Containing the Indicated Elements									
OCTOBER	GMT	# PARTICLES	Al	Mg	Ca	Na	Cl	S	P	K	Fe	Si
9	9:25	50	34	10	10	54	80	8	74	6	20	40
9	11:55	50	58	34	36	48	62	48	76	24	18	88
9	15:59	50	80	54	72	68	82	34	60	40	16	74
9	18:10	50	64	38	30	56	66	26	62	22	14	64
10	6:25	100	42	9	42	34	35	19	44	25	31	44
10	9:30	100	57	29	21	50	66	53	31	46	46	72
10	10:20	100	69	29	74	29	49	7	64	18	27	13
10	12:10	100	63	33	69	31	44	7	90	69	4	66
10	15:00	100	70	41	67	63	77	14	84	28	17	70
10	18:00	100	68	50	48	47	46	34	65	27	15	74
10	21:50	100	35	24	17	22	21	9	93	12	4	82
11	6:50	100	40	30	57	66	87	44	69	29	8	43
11	7:55	100	23	16	28	75	92	18	28	17	6	24
11	9:00	100	34	21	47	50	68	25	34	12	33	49
11	12:30	100	29	16	22	72	81	17	22	10	19	37
11	14:55	100	48	38	45	49	47	30	45	17	39	53
11	18:00	100	50	31	38	56	56	29	36	17	40	47
12	6:15	100	74	36	26	7	1	76	24	31	43	78
12	8:55	100	53	68	60	23	6	54	43	21	26	60
12	11:03	100	43	31	25	40	31	36	78	7	12	47
12	12:30	100	50	36	41	63	31	16	78	11	7	54
12	15:05	100	38	25	49	41	75	16	67	14	19	44
13	6:10	100	74	43	14	29	51	58	30	14	4	95
13	8:35	100	20	12	21	62	67	4	64	6	2	36
13	11:50	50	12	10	10	90	94	14	20	4	0	10
13	15:10	50	64	38	86	14	32	16	72	14	10	70
13	17:30	50	18	8	8	96	98	2	2	4	4	24

B-4.1 Contd.

BARTLETT CASELLA ANALYSIS

OCTOBER	GMT	# PARTICLES	Al	Mg	Ca	Na	Cl	S	P	K	Fe	Si
14	6:00	50	6	2	4	98	100	6	2	0	0	6
14	7:45	50	8	12	2	98	96	2	2	0	0	10
14	9:10	50	22	26	40	62	68	18	0	12	4	46
14	12:00	50	2	0	0	100	100	0	0	0	0	2
14	13:07	50	12	12	28	84	82	10	0	0	4	18
14	15:00	50	0	6	0	100	100	4	0	0	0	0
14	17:55	50	2	4	4	98	98	2	0	0	0	4
15	6:25	50	10	16	14	94	92	20	2	0	0	16
15	9:00	50	6	8	4	96	96	0	0	2	0	6
15	12:00	50	6	6	15	82	80	10	0	4	2	14
15	15:10	50	10	22	12	88	92	22	0	6	2	12
16	6:20	50	40	30	42	78	86	4	2	16	12	38
16	9:00	50	54	46	40	62	54	16	0	14	16	52
16	11:25	50	58	32	42	58	32	28	4	16	8	60
16	12:30	50	40	46	40	72	32	34	0	16	14	48
16	13:30	50	72	48	50	54	4	26	2	28	22	84
16	14:30	50	24	18	18	90	88	16	0	12	2	36
16	15:25	50	52	56	58	54	42	76	94	52	32	64
17	6:15	50	2	4	4	94	94	4	0	2	2	4
17	10:05	50	2	6	2	100	98	6	0	0	0	2
17	12:37	50	2	0	6	98	98	4	0	0	2	2
17	17:35	50	4	4	2	100	100	10	0	0	0	2
18	8:45	50	2	4	2	100	100	2	0	0	0	2
18	10:40	50	6	12	2	100	100	6	0	2	0	8
18	13:20	50	2	6	4	100	100	8	0	2	0	4
18	15:00	50	2	8	4	92	94	12	0	0	2	6
18	18:00	50	2	12	2	100	100	8	0	0	0	4

NAUCRATES DATA

NAUCRATES CASELLA ANALYSIS

OCTOBER	GMT	# PARTICLES	Al	Mg	Ca	Na	Cl	S	P	K	Fe	Si
11	11:00	50	56	28	56	18	24	38	0	24	24	84
11	12:00	50	66	30	48	18	30	68	2	30	18	86
11	13:15	50	32	36	12	76	68	26	0	4	6	48
11	15:20	50	38	38	56	46	22	34	6	20	20	44
12	11:30	50	52	36	38	38	26	36	44	10	8	52
12	15:00	50	34	40	18	68	86	26	4	14	6	30
12	17:00	50	16	26	20	74	80	20	0	4	4	20

Table B-4.2

PARTICLE TYPE CLASSIFICATION

BARTLETT DATA

% Particles of the Indicated Classification

OCTOBER	GMT	# PARTICLES	ORG.	NaCl	NaCl MIXED	Si COMP.	S COMP.	OTHER
9	11:25	50	0	0	62	24	10	4
9	15:59	50	2	6	76	10	4	2
9	18:10	50	0	12	54	20	8	6
10	6:25	100	0	1	33	21	4	41
10	8:30	100	0	0	66	12	4	18
10	10:20	100	0	0	49	27	1	23
10	12:10	100	0	0	44	30	0	26
10	15:00	100	0	8	69	9	0	14
10	18:00	100	0	1	47	23	19	10
10	21:50	100	0	2	19	68	1	10
11	6:50	100	0	7	80	2	7	4
11	7:55	100	0	50	42	2	3	3
11	9:00	100	0	25	44	13	11	7
11	12:30	100	0	41	40	8	7	4
11	14:33	100	0	9	38	20	23	10
11	18:00	100	0	19	38	15	20	8
12	6:15	100	0	0	1	21	75	3
12	8:55	100	0	1	5	30	51	13
12	11:03	100	0	1	29	21	33	16
12	12:30	100	0	5	26	34	15	20
12	15:05	100	0	14	61	10	8	7
13	6:10	100	0	0	51	27	22	0
13	8:35	100	0	27	40	19	3	11
13	11:50	50	0	68	26	0	4	2
13	15:10	50	0	0	32	40	8	20
13	17:30	50	0	74	24	2	0	0

B-4.2 Contd.

BARTLETT CASELLA ANALYSIS

OCTOBER	GMT	# PARTICLES	ORG.	NaCl	NaCl MIXED	Si COMP.	S COMP.	OTHER
14	6:00	50	0	94	6	0	0	0
14	7:45	50	0	78	18	4	0	0
14	9:10	50	0	34	34	18	6	8
14	12:00	50	0	96	4	0	0	0
14	13:07	50	0	70	12	0	8	10
14	15:00	50	0	94	6	0	0	0
14	17:55	50	0	90	8	2	0	0
15	6:25	50	0	68	24	2	6	0
15	9:00	50	2	84	12	2	0	0
15	12:00	50	0	68	12	4	6	10
15	15:10	50	0	66	26	0	8	0
16	6:20	50	0	42	44	8	2	4
16	9:00	50	2	18	36	24	10	10
16	11:25	50	4	4	28	34	14	16
16	12:30	50	2	2	30	20	20	26
16	13:30	50	0	0	4	64	26	6
16	14:30	50	0	50	38	2	10	0
16	15:25	50	0	0	42	10	40	8
17	6:15	50	0	94	0	2	4	0
17	10:05	50	0	94	4	0	2	0
17	12:37	50	0	90	8	0	2	0
17	17:35	50	0	88	12	0	0	0
18	8:45	50	0	96	4	0	0	0
18	10:40	50	0	84	16	0	0	0
18	13:20	50	0	92	8	0	0	0
18	15:00	50	0	82	12	4	2	0
18	18:00	50	0	78	22	0	0	0

NAUCRATES DATA

NAUCRATES CASELLA ANALYSIS

OCTOBER	GMT	# PARTICLES	ORG.	NaCl	NaCl MIXED	Si COMP.	S COMP.	OTHER
11	11:00	50	0	0	24	40	30	6
11		50	0	0	30	16	52	2
11	13:15	50	0	42	26	18	12	2
11	15:20	50	0	6	16	22	28	28
12	11:30	50	0	8	18	30	32	12
12	15:00	50	0	42	44	4	8	2
12	17:00	50	0	46	34	4	6	10

B-5: Summary Discussion of the Alboran Gyre

The following summary is supplied to provide the reader with immediate access to a description of the Alboran Gyre. This discussion is reproduced from Reference 3:

"BACKGROUND AND OBJECTIVES OF THE ALBORAN SEA PROJECT"

by

T. H. Kinder, et. al

"Operation Plan, DONDE VA?"

July 1982

NORDA Informal Prospectus

Sea straits impose a geographic constriction on the flow of water and frequently on the flow of air above the sea surface. Bathymetric gradients are also large, with continental slopes, submarine canyons, and seamounts often located near straits. These features cause an intensification in water flow, a juxtaposition of different water masses, and a modification of atmospheric forcing. The geometry of straits make various boundary effects important, such as lateral and bottom friction, coastal upwelling, sidewall eddies, setup, and sharp curvature of streamlines. Moreover for straits of large size the earth's rotation remains important.

Because straits are both a constriction to flow and a connection between two water bodies, flow in straits is influenced by phenomena over a wide range of spatial and temporal scales. On the smallest spatial scales density finestructure and boundary layer turbulence are found. Larger scales include those of fronts, of bottom topography, of water depth, width of the strait, length of the strait, and mesoscale features such as eddies at the inlet and outlet. Finally, the scales of the largest atmospheric systems (e.g. Bermuda high) and current systems (e.g. North Atlantic subtropical gyre) can influence straits. Concomitant temporal scales range from periods of the smallest turbulent eddies and internal waves through tidal periods and local weather phenomena to seasonal time scales. Other processes imbedded in the flow regime such as chemical reactions, phytoplankton growth, and sediment transport add their own scales.

Effects resulting from sea straits are not localized within the straits themselves, but may be found far downstream as jets, eddies, internal tides, or finestructure. These downstream phenomena (and also upstream blocking effects) are sometimes more tractable objects for study because they are in a quieter background than exists within the strait. For example, direct effects of flow through the Strait of Gibraltar extend over 200 km into both the Alboran Sea to the east and the Gulf of Cadiz to the west.

Clearly, to progress on understanding physical phenomena near sea straits it is necessary to identify one or two important phenomena and to mitigate interference from competing processes. This self-evident homily can often be ignored where phenomena are geographically separated, (e.g., coastal upwelling does not interfere with measurements of mid-ocean eddies), but sea straits bring many phenomena close together. Our approach will be to concentrate on dynamical effects of the sea straits that occur in the regions on either side of the strait, rather than concentrating within the straits themselves. We thus intend to focus on mesoscale and submesoscale phenomena (e.g. jets, eddies, fronts) with length scales defined by the width and depth of the strait and by the Rossby radius, and temporal scales longer than tidal. We believe that the energetic high wavenumber and high frequency regimes in the straits are less accessible by our techniques than the equally-important downstream flow regimes. We thus consider the strait itself as a boundary condition or a forcing term for the downstream variability. For example, the inflowing Atlantic water jet, which dominates mesoscale processes in the Alboran Sea, would not exist without the constriction at the Strait of Gibraltar. Many details of the dynamics within the strait, however, may not be important in forming mesoscale structure in the Alboran Sea.

Mean flow through the Strait of Gibraltar is driven by sea level and density differences resulting from the evaporative loss of water from the Mediterranean Sea. By using mass budgets, heat budgets, and current measurements, annual mean inflows (and outflows) of 1 to 2 x 10^6 m^3/sec have been estimated (Lacombe, 1971; Bethoux, 1979; Lacombe and Richez, 1982). The inflowing Atlantic water is always less dense and much less saline (salinity of about 36^o/oo) than the outflowing waters, and in the Strait and Alboran Sea it is always found as a surface layer. The outflowing Mediterranean water is always denser and more saline (salinity of about 38^o/oo) than the inflowing waters, and is found as a subsurface layer everywhere (outside upwelling regions). These large volume transports of inflowing Atlantic water and outflowing Mediterranean water through the narrow (less than 20 km) and shallow (about 300 m) Strait of Gibraltar produce mean current speeds of 50 to 100 cm/sec.

East of the Strait, the Atlantic water appears to retain identification as a narrow (about 30 km wide) jet, and it forms a gyre in the Alboran Sea (Peluchon and Donguy, 1962; Grousson and Faroux, 1963; Lanoix, 1974; May and Porter, 1975; Petit et al., 1978; Wannamaker, 1979; Cheney and Doblar, 1982). The gyre fills the western half of the sea, from Cape Tres Forcas (3°W) to the Strait. Although there has been some controversy, the gyre apparently is either permanent or nearly so: the more comprehensive measurements reported in the literature all show the gyre.

Part of the evidence for this permanence comes from satellite infrared images. Because of upwelling along the southern Spanish coast, the gyre often shows clearly as a warm core eddy (Stevenson, 1977; Cheney, 1978a; Wannamaker, 1979; Philippe et al., 1979; Gallagher, et al., 1981; Philippe and Harang, 1982). The notion that the gyre is permanent and detectable nearly year-round (Cheney, 1978a) is also supported by the satellite imagery made during 1979-1982 that we have examined.

Included in discussions of the permanence of the gyre has been the question of its variability and the attendant forcing. The gyre seems to vary in size, shape, and intensity. Wind stress has been proposed as an important modifying force (Cano and Castillejo, 1972; Ovchinnikov, Krivosheya, and Muskalenka, 1976; Cheney, 1978b; Cheney and Doblar, 1982).

Whitehead and Miller (1979) used a rotating turntable to model the Alboran Gyre. The model was transient, but included stratification and realistic lateral boundaries. Neither wind stress nor bottom topography were included. Over a reasonable (scaled) parameter range, they simulated the anticyclonic gyre. They suggested that the gyre results from the density driven flow interacting with the lateral boundaries (especially Cape Tres Forcas) under the constraint of rotation.

Preller and Hurlburt (1982) have applied the reduced gravity model of Hurlburt and Thompson (1980) and obtained solutions that closely resemble the classical gyre (Lanoix, 1974). This was done with a highly idealized model: no topography, straight coastlines, and no winds. These results suggest that the angle of the inflow and the inflow vorticity are important for the resulting gyre formation.

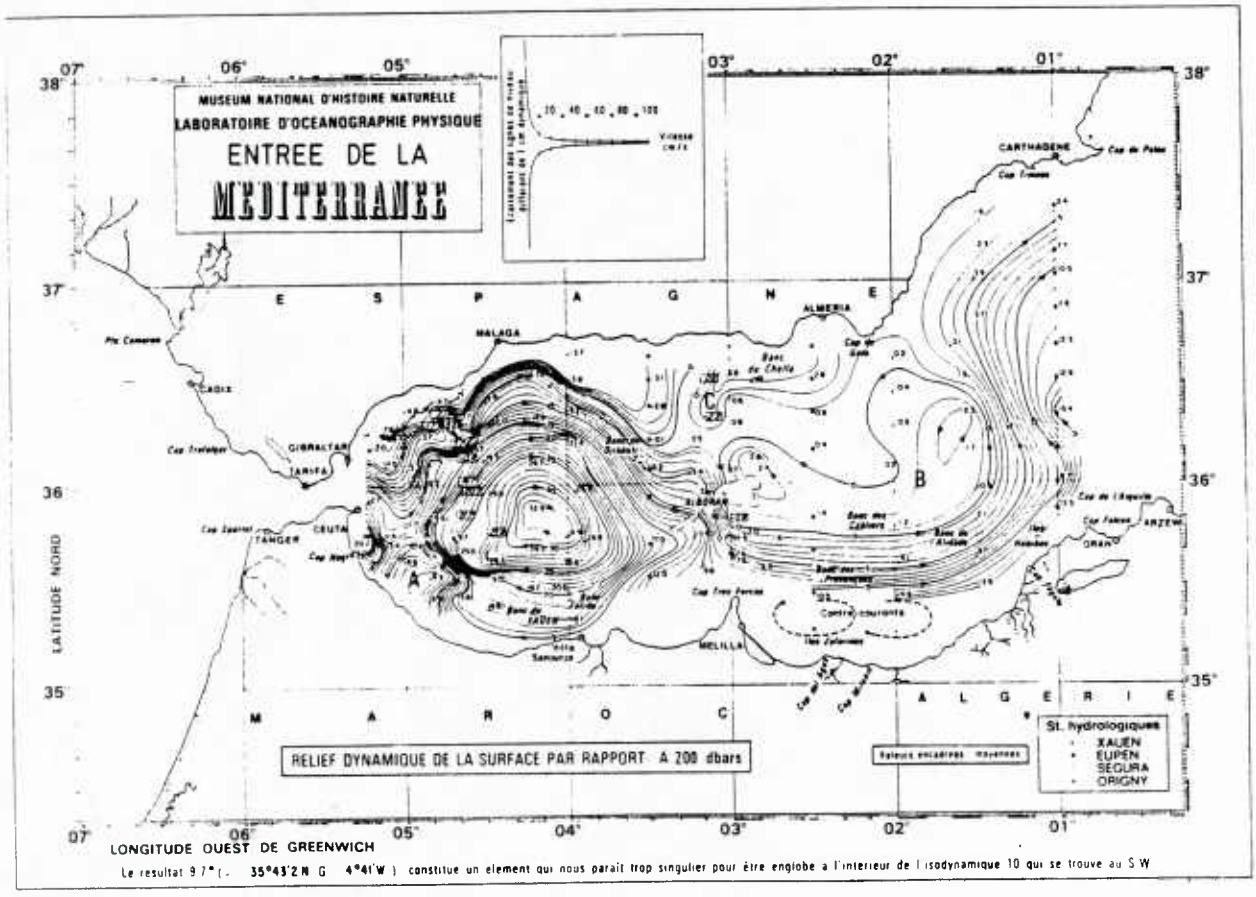

Dynamic topography for the surface for the period July and August 1962 (Lanoix, 1974)

DISTRIBUTION

COMMANDER IN CHIEF
U.S. ATLANTIC FLEET
CODE N04E
NORFOLK, VA 23511

CINCUSNAVEUR
NAVELEX DET.
ATTN: NSAP SCIENCE ADVISOR
BOX 100
FPO NEW YORK 09501

COMSIXTHFLT
ATTN: FLT METEOROLOGIST
FPO NEW YORK 09501

COMFLTAIR, MEDITERRANEAN
ATTN: NSAP SCIENCE ADVISOR
CODE 03A
FPO NEW YORK 09521

COMMANDING OFFICER
31 OCEANO. DEV. SQDN 8-VXN-8
NAVAL AIR STATION
PATUXENT RIVER, MD 20670

COMMANDING OFFICER
AIR TEST & EVAL SQDN 5-VX-5
NAVAL WEAPONS CENTER
CHINA LAKE, CA 93555

SPECIAL ASST. TO THE ASST.
SECRETARY OF THE NAVY (R&D)
ROOM 4E741, THE PENTAGON
WASHINGTON, DC 20350

CHIEF OF NAVAL RESEARCH (2)
LIBRARY SERVICES, CODE 734
RM 633, BALLSTON TOWER #1
800 QUINCY ST.
ARLINGTON, VA 22217

OFFICE OF NAVAL RESEARCH
CODE 420
ARLINGTON, VA 22217

OFFICE OF NAVAL RESEARCH
COASTAL SCIENCES PROGRAM
CODE 422 CS
ARLINGTON, VA 22217

CHIEF OF NAVAL OPERATIONS
U.S. NAVAL OBSERVATORY
DR. RECHNITZER, OP-952F
34TH & MASS AVE.
WASHINGTON, DC 20390

OFFICER IN CHARGE
U.S. NAVOCEANCOMDET
NAPLES, BOX 23
FPO NEW YORK 09520

OFFICER IN CHARGE
NAVOCEANCOMDET
U.S. NAVAL AIR FACILITY
FPO NEW YORK 09523

COMMANDING OFFICER
NAVAL RESEARCH LAB
ATTN: LIBRARY, CODE 2620
WASHINGTON, DC 20390

OFFICE OF NAVAL RESEARCH
SCRIPPS INSTITUTION OF
OCEANOGRAPHY
LA JOLLA, CA 92037

COMMANDING OFFICER
NORDA, CODE 335
NSTL STATION, MS 39529

COMMANDING OFFICER
U.S. NAVOCEANCOMCEN
BOX 31 (ROTA)
FPO NEW YORK 09540

SUPERINTENDENT
LIBRARY REPORTS
U.S. NAVAL ACADEMY
ANNAPOLIS, MD 21402

NAVAL POSTGRADUATE SCHOOL
METEOROLOGY DEPT.
MONTEREY, CA 93943

NAVAL POSTGRADUATE SCHOOL
OCEANOGRAPHY DEPT.
MONTEREY, CA 93943

NAVAL POSTGRADUATE SCHOOL
PHYSICS & CHEMISTRY DEPT.
MONTEREY, CA 93943

LIBRARY
NAVAL POSTGRADUATE SCHOOL
MONTEREY, CA 93943

PRESIDENT
NAVAL WAR COLLEGE
ATTN: GEOPHYSICS OFFICER
NEWPORT, RI 02840

COMMANDER (2)
NAVAIRSYSCOM
ATTN: LIBRARY (AIR-7226)
WASHINGTON, DC 20361

COMMANDER
NAVAIRSYSCOM (AIR-330)
WASHINGTON, DC 20361

COMMANDER
NAVAL SEA SYSTEMS COMMAND
ATTN: LCDR S. GRIGSBY
PMS-405/PM-22
WASHINGTON, DC 20362

COMMANDER
NAVOCEANSYSCEN
DR. J. RICHTER, CODE 532
SAN DIEGO, CA 92152

COMMANDER
NAVAL WEAPONS CENTER
DR. A. SHLANTA, CODE 3918
CHINA LAKE, CA 93555

COMMANDER
NAVAL SURFACE WEAPONS CENTER
DAHLGREN,VA 22448

COMMANDER
NAVSURFWEACEN, CODE R42
DR. B. KATZ, WHITE OAKS LAB
SILVER SPRING, MD 20910

COMMANDER
PACMISTESTCEN
GEOPHYSICS OFFICER
PT. MUGU, CA 93042

USAFETAC/TS
SCOTT AFB, IL 62225

AFGL/LY
HANSCOM AFB, MA 01731

OFFICE OF NAVAL RESEARCH
CODE 422AT
ARLINGTON, VA 22217

ROBERT ARNONE
NORDA CODE 335
NSTL STATION, MS 39529

COMMANDER & DIRECTOR
ATTN: DELAS-AS-P
U.S. ARMY ATMOS. SCI. LAB
WHITE SANDS MISSILE RANGE,
NEW MEXICO 88002

DIRECTOR (12)
DEFENSE TECH. INFORMATION
CENTER, CAMERON STATION
ALEXANDRIA, VA 22314

DIRECTOR
COASTAL STUDIES INSTITUTE
LOUISIANA STATE UNIVERSITY
ATTN: O. HUH
BATON ROUGE, LA 70803

WOODS HOLE OCEANO. INSTITUTE
DOCUMENT LIBRARY LO-206
WOODS HOLE, MA 02543

UNIVERSITY OF WASHINGTON
ATMOSPHERIC SCIENCES DEPT.
SEATTLE, WA 98195

COLORADO STATE UNIVERSITY
ATMOSPHERIC SCIENCES DEPT.
FORT COLLINS, CO 80523

CHAIRMAN, METEOROLOGY DEPT.
PENNSYLVANIA STATE UNIV.
503 DEIKE BLDG.
UNIVERSITY PARK, PA 16802

ARVIN/CALSPAN ADVANCED
TECH. CENTER
ATMOS. SCI./ENV. SCI. DEPT.
P.O. BOX 400
BUFFALO, NY 14225

DIRECTOR, SACLANT ASW
RESEARCH CENTRE
VIALE SAN BARTOLOMEO, 400
I-19026 LA SPEZIA, ITLAY

S. A. HSU
COASTAL STUDIES INSTITUTE
LOUISIANA STATE UNIVERSITY
BATON ROUGE, LA 70803

THOMAS H. KINDER
NORDA CODE 331
NSTL STATION, MS 39529

PAUL LAVIOLETE
NORDA CODE 335
NSTL STATION, MS 39529

GREGORIO PARRILLA
INSTITUTO ESPANOL DE
OCEANOGRAFIA
ALCALA 27-4
MADRID, 14, ESPANA

MICHELE CHAMPAGNE PHILIPPE
CENTRE DE METEOROLOGIE
SPATIALE
BP 147 22301 LANNION,
CEDEX, FRANCE

HEINZ VAN DER PIEPEN
DEUTSCHE FORSCHUNGS-UND
VERSUCHSANSTALT FUR LUFT-UND
RAMFAHRT E.V. (DFVLR)
OBERPFAFFENHOFEN 8030 WESSLING
FEDERAL REPUBLIC OF GRMANY